

Impact of Exposure to Benzo[*b*]fluoranthene and Aging on Mutations in Male Mouse Germ Cells

Madison Stewart

Thesis submitted to the University of Ottawa in partial fulfillment of the
requirements for the degree of
Master of Science in Biology Specialization in Bioinformatics

Department of Biology
Faculty of Science
University of Ottawa,
Ottawa, ON

Abstract

Mutations in germ cells accumulate with age and can lead to inherited disorders; thus, it is critical to identify the endogenous and exogenous factors that contribute to their formation. Polycyclic aromatic hydrocarbons (PAHs) are widespread combustion by-products that are ubiquitous in the environment. Long-term exposure to these harmful compounds can have serious implications to health. Benzo[*b*]fluoranthene (BbF) is a PAH that induces mutations in mouse somatic tissues and is classified as a possible human carcinogen. However, the effects of BbF on germ cells are unknown. Age-related spontaneous mutations in male germ cells are attributed to lower fertility and elevated risk of genetic disease in the offspring; making it necessary to deeply characterize the effects of aging on the male germline. We evaluated the effects of long-term BbF exposure and aging on male germ cells. Adult MutaMouse males were exposed orally to BbF dissolved in olive oil at doses of 0 (controls), 3.25, 6.25, 12.5, 25, or 50 mg/kg BW/day for 90 days or at 0, 1.5625, 3.125, 6.25, 12.5, or 25 mg/kg body weight per day (BW/day) for 180 days. Mutant frequencies were determined in germ cells from the seminiferous tubules using the *lacZ* assay (n = 8 per dose group). Control and high dose groups for each time point were then sequenced to detect mutations using Duplex Sequencing (DS; n = 6 per group). The effects of aging were investigated in unexposed male mice at 3, 13-15, 25-27, and 35-37 weeks of age. There were no significant effects of BbF at 90 or 180 days using either methodology. Similarly, there were no significant increases in C:G > A:T mutations, the major mutation induced by BbF in somatic tissues. Our power analysis based on observed variation and mutation frequencies shows that a larger sample size is required to detect an effect of BbF with 80% power relative to somatic tissues. We also did not observe an age-related increase in spontaneous mutation frequency using DS; however, a significant age-dependent increase in mutant frequency was detected using the *lacZ* assay, which may be explained by an unusually low mutant frequency at 13-15 weeks relative to the historical control database. There were no significant increases in C:G > T:A mutations, the predominant age-associated mutation expected, at 35-37 weeks relative to 3 weeks; however, there was a significant age-related trend in these mutations. Overall, lack of a BbF effect may be explained by high germline DNA repair capacity or by pharmacokinetic differences between somatic and germ cell tissues (e.g.,

distribution of BbF to the germ cells and metabolic activation). Our results also suggest that older animals may be required to detect an age-related effect on mutations in male mouse germ cells.

Acknowledgments

I would to acknowledge so many incredible people who have supported me over the course of my master's and who I am deeply grateful for.

Firstly, I want to thank my two amazing supervisors, Drs. Francesco Marchetti and Carole Yauk. Prior to beginning my master's, I never thought I would be so lucky to have two remarkably supportive, insightful, and dedicated mentors who have continuously gone above and beyond to guide, challenge, and encourage me throughout my academic journey. Their expertise and feedback have allowed me to strengthen my scientific written communication and critical thinking skills. I am incredibly grateful for their determination to challenge me in ways that strengthened my weaknesses and truly shaped my growth. Thank you both for always being my biggest cheerleaders - the knowledge I have gained and the confidence I have built would not have been possible without you both.

I would also like to thank my committee members, Drs. Paul White and Iain Lambert. I am immensely grateful to have you both on my thesis advisory committee. During my masters, your insights, knowledge, and feedback have been extremely helpful and have allowed to gain a better understanding of my research. Your suggestions and input have advanced my analytical thinking skills and have strengthened this thesis.

I want to extend my gratitude to my colleagues at Health Canada. To Danielle LeBlanc and to Gu Zhou, who dedicated time to training me in the lab. I am incredibly thankful for your unwavering support, patience, and generosity; this work would have not been possible without your help. I would also like to thank Andrew Williams and Dr. Matthew Meier, for their knowledge and assistance in conducting statistical analyses for this work. To Annette Dodge, for the countless meetings on using the MutSeqR package in R software, your bioinformatics knowledge has been a tremendous help. To all five of you, I am profoundly grateful for your guidance and kindness, it has truly been invaluable to me.

I would also like to show my admiration to my peers at the University of Ottawa. To David Schuster, thank you for being an outstanding mentor who I have always been able to turn to. It has been a pleasure working alongside you, your encouragement and leadership has been greatly appreciated. To our lab technician David Eickmeyer, thank you for making the lab so warm and welcoming during my time at uOttawa. It truly made my experience enjoyable and memorable. To Geronimo Parodi-Matteo, Emmanuelle Monniez, Alper James Alcaez, Elena Esina, Hyojin Lee, Reyna Tao, Vicky Wang, and Josie Jabbour, I express my deepest gratitude for your ongoing support and compassion. I will cherish every moment we have all spent working together, I know you will all achieve amazing things throughout your studies and in your future endeavours.

I am beyond thankful for the faculty members of the Department of Biology at the University of Ottawa and Carleton University for their outstanding teaching and their dedication to creating an inspiring environment that enables students to excel academically. The convenient access to resources and graduate information was greatly appreciated. Along with the Department of Biology, I want to extend my thanks to the Biology Graduate Student's Association for their guidance and their contribution to the Biology Grad Handbook that effectively assisted me in navigating the transition from undergraduate to graduate studies.

Finally, I am so deeply grateful to my friends and family for their unwavering love, endless patience, and continuous motivation. You all believed in me even when I doubted myself and have all been instrumental in getting me here. I want to thank my sister Kaylie and my boyfriend Ryan, who have always provided me with comfort and belief during the most stressful times. Your faith in me gave me the strength I needed to overcome every challenge. To all my friends, who have been my biggest supporters along this journey and for reminding me that I am not alone, I am incredibly thankful to you all. I want to also acknowledge my uncle Luigi Lorusso, the only one in my family who understood my research and my project. Thank you for your genuine interest in my studies, it has truly been amazing having someone in the family that I could turn to for meaningful conversations. Most of all, I want to thank my parents.

Without your unconditional love and care, I would not be the person I am today. Your encouragement has truly helped me stay motivated and it is because of you that I have had the strength to achieve my goals and pursue my dreams with confidence. I hope I have made you proud.

Contents

Abstract.....	ii
Acknowledgments.....	iv
List of Tables.....	x
List of Figures.....	xi
List of Supplementary Material.....	xiii
List of Abbreviations.....	xiv
Statement of Contribution.....	xvi
Chapter One.....	1
1.1 Germ Cell Mutagenesis.....	2
1.2 Spermatogenesis.....	3
1.2.1 Experimental Variable Considerations for Germ Cell Mutagenicity Testing.....	4
1.3 “Gold standard” Transgenic Rodent Gene (TGR) Mutation Assay.....	5
1.3.1 Limitations Associated with the TGR <i>lacZ</i> Assay.....	6
1.4 Duplex Sequencing: An Innovative Approach to Mutagenicity Testing.....	8
1.5 Polycyclic Aromatic Hydrocarbons (PAHs).....	10
1.5.1 Benzo[<i>b</i>]fluoranthene (BbF).....	11
1.6 Aging in Germ Cells.....	13
1.7 Thesis Hypotheses and Objectives.....	14
1.8 References.....	16
Chapter Two.....	24
2.1 Abstract.....	26
2.2 Introduction.....	27
2.3 Materials & Methods.....	29
2.3.1 Animal Exposures and Tissue Collection.....	29
2.3.2 Transgenic Rodent Gene Mutation Assay (<i>LacZ</i> assay).....	30
2.3.3 Duplex Sequencing (DS).....	30
2.3.4 TwinStrand Mouse Mutagenesis Panel.....	31
2.3.5 Statistical Analyses.....	32
2.3.5.1 Body and Tissue Weight Analyses.....	32
2.3.5.2 TGR Analyses.....	32
2.3.5.3 DS Analyses.....	33
2.3.5.4 Power Analyses.....	33
2.4 Results.....	34
2.4.1 Top Dose Selection.....	34
2.4.2 Body and Testes Weights.....	34
2.4.3 <i>LacZ</i> Mutant Frequencies.....	36

2.4.4 DS Mutation Frequencies.....	38
2.4.5 DS Mutation Frequency by Target.....	40
2.4.6 Mutation Spectrum.....	41
2.4.7 Power Analyses.....	43
2.5 Discussion.....	43
2.6 Conclusions.....	47
2.7 References.....	48
Chapter Three.....	54
3.1 Abstract.....	56
3.2 Introduction.....	57
3.3 Materials and Methods.....	59
3.3.1 Animal and Tissue Collection.....	59
3.3.2 Transgenic Rodent Gene Mutation Assay (<i>LacZ</i> assay).....	59
3.3.3 Duplex Sequencing (DS).....	60
3.3.4 Statistical Analyses.....	61
3.3.4.1 TGR Analyses.....	61
3.3.4.2 DS Analyses.....	61
3.4 Results.....	62
3.4.1 <i>LacZ</i> Mutant Frequencies.....	62
3.4.2 DS Mutation Frequencies.....	63
3.4.3 DS Mutation Frequency by Target.....	66
3.4.4 DS Mutation Spectrum.....	67
3.5 Discussion.....	69
3.6 Conclusions.....	71
3.7 References.....	72
Chapter Four.....	78
4.1 Summary of Study Outcomes.....	79
4.2 Fulfillment of Objectives.....	80
Objective 1. Quantify the impact of BbF exposure on mutant frequency and MF in MutaMouse male germ cells.....	80
Objective 2. Measure spectral changes induced by BbF in male germ cell.....	81
Objective 3. Perform <i>lacZ</i> and DS power analyses on BbF-induced male germ cell mutant frequency and MF.....	81
Objective 4. Measure the impact of age on spontaneous mutant frequency, MF and spectrum in MutaMouse male germ cells.....	82
4.3 Contribution to Scientific Knowledge.....	82
4.3.1 BbF Does Not Induce Mutations in Mouse Germ Cells after 90-day and 180-day Exposures.....	82

4.3.2 Germ Cells Do Not Metabolically Activate BbF and/or Possess Differential Responses to DNA Damage.....	83
4.3.3 Aging Does Not Induce Mutations in 35-37-week-old Mice.....	84
4.4 Future Directions.....	84
4.4.1 Level of DNA Damage in Testis Versus Somatic Tissues.....	85
4.4.2 Different Experimental Design (e.g., 28 + 28d).....	85
4.4.3 Effects of Aging in Older Mice.....	86
4.5 Concluding Remarks.....	86
4.6 References.....	87
Appendix.....	91
Supplementary Material for Chapter Two.....	91
Supplementary Material for Chapter Three.....	102

List of Tables

Chapter Two

Table 2.1. Average *lacZ* mutant frequencies in MutaMouse male germ cells after 90 and 180 days of exposure to BbF.....38

Table 2.2. Average DS MF_{min} and MF_{max} in MutaMouse male germ cells after 90 and 180 days of exposure to BbF.....40

Table 2.3. Power analysis of *lacZ* and DS 90-day and 180-day combined datasets.....43

Chapter Three

Table 3.1. Average *lacZ* mutant frequencies in MutaMouse male germ cells at 13-15, 25-27, and 35-37 weeks.....63

Table 3.2. Average DS MF_{min} and MF_{max} in MutaMouse male germ cells at 3, 13-15, 25-27, and 35-37 weeks.....65

List of Figures

Chapter One

Figure 1.1. Spermatogonial proliferation and stem cell renewal (A_s model).....	4
Figure 1.2. Summary of TGR <i>lacZ</i> assay using MutaMouse and <i>E. coli C, lacZ-, galE-</i>	7
Figure 1.3. Summary of duplex sequencing.....	9
Figure 1.4. Metabolic activation of PAHs.....	11
Figure 1.5. Structure of benzo[<i>b</i>]fluoranthene (BbF).....	12

Chapter Two

Figure 2.1. Change in body weights and sum of testes weights of MutaMouse males exposed to BbF for 90 days (A, C) and 180 days (B, D).....	35
Figure 2.2. <i>LacZ</i> mutant frequencies in the germ cells of MutaMouse males exposed to BbF for 90 days (A) and 180 days (B).....	37
Figure 2.3. Duplex sequencing MF in germ cells of MutaMouse males in control and BbF exposed groups (N = 5 to 6 mice per dose group) at 90 days (A) and 180 days (B).....	39
Figure 2.4. DS locus-specific MF _{min} for controls and BbF-treated mice at 90 days (A) and 180 days (B).	41
Figure 2.5. Mutation spectrum in control and BbF-treated MutaMouse male germ cells quantified using DS following 90-day (A) and 180-day (B) exposures (N = 5 to 6 per dose group).....	42

Chapter Three

Figure 3.1. <i>LacZ</i> mutant frequencies in MutaMouse male germ cells at 13-15, 25-27, and 35-37 weeks.....	63
Figure 3.2. MF in MutaMouse male germs cells at 3, 13-15, 25-27, and 35-37 weeks using the MF _{min} assumption (A) and the MF _{max} assumption (B).....	65
Figure 3.3. Average MF for intergenic and genic targets using MF _{min} (A) and MF _{max} (B) assumptions at 3, 13-15, 25-27, and 35-37 weeks.....	67

Figure 3.4. DS mutation spectrum in germ cells of MutaMouse males at 3, 13-15, 25-27, and 35-37 weeks.....68

List of Supplementary Material

Chapter Two

- Supplementary Figure 2.1.** Informative duplex bases per animal for the control and BbF treated dose groups at 90 days (A) and 180 days (B).....91
- Supplementary Figure 2.2.** Top dose selection for 90-day and 180-day exposure durations.....92
- Supplementary Table 2.1.** Body weight change in MutaMouse animals after 90 days and 180 days relative to start of exposure.....93
- Supplementary Figure 2.3.** Cochran Armitage Trend Test of BbF-induced mutant frequencies at 90 days (A) and 180 days (B) using *lacZ* assay.....96
- Supplementary Table 2.2.** Historical control database of *lacZ* mutant frequencies in seminiferous tubules of control MutaMouse animals.....97
- Supplementary Figure 2.4.** Single nucleotide variant (SNV) proportions of total mutations in percent for the control and BbF treated mice at 90 days (A) and 180 days (B).....101

Chapter Three

- Supplementary Figure 3.1.** Informative duplex bases per mouse at 3, 13-15, 25-27, and 35-37 weeks.....102
- Supplementary Figure 3.2.** Cochran Armitage Trend Test of MF_{min} for C:G > T:A transitions at 3-, 13-15-, 25-27-, and 35-37-week time points.....103
- Supplementary Figure 3.3.** Trinucleotide plots at 3, 13-15, 25-27, and 35-37 weeks.....104

List of Abbreviations

BaP	Benzo[<i>a</i>]pyrene
BbF	Benzo[<i>b</i>]fluoranthene
bp	Base pairs
BW	Body weight
chr	Chromosome
CYP	Cytochrome
DCS	Duplex consensus sequence
DS	Duplex sequencing
ecNGS	Error-corrected next-generation sequencing
ED	Elongated spermatids
EL	Elongating spermatids
ENU	<i>N</i> -ethyl- <i>N</i> -nitrosourea
<i>E. coli</i>	<i>Escherichia coli</i>
GHS	Globally Harmonized System (GHS) of classification
GLM	Generalized Linear Model
GLMM	Generalized Linear Mixed Model
IARC	International Agency for Research on Cancer
MF	Mutation Frequency
MF_{max}	Mutation Frequency Maximum
MF_{min}	Mutation Frequency Minimum
MMP	Mouse Mutagenesis Panel

MNV	Multi-nucleotide variants
NER	Nucleotide excision repair
NGS	Next-generation sequencing
OECD	Organisation for Economic Co-operation and Development
PAHs	Polycyclic aromatic hydrocarbons
PCR	Polymerase Chain Reaction
PFU	Plaque forming units
P-gal	phenyl β -d-galactopyranoside
RD	Round spermatids
SEM	Standard error of the mean
SNVs	Single-nucleotide variants
SSCs	Spermatogonial stem cells
TG	Test guideline
TGR	Transgenic rodent somatic and germ cell gene mutation assay
VCF	Variant call file

Statement of Contribution

Chapter 2: Long Term Exposure to Benzo[*b*]fluoranthene Does Not Induce Mutations in MutaMouse Male Germ Cells

Authors:

Madison Stewart^{1,2}, Gu Zhou¹, Danielle P.M. LeBlanc¹, Annette E. Dodge¹, Matthew J. Meier¹, Andrew Williams¹, Alexandra S. Long³, Paul A. White¹, Carole L. Yauk^{2,*}, Francesco Marchetti^{1,4,*}

Affiliations:

¹Environmental Health Science and Research Bureau, HECSB, Health Canada, Ottawa, ON, Canada; ²Department of Biology, University of Ottawa, Ottawa, ON, Canada; ³Existing Substances Risk Assessment Bureau, HECSB, Health Canada, Ottawa, ON, Canada; ⁴Department of Biology, Carleton University, Ottawa, ON, Canada.

Study Concept and Design.....	Madison Stewart Carole L. Yauk Francesco Marchetti
Animal Study and Tissue Collection.....	Gu Zhou Danielle P.M. LeBlanc
Transgenic Rodent Gene Mutation Assay (<i>LacZ</i> assay).....	Madison Stewart
Library Preparation and Bioinformatic Processing.....	Madison Stewart Danielle P.M. LeBlanc
Data Analysis.....	Madison Stewart Annette E. Dodge Matthew J. Meier Andrew Williams
Manuscript Preparation.....	Madison Stewart Gu Zhou Danielle P.M. LeBlanc Annette E. Dodge Matthew J. Meier Andrew Williams Alexandra S. Long Paul A. White Carole L. Yauk Francesco Marchetti

Chapter 3: Aging Does Not Induce Spontaneous Mutations in Unexposed MutaMouse Male Germ Cells Spanning 3 Weeks to 37 Weeks

Authors:

Madison Stewart^{1,2}, Gu Zhou¹, Danielle P.M. LeBlanc¹, Annette E. Dodge¹, Matthew J. Meier¹, Andrew Williams¹, Carole L. Yauk^{2,*}, Francesco Marchetti^{1,3,*}

Affiliations:

¹Environmental Health Science and Research Bureau, HECSB, Health Canada, Ottawa, ON, Canada; ²Department of Biology, University of Ottawa, Ottawa, ON, Canada; ³Department of Biology, Carleton University, Ottawa, ON, Canada.

Study Concept and Design.....	Madison Stewart Carole L. Yauk Francesco Marchetti
Animal Study and Tissue Collection.....	Gu Zhou Danielle P.M. LeBlanc
Transgenic Rodent Gene Mutation Assay (<i>LacZ</i> assay).....	Madison T. Stewart
Library Preparation and Bioinformatic Processing.....	Madison T. Stewart Danielle P.M. LeBlanc
Data Analysis.....	Madison T. Stewart Annette E. Dodge Matthew J. Meier Andrew Williams
Manuscript Preparation.....	Madison T. Stewart Gu Zhou Danielle P.M. LeBlanc Annette E. Dodge Matthew J. Meier Andrew Williams Carole L. Yauk Francesco Marchetti

CHAPTER ONE

INTRODUCTION
MADISON T. STEWART

1.1 Germ Cell Mutagenesis

Mutations refer to changes in the DNA sequence of a cell. They are caused by a variety of physical and environmental factors including ionizing radiation, harmful viruses, and toxic chemicals. Mutations can also be the result of errors occurring during DNA replication, repair, and recombination leading to a variety of changes including point mutations, insertions and deletions, chromosomal aberrations, and more (Huk et al., 2015, Lagadec et al., 2012). Somatic mutations are unavoidable in normal tissues and can occur in genes that are known to be drivers of cancer (Rahal et al., 2024).

Germline mutations can lead to a wide range of adverse outcomes from embryonic death to genetic disorder in the progeny (Singer & Yauk, 2010). One mutation in a germ cell will result in a new organism carrying that mutation in every cell in its body. Thus, a germline mutation can result in a larger spectrum of disease outcomes than what would occur from a somatic mutation (Marchetti et al., 2020). According to recent estimates, up to 400,000 babies across the world every year suffer developmental disorders as a result of *de novo* mutations (Deciphering Developmental Disorders Study, 2017). In addition, even a slight increase in the mutation rate brought about by an environmental exposure can have remarkable implications at the population level (Beal et al., 2017).

Many challenges are associated with germ cell mutagenicity testing given the rarity of these mutations. Moreover, there is no clear evidence for human germ cell mutagens (Wyrobek et al., 2007). Thus, regulatory assessments are centered around the premise that decisions based on somatic cell mutation assays protect the germline; however, these approaches may fail to detect effects specific to gametes, given the many distinct features of the germline. Research involving high-throughput methods to study germline mutations is required to address data and knowledge gaps to protect the germline and future generations (Singer & Yauk, 2010).

De novo mutations, i.e., mutations present in the child but not in the parents, typically occur in the male germline (Wilson Sayres & Makova, 2011). This higher proportion of male mutations is primarily a result of cell division occurring throughout a lifetime during spermatogenesis; this contrasts with the proliferating phase of oogenesis being restricted to the fetal life. Therefore, mutations affecting the male germline are the focus of my thesis.

1.2 Spermatogenesis

Spermatogenesis is the process by which sperm are produced from spermatogonial stem cells in the seminiferous tubules of the testis (Griswold et al., 2016). This process is characterized by three distinct phases: mitosis, meiosis, and post-meiosis (Adler, 1996).

The mitotic phase of spermatogenesis consists of three types of spermatogonia including spermatogonial stem cells, proliferating spermatogonia, and differentiated spermatogonia (Figure 1.1). Before differentiating spermatogonia commit to meiosis in the mouse, there are about 10 mitotic divisions spread out over approximately two weeks (De Rooji, 2001). Meiosis also occurs over a period of around two weeks. When two meiotic divisions are completed, haploid spermatids are produced. The haploid population contains round (RD), elongating (EL), and elongated (ED) spermatids, with RD spermatids constituting the longest period of the post-meiotic phase. In the mouse, spermatids exit the testis after two weeks and complete sperm maturation while travelling through the epididymis and aggregating in the cauda awaiting ejaculation. Overall, spermatogenesis lasts roughly 35 days in the mouse from the start of meiosis to the storage of sperm in the cauda (Oakberg, 1956, Marchetti et. al, 2018a).

In the final two weeks of post-meiosis, DNA repair progressively declines. Because of the increasing loss of DNA repair and lack of DNA replication, exposures that take place during the post-meiotic phase are not appropriate for analysis of mutations in germ cells (Marchetti et al., 2018b). However, exposures that target the mitotic phase of spermatogenesis are effective in inducing germ cell mutations. This is because the mitotic phase is the only phase of spermatogenesis where there is active DNA replication and cell proliferation, which are crucial for the formation of mutations in germ cells. Given the cyclical nature of spermatogenesis, only compounds that impact spermatogonial stem cells generate a long-lasting increase in sperm mutations (Marchetti et al., 2018b).

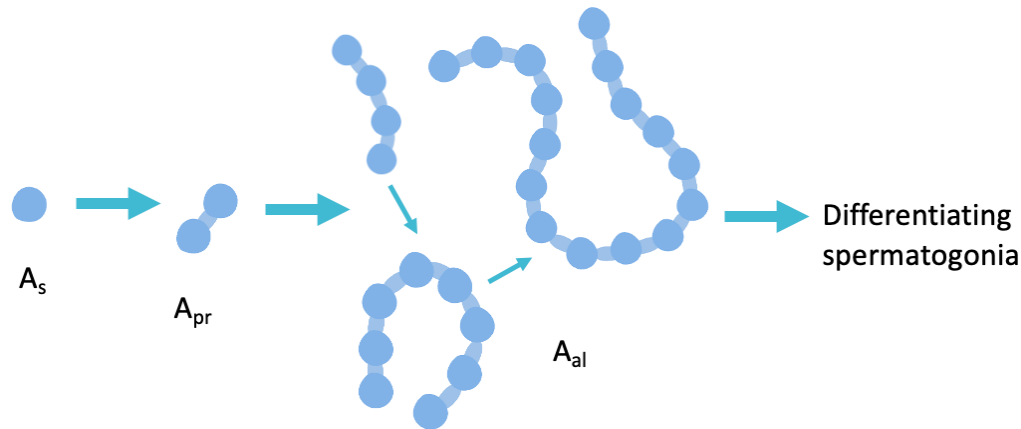


Figure 1.1. Spermatogonial proliferation and stem cell renewal (A_s model). Prior to differentiation, the population of undifferentiated spermatogonia includes single spermatogonia (A_{single} , A_s), pairs of spermatogonia (A_{paired} , A_{pr}), and chains of four, eight, or sixteen cells ($A_{aligned}$, A_{al}). The ' A_s model' implies that A_s spermatogonia are the spermatogonial stem cells (SSCs). After SSCs divide, their daughter cells either separate and form two additional SSCs or form an intercellular bridge through incomplete cytokinesis (A_{pr} spermatogonia). Afterwards, pairings can proliferate to produce clones of 4, 8, or 16 interconnected A_{al} spermatogonia. A_{al} spermatogonia commit to differentiation, completing six successive divisions before entering meiosis, and generating spermatocytes and spermatids (Figure adapted from from: De Rooji, 2001).

1.2.1 Experimental Variable Considerations for Germ Cell Mutagenicity Testing

Determining whether a chemical is a germ cell mutagen requires careful consideration of the duration of spermatogenesis when selecting the experimental design. Experimental variables that must be taken into consideration include: (a) the selection of germ cell population for analysis, (b) the administration time, and (c) the sampling time.

Effects on different phases of spermatogenesis are analyzed depending on the germ cell population or tissue sample being tested (e.g., entire testis, tubule germ cells, or sperm) (Marchetti et al., 2018b). Tubule germ cells contain approximately 2% spermatogonia, 23% spermatocytes, and 75% spermatids (Marchetti et al., 2018a). These will be the cell types tested for mutagenicity in my thesis.

The administration time determines how long target cells are exposed to the chemical being tested. The duration of the administration period can focus exposures to specific phases of spermatogenesis. The sampling time is the fixation period between end of the exposure and collection of tubule germ cells used to analyze the effects of exposure on different phases of spermatogenesis. Longer sampling times enable the investigation of effects occurring in earlier stages of sperm development (Marchetti et al., 2018b). For example, a sampling time of at least 49 days is required to demonstrate a true stem cell effect. This design provides enough time for the elimination of cells exposed at later phases of spermatogenesis (O'Brien et al., 2014). Although many studies analyzing the effects of various sampling times on different phases of spermatogenesis have been conducted, studying the effects of chronic, continuous exposure with no fixation period is uncommon. Chronic and sub-chronic exposures with no sampling times, i.e., 90 days and 180 days, respectively were employed in my study.

1.3 “Gold standard” Transgenic Rodent Gene (TGR) Mutation Assay

The current "gold standard" for in vivo mutagenicity assessment is the transgenic rodent somatic and germ cell gene (TGR) mutation assay (OECD 488, 2022). TGR models contain multiple copies of vectors containing one or two bacterial genes known as transgenes (Shwed et al., 2010). These transgenes may be easily retrieved and analyzed for mutations. The advantage of these TGR assays over bacterial and *in vitro* assays is the retention of intact metabolic and DNA repair processes since they use *in vivo* rodent models (Gingerich et al., 2014).

A test guideline on transgenic rodent somatic and germ cell gene mutation assays was adopted by the Organisation for Economic Co-operation and Development (OECD) in 2011 (updated in 2022). This guideline uses the following model systems: MutaMouse (Gossen et al., 1992, Jakubczak et al., 1996), *lacZ* plasmid mouse (Boerrigter et al., 1995), Big Blue[®] mouse and rat (Jakubczak et al., 1996, Kohler et al., 1991), and *gpt* delta mouse and rat (Nohmi et al., 1996). MutaMouse is a transgenic mouse model that contains multiple concatenated copies of a recombinant λ gt10 phage vector carrying an *Escherichia coli* (*E. coli*) *lacZ* reporter gene (Shwed et al, 2010). Using this model, mice are exposed to the toxicant via an appropriate

route. The OECD test guideline requires a 28-day administration period followed by a 28-day sampling time for male germ cells collected from the testes (OECD 488, 2022). Following exposure, germ cells are isolated from the seminiferous tubules and high molecular weight DNA extracted. Infectious λ phage particles are created by packaging transgenic inserts into empty λ phage capsids. These infectious λ phage particles are then used to infect an *E. coli* host. The infected bacteria are grown on selective media that can differentiate cells carrying a vector with wild-type *lacZ* and cells containing a vector with a mutant copy of *lacZ*. The frequency of mutant transgenes in the control and treated mice are compared to assess the mutagenic effect of the exposure on the male germline (Figure 1.2) (Gingerich et al., 2014, O'Brien et al., 2014). In my thesis, the MutaMouse model was used to determine the mutagenic potential of benzo[*b*]fluoranthene (BbF), a priority polycyclic aromatic hydrocarbon (PAH), on male germ cells.

1.3.1 Limitations Associated with the TGR *lacZ* Assay

TGR mutation assays are frequently used to produce data to inform regulatory decisions, but their utility in quantifying relative mutagen susceptibility is limited by their reliance on exogenous bacterial genes that do not accurately reflect the natural variation in sequence context, chromatin structure, and transcription status in the mammalian genome. Additionally, these assays provide little mechanistic information based on mutation type. The ability to identify mutation subtypes induced by a given chemical can reveal the mechanism behind its mutagenicity which is impractical with the TGR assay given the need to individually select and sequence several viral plaques (Beal et al., 2020). All these factors can affect mutagenesis and the frequency of detected mutations. Although the TGR assays have been useful to the regulatory community, they have shortcomings that hinder their capacity to resolve crucial aspects of mutagenesis (LeBlanc et al., 2022). Advancements in methodologies are needed to more accurately understand the impacts of chemical exposure on endogenous mammalian loci and provide information on the mechanisms of chemical action.

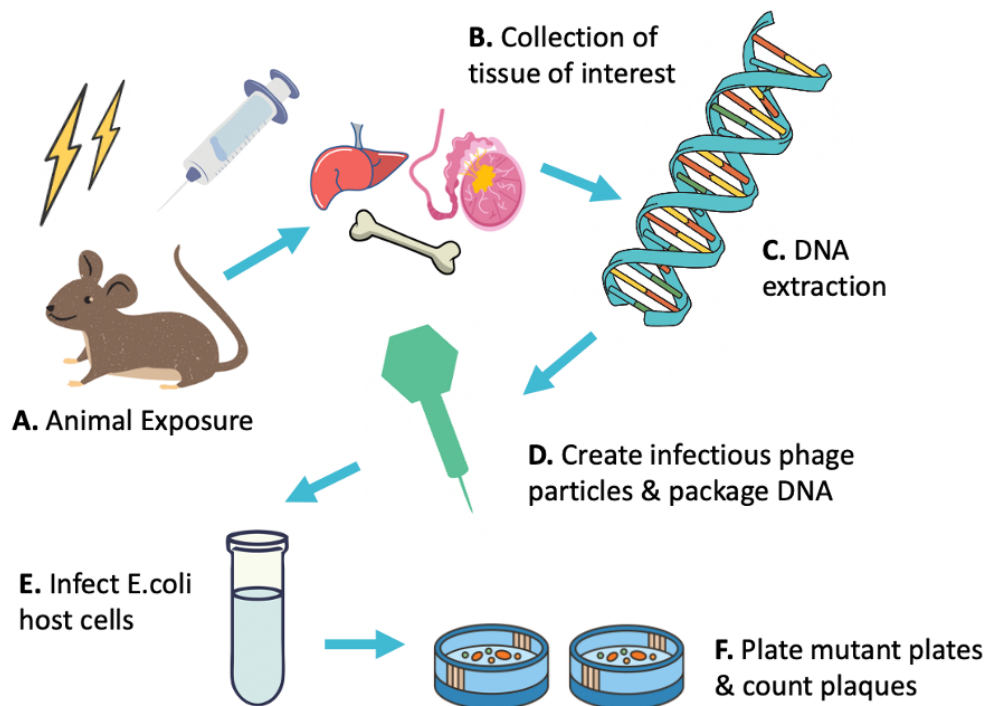


Figure 1.2. Summary of TGR *lacZ* assay using MutaMouse and *E. coli C, lacZ⁻, galE⁻*. **A.** In accordance with the OECD test guidelines, animals are treated daily over the exposure duration. **B.** After final administration, tissues are collected and frozen for storage. **C.** Frozen tissues are then used to isolate genomic DNA. **D.** Using Transpack packaging extracts, viable phages are recovered from the genomic DNA preparation (Agilent Technologies). **E.** The host cells of *E. coli C, lacZ⁻, galE⁻* are infected with the phage generated through packaging. **F.** Cells are plated on minimal agar plates with and without the selective agent, phenyl-D-galactopyranoside (p-gal). In the absence of p-gal, cells infected with both wild-type (*lacZ⁺*) and mutant phages propagate and form plaques since there is no supply of galactose. In the presence of p-gal, using their *lacZ* gene, cells infected with wild-type phages will cleave p-gal and produce galactose. Given the lack of a functional *galE* gene, host cells are unable to complete the conversion of galactose to UDP-glucose, which leads to early cell death, no phage propagation, and thus no plaque formation. Infection of host cells with a mutant phage (non-functional *lacZ* gene) will lead to plaque formation as they are unaffected by the presence of p-gal. Plaques are scored and the data are used to calculate mutant frequency after overnight incubation at 37°C. (Figure adapted from: Gingerich et al., 2014).

1.4 Duplex Sequencing: An Innovative Approach to Mutagenicity Testing

Mutations can be analyzed using next-generation sequencing (NGS) technology to determine the nucleotide change and location. The use of NGS to identify the genetic drivers of human disease is now a common approach in the clinics (Qin, 2019). However, using this technology to detect mutation induction by chemicals can be challenging because the technical error rate of standard NGS is significantly higher than the spontaneous mutation frequency (MF) of normal tissues. By using consensus-based error correction approaches, emerging technologies are increasing the accuracy of mutation detection by NGS (Salk & Kennedy, 2020).

One such error-corrected NGS (ecNGS) technology is Duplex Sequencing (DS), which can resolve spontaneous and chemically induced mutations at extremely low frequencies directly from extracted DNA (Salk et al., 2018). By uniquely barcoding, creating a consensus sequence for each strand of DNA, and reporting only mutations complementary on both strands, DS reduces sequencing-derived errors from 1 in 1000 to 1 in 10 million (Figure 1.3) (Salk et al., 2018). Because of this, DS can detect rare mutations that are caused by mutagenic exposure (LeBlanc et al., 2022, Valentine et al., 2020).

Unlike the TGR assay, DS can detect mutations in any region or target gene of interest. Variation in the type and rate of mutations has been observed across the genome due to differences in sequence context, recombination rate, replication timing, transcription status, and gene presence (LeBlanc et al., 2022). Thus, it is essential to study mutagenesis across a representative sampling of the genome. Additionally, mutation spectrum, trinucleotide mutation signatures, and expected functional implications of mutations can be derived from sequenced data (Valentine et al., 2020). Mutational signatures consider the context of the flanking nucleotides, in contrast to traditional mutation characterization, which solely describes the frequency of individual nucleotide changes (Beal et al., 2020). DS can provide information on mutation spectrum and sequence context by identifying nucleotide changes and enabling more in-depth investigations into the mechanisms of chemical action (Valentine et al., 2020).

My thesis investigated BbF mutagenicity in male mouse germ cells using DS and the TGR *lacZ* assay. I used tubules from mice collected in a parallel study examining the utility of DS to measure mutations in somatic tissues to understand the implications of exposure duration on

MF. These tissues were used to deeply characterize the germ cell mutagenicity of BbF. Specifically, tubule germ cells were collected 24 hours after continuous BbF exposure for 90 days and 180 days. Exposure durations were chosen to match repeated dose toxicity (OECD 408, 2018) and chronic toxicity (OECD 453, 2018) studies.

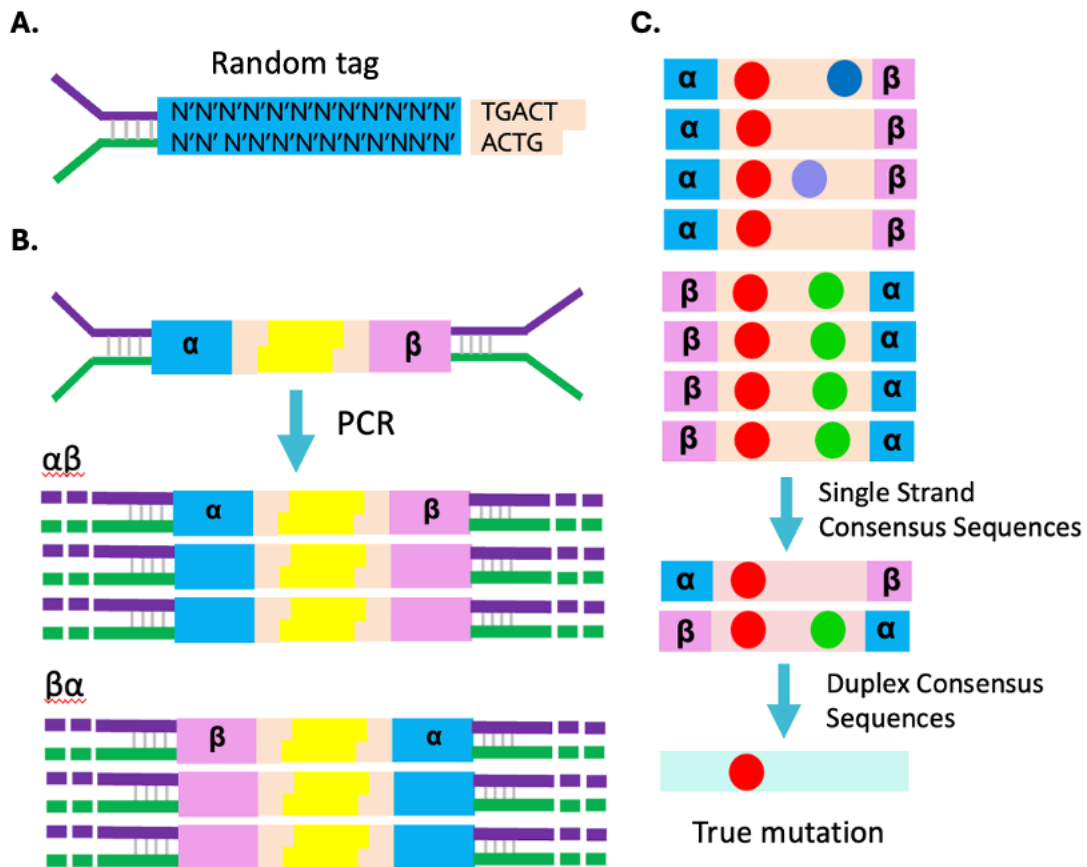


Figure 1.3. Summary of duplex sequencing. DS uses degenerate molecular tags to identify complementarity of double-stranded DNA fragments from the same original molecule. **A.** Illustration of a DS adaptor, displaying the invariant spacer sequence and random double-stranded tag. **B.** After the adaptors are ligated to the sample DNA, the molecule acquires a distinctive 12-nt tag sequence on both ends. Each strand of the DNA duplex is amplified separately by PCR, yielding two unique but related PCR products. **C.** Reads that share distinct “α” and “β” tag sequences are classified into “αβ” or “βα” tag families, and a single strand consensus sequence (SSCS) is generated for each tag family. Three mutation types are illustrated: true mutations (red dots), first-round PCR errors (green dots), and sequencing errors

(blue or purple dots). Sequencing errors are eliminated by the formation of the SSCS; however, this does not eliminate first-round PCR errors. First-round PCR errors are removed by generating a duplex consensus sequence (DCS) through comparison of SSCSs from the “αβ” and “βα” tag families. True mutations are only scored if they are located at the same position in both strands of DNA (Figure adapted from: Kennedy et al., 2014).

1.5 Polycyclic Aromatic Hydrocarbons (PAHs)

PAHs are ubiquitous organic compounds that are prevalent in the environment (Baklanov et al., 2007, Latimer & Zheng, 2003). PAHs can be present in the human diet (e.g., grilled and smoked foods), tobacco products, environmental pollution, and in numerous occupational settings (Sahoo et al., 2020). PAHs are formed through incomplete combustion processes. Due to the extensive use of fuels for industrial applications, heating and transportation, these compounds are abundant in the environment (Boström et al., 2002, Abdel-Shafy & Mansour, 2016). The International Agency for Research on Cancer (IARC) has classified numerous PAHs as carcinogenic in mammals and other vertebrates. IARC currently identifies three PAHs as probable human carcinogens (IARC Group 2A), eleven PAHs as possible human carcinogens (IARC Group 2B), and one PAH (Benzo[*a*]pyrene; BaP) as a known human carcinogen (IARC Group 1) (IARC, 2010).

For PAHs to be DNA reactive, they must undergo metabolic transformation. The main mutagenic pathway of PAH activation involves the production of DNA reactive dihydrodiol-epoxides through cytochrome P450 (CYP) isozymes and epoxide hydrolase (Figure 1.4) (Shimada, 2002, Shimada, 2004, Xue & Warshawsky). The PAH-dihydrodiol-epoxides cause mutations by generating a large DNA adduct. These adducts, if inadequately repaired, can lead to permanent DNA sequence changes (Cairns, 1998, Long et al., 2016).

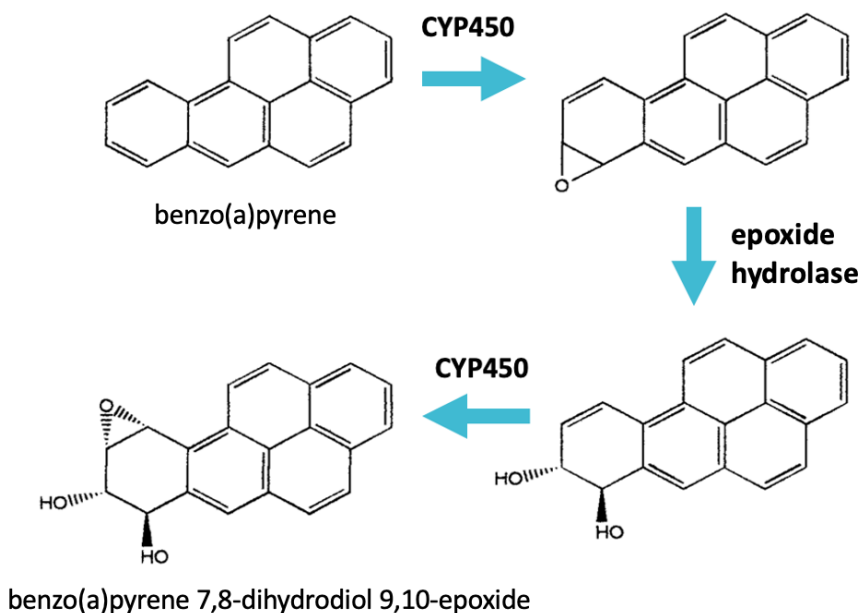


Figure 1.4. Metabolic activation of PAHs. Illustrated is the metabolism of Benzo[*a*]pyrene (BaP), the most well studied PAH. BaP is metabolized by cytochrome P450 (CYP450) and epoxide hydrolase to produce 7,8-dihydrodiol 9,10-epoxide. This dihydrodiol-epoxide is DNA-reactive and carcinogenic (Figure adapted from: Wormhoudt et al., 1999).

1.5.1 Benzo[*b*]fluoranthene (BbF)

BbF (Figure 1.5) is a priority, yet understudied, PAH that is metabolized to produce reactive epoxides through CYP450 enzymes (Amin et al., 1982, Yang, 1988, Lehr et al., 1985). BbF has been linked to serious consequences including genotoxicity, carcinogenicity, hormonal alterations, kidney damage, and reproductive disorders (Thurston et al., 2000, Tomei et al., 2006, Mass et al., 1996, Zhang et al., 2020).

Although there are no data available regarding the carcinogenicity of BbF in humans, there are adequate data to show that it is carcinogenic in mice (Wynder & Hoffmann, 1959). Consequently, BbF has been classified by IARC as a possible human carcinogen (IARC, 2010). The mutagenicity of BbF in somatic tissues is well established. Long et al. (2016) evaluated the effects of sub-chronic oral exposures of MutaMouse males to nine carcinogenic PAHs including BbF using two genotoxicity endpoints. Micronuclei were induced in peripheral blood indicating

clastogenicity, while *lacZ* transgene mutations were induced in bone marrow, glandular stroma, small intestine, liver, and lung. Bulky PAH-DNA adducts also showed dose-dependent increases in response, supporting their involvement in the observed genotoxic effects. For each endpoint, the potency of each chemical (i.e., slope of the linear region of the dose-response curve) was also determined and ranked by tissue (1 = most potent, 5 = least potent). For the *lacZ* endpoint, BbF along with 4 other PAH compounds (BaP, Benzo[*k*]fluoranthene (BkF), Indeno[1,2,3-*cd*]pyrene (IDENO), Dibenz[*a,l*]pyrene (DBaP)) demonstrated mutagenicity in all tissues analyzed. BbF exhibited the highest potency in the small intestine (rank = 1) and the lowest potency in the bone marrow (rank = 5) (Long, et al., 2016). Additionally, Schuster et al. (2024) investigated the effects of BbF after 28-day oral exposure in male mouse bone marrow and liver with DS and demonstrated strong dose-dependent mutagenic responses of BbF, with larger mutagenic responses in liver compared to bone marrow.

No study has examined the mutagenicity of BbF in germ cells. Given that BaP is an established germ cell mutagen (Beal et al., 2019, O'Brien et al., 2016) and given the strong evidence for BbF mutagenicity in somatic tissues, I hypothesized that BbF will also be a germ cell mutagen. Because of this and the widespread exposure to PAHs, it is critical to fully understand BbF-induced mutagenicity in germ cells.

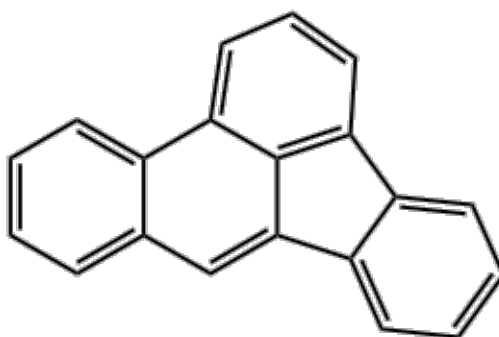


Figure 1.5. Structure of benzo[*b*]fluoranthene (BbF). BbF is an ortho- and peri-fused polycyclic arene consisting of a benzene ring fused with an acephenanthrylene ring. BbF has a chemical formula of C₂₀H₁₂ and a molecular weight of 252.3 g/mol (Figure from: National Center for Biotechnology Information, 2025).

1.6 Aging in Germ Cells

Spontaneous mutations in male germ cells increase with age and have been linked to reduced fertility and increased risk of disorders in progeny (Jenkins et al., 2014). Although SSCs exhibit one of the lowest spontaneous mutation rates among cell types (Hill et al., 2004, Xavier et al., 2018), research has demonstrated that germ cells accumulate genetic mutations with age (Aitken, 1999, Crow, 2000). In addition, *de novo* mutations can arise during gametogenesis, post-zygotically or throughout postnatal life; however, only germline *de novo* mutations present in the parental germ cells can be inherited and affect all cells in the progeny (Goldmann et al., 2019). Sequencing studies have shown a progressive increase in germline *de novo* mutations with paternal age at conception (Kong et al., 2012, Goldmann et al., 2019), which has been termed the paternal age effect (Crow, 2000, Shojaeisaadi et al., 2024). Investigating male germline mutations associated with age would allow us to better understand the paternal age effect and the implications of these mutations on future generations.

Germline *de novo* mutations are contributing factors to neurodevelopmental and psychiatric conditions including intellectual disability, autism (Turner et al., 2017), and schizophrenia (Howrigan et al., 2020). Several rare genetic disorders exhibit a higher correlation with paternal age than maternal age (Penrose, 1955). It was hypothesized that the origin of this association could be improper genome copying throughout the numerous cell divisions required for ongoing sperm cell production in males (Penrose, 1955, Crow, 2000). Research on historic population suggests that on average, late-born children have lower genetic fitness and are less likely to pursue marriage (Arslan et al., 2017, Hayward et al., 2015, Nybo Andersen & Urhoj, 2017). Moreover, in modern populations, a significant trend towards delayed parenthood is prominent, which elevates the likelihood of genetic disease. This trend is expected to significantly increase the influence of *de novo* disorders on society in the future (Goldmann et al., 2019). Thus, further research is required to better understand the effects of aging and their impact on germ cell mutagenesis.

In my thesis, the effects of aging on male mouse germ cell mutations were evaluated using the TGR *lacZ* assay and DS. Male mice of 3, 13-15, 25-27, and 35-37 weeks were assessed using

both methodologies to further our knowledge and understanding of the impact of age on the male germline.

1.7 Thesis Hypotheses and Objectives

I tested four hypotheses in this thesis.

1. Long-term exposure to BbF causes mutations in male germ cells.
2. Increased exposure duration to BbF causes increases in mutant frequency and MF in germ cells.
3. The mutation spectrum of BbF will be similar to those of other PAHs (i.e., BaP).
4. Spontaneous mutant frequency and MF in germ cells will increase with age.

To test these hypotheses, DNA was extracted from tubule germ cells of MutaMouse males exposed to five doses of BbF plus controls for 90 or 180 days. The TGR assay was used to calculate *lacZ* mutant frequency. DS was then performed to determine MF in the control and high dose groups for the 90- and 180-day time points. A panel of twenty 2.4 kb genomic targets was sequenced using this technology. DNA was also extracted from tubule germ cells of unexposed male mice of different ages (3, 13-15, 25-27, and 35-37 weeks) and the *lacZ* assay and DS were performed.

There are four objectives in my thesis.

1. **Quantify the impact of BbF exposure on MutaMouse male germ cell mutant frequency and MF.** Mutant frequency and MF in tubule germ cells of MutaMouse males exposed to BbF alongside controls were quantified using the *lacZ* assay and DS, respectively. Mutant frequency and MF observed from BbF exposure in somatic cells was compared to germ cell effects.
2. **Measure spectral changes induced by BbF in male germ cell.** Mutation spectrum was characterized using DS. The spectrum was compared to that observed in BbF- exposed somatic tissues and to the spectrum of BaP. These

spectra were used to determine if there are mechanistically unique effects occurring in germ cells exposed to BbF.

- 3. Perform *lacZ* and DS power analyses on BbF-induced male germ cell mutant frequency and MF.** The empirical data was used to determine what effect size we were powered to detect with our study design and endpoints.
- 4. Measure the impact of age on spontaneous mutant frequency, MF, and spectrum in MutaMouse male germ cells.** Mutant frequency and MF in tubule germ cells of unexposed MutaMouse males at different ages (3, 13-15, 25-27, and 35-37 weeks) were measured using the *lacZ* assay and DS, respectively to determine whether spontaneous mutations increase with age. Spectrum obtained using DS was also analyzed to observe any shift in mutations with age.

1.8 References

- Abdel-Shafy, H. I., & Mansour, M. S. M. (2016). A review on polycyclic aromatic hydrocarbons: Source, environmental impact, effect on human health and remediation. *Egyptian Journal of Petroleum*, 25(1), 107–123. <https://doi.org/10.1016/j.ejpe.2015.03.011>
- Adler, I.-D. (1996). Comparison of the duration of spermatogenesis between male rodents and humans. *Mutation Research/Fundamental and Molecular Mechanisms of Mutagenesis*, 352(1–2), 169–172. [https://doi.org/10.1016/0027-5107\(95\)00223-5](https://doi.org/10.1016/0027-5107(95)00223-5)
- Aitken, R. J. (1999). The Amoroso Lecture The human spermatozoon—A cell in crisis? *Reproduction*, 115(1), 1–7. <https://doi.org/10.1530/jrf.0.1150001>
- Amin, S., LaVoie, E. J., & Hecht, S. S. (1982). Identification of metabolites of benzo[b]fluoranthene. *Carcinogenesis*, 3(2), 171–174. <https://doi.org/10.1093/carcin/3.2.171>
- Arslan, R. C., Willführ, K. P., Frans, E. M., Verweij, K. J. H., Bürkner, P.-C., Myrskylä, M., Volland, E., Almqvist, C., Zietsch, B. P., & Penke, L. (2017). Older fathers' children have lower evolutionary fitness across four centuries and in four populations. *Proceedings of the Royal Society B: Biological Sciences*, 284(1862), 20171562. <https://doi.org/10.1098/rspb.2017.1562>
- Baklanov, A., Hänninen, O., Slørdal, L. H., Kukkonen, J., Bjergene, N., Fay, B., Finardi, S., Hoe, S. C., Jantunen, M., Karppinen, A., Rasmussen, A., Skouloudis, A., Sokhi, R. S., Sørensen, J. H., & Ødegaard, V. (2007). Integrated systems for forecasting urban meteorology, air pollution and population exposure. *Atmospheric Chemistry and Physics*, 7(3), 855–874. <https://doi.org/10.5194/acp-7-855-2007>
- Beal, M. A., Gagné, R., Williams, A., Marchetti, F., & Yauk, C. L. (2015). Characterizing Benzo[a]pyrene-induced lacZ mutation spectrum in transgenic mice using next-generation sequencing. *BMC Genomics*, 16(1), 812. <https://doi.org/10.1186/s12864-015-2004-4>
- Beal, M. A., Meier, M. J., LeBlanc, D. P., Maurice, C., O'Brien, J. M., Yauk, C. L., & Marchetti, F. (2020a). Chemically induced mutations in a MutaMouse reporter gene inform mechanisms underlying human cancer mutational signatures. *Communications Biology*, 3(1), 438. <https://doi.org/10.1038/s42003-020-01174-y>
- Beal, M. A., Meier, M. J., LeBlanc, D. P., Maurice, C., O'Brien, J. M., Yauk, C. L., & Marchetti, F. (2020b). Chemically induced mutations in a MutaMouse reporter gene inform mechanisms underlying human cancer mutational signatures. *Communications Biology*, 3(1), 438. <https://doi.org/10.1038/s42003-020-01174-y>
- Beal, M. A., Yauk, C. L., & Marchetti, F. (2017). From sperm to offspring: Assessing the heritable genetic consequences of paternal smoking and potential public health impacts. *Mutation*

Research/Reviews in Mutation Research, 773, 26–50.

<https://doi.org/10.1016/j.mrrev.2017.04.001>

Boerrigter, M. E. T. I., Dollé, M. E. T., Martus, H.-J., Gossen, J. A., & Vijg, J. (1995). Plasmid-based transgenic mouse model for studying in vivomutations. *Nature*, 377(6550), 657–659.

<https://doi.org/10.1038/377657a0>

Boström, C.-E., Gerde, P., Hanberg, A., Jernström, B., Johansson, C., Kyrklund, T., Rannug, A., Törnqvist, M., Victorin, K., & Westerholm, R. (2002). Cancer risk assessment, indicators, and guidelines for polycyclic aromatic hydrocarbons in the ambient air. *Environmental Health Perspectives*, 110(suppl 3), 451–488. <https://doi.org/10.1289/ehp.110-1241197>

Cairns, J. (1998). Mutation and Cancer: The Antecedents to Our Studies of Adaptive Mutation. *Genetics*, 148(4), 1433–1440. <https://doi.org/10.1093/genetics/148.4.1433>

Crow, J. F. (2000). The origins, patterns and implications of human spontaneous mutation. *Nature Reviews Genetics*, 1(1), 40–47. <https://doi.org/10.1038/35049558>

Qin, D. (2019). Next-generation sequencing and its clinical application. *Cancer Biology & Medicine*, 16(1), 4–10. <https://doi.org/10.20892/j.issn.2095-3941.2018.0055>

De Rooij, D. (2001). Proliferation and differentiation of spermatogonial stem cells. *Reproduction*, 121(3), 347–354. <https://doi.org/10.1530/rep.0.1210347>

Deciphering Developmental Disorders Study. (2017). Prevalence and architecture of de novo mutations in developmental disorders. *Nature*, 542, 433–438.

Gingerich, J. D., Soper, L., Lemieux, C. L., Marchetti, F., & Douglas, G. R. (2014). Transgenic Rodent Gene Mutation Assay in Somatic Tissues. In L. M. Sierra & I. Gaivão (Eds.), *Genotoxicity and DNA Repair* (pp. 305–321). Springer New York. https://doi.org/10.1007/978-1-4939-1068-7_18

Goldmann, J. M., Veltman, J. A., & Gilissen, C. (2019). De Novo Mutations Reflect Development and Aging of the Human Germline. *Trends in Genetics*, 35(11), 828–839.

<https://doi.org/10.1016/j.tig.2019.08.005>

Gossen, J. A., Molijn, A. C., Douglas, G. R., & Vijg, J. (1992). Application of galactose-sensitive *E.coli* strains as selective hosts for *LacZ*⁻ plasmids. *Nucleic Acids Research*, 20(12), 3254–3254.

<https://doi.org/10.1093/nar/20.12.3254>

Griswold, M. D. (2016). Spermatogenesis: The Commitment to Meiosis. *Physiological Reviews*, 96(1), 1–17. <https://doi.org/10.1152/physrev.00013.2015>

Hayward, A. D., Lummaa, V., & Bazykin, G. A. (2015). Fitness Consequences of Advanced

Ancestral Age over Three Generations in Humans. *PLOS ONE*, 10(6), e0128197.
<https://doi.org/10.1371/journal.pone.0128197>

Hill, K. A., Buettner, V. L., Halangoda, A., Kunishige, M., Moore, S. R., Longmate, J., Scaringe, W. A., & Sommer, S. S. (2004). Spontaneous mutation in Big Blue® mice from fetus to old age: Tissue-specific time courses of mutation frequency but similar mutation types. *Environmental and Molecular Mutagenesis*, 43(2), 110–120. <https://doi.org/10.1002/em.20004>

Howrigan, D. P., Rose, S. A., Samocha, K. E., Fromer, M., Cerrato, F., Chen, W. J., Churchhouse, C., Chambert, K., Chandler, S. D., Daly, M. J., Dumont, A., Genovese, G., Hwu, H.-G., Laird, N., Kosmicki, J. A., Moran, J. L., Roe, C., Singh, T., Wang, S.-H., ... Neale, B. M. (2020). Exome sequencing in schizophrenia-affected parent–offspring trios reveals risk conferred by protein-coding de novo mutations. *Nature Neuroscience*, 23(2), 185–193.
<https://doi.org/10.1038/s41593-019-0564-3>

Huk, A., Izak-Nau, E., El Yamani, N., Uggerud, H., Vadset, M., Zasonska, B., Duschl, A., & Dusinska, M. (2015). Impact of nanosilver on various DNA lesions and HPRT gene mutations – effects of charge and surface coating. *Particle and Fibre Toxicology*, 12(1), 25.
<https://doi.org/10.1186/s12989-015-0100-x>

IARC (2010) Some non-heterocyclic polycyclic aromatic hydrocarbons and some related exposures. *IARC Monographs on the Evaluation of Carcinogenic Risks to Humans*, 92. International Agency for Research on Cancer, Lyon.

Jakubczak, J. L., Merlino, G., French, J. E., Muller, W. J., Paul, B., Adhya, S., & Garges, S. (1996). Analysis of genetic instability during mammary tumor progression using a novel selection-based assay for in vivo mutations in a bacteriophage lambda transgene target. *Proceedings of the National Academy of Sciences*, 93(17), 9073–9078. <https://doi.org/10.1073/pnas.93.17.9073>

Jenkins, T. G., Aston, K. I., Pflueger, C., Cairns, B. R., & Carrell, D. T. (2014). Age-Associated Sperm DNA Methylation Alterations: Possible Implications in Offspring Disease Susceptibility. *PLoS Genetics*, 10(7), e1004458. <https://doi.org/10.1371/journal.pgen.1004458>

Kennedy, S. R., Schmitt, M. W., Fox, E. J., Kohn, B. F., Salk, J. J., Ahn, E. H., Prindle, M. J., Kuong, K. J., Shen, J.-C., Risques, R.-A., & Loeb, L. A. (2014). Detecting ultralow-frequency mutations by Duplex Sequencing. *Nature Protocols*, 9(11), 2586–2606.
<https://doi.org/10.1038/nprot.2014.170>

Kohler, S. W., Provost, G. S., Fieck, A., Kretz, P. L., Bullock, W. O., Putman, D. L., Sorge, J. A., & Short, J. M. (1991). Analysis of spontaneous and induced mutations in transgenic mice using a lambda ZAP/ *lacI* shuttle vector. *Environmental and Molecular Mutagenesis*, 18(4), 316–321.
<https://doi.org/10.1002/em.2850180421>

Kong, A., Frigge, M. L., Masson, G., Besenbacher, S., Sulem, P., Magnusson, G., Gudjonsson, S. A., Sigurdsson, A., Jonasdottir, A., Jonasdottir, A., Wong, W. S. W., Sigurdsson, G., Walters, G. B., Steinberg, S., Helgason, H., Thorleifsson, G., Gudbjartsson, D. F., Helgason, A., Magnusson, O. Th., ... Stefansson, K. (2012). Rate of de novo mutations and the importance of father's age to disease risk. *Nature*, *488*(7412), 471–475. <https://doi.org/10.1038/nature11396>

Lagadec, C., Vlashi, E., Della Donna, L., Dekmezian, C., & Pajonk, F. (2012). Radiation-Induced Reprogramming of Breast Cancer Cells. *STEM CELLS*, *30*(5), 833–844. <https://doi.org/10.1002/stem.1058>

Latimer, J. S., & Zheng, J. (2003). The Sources, Transport, and Fate of PAHs in the Marine Environment. In P. E. T. Douben (Ed.), *PAHs: An Ecotoxicological Perspective* (1st ed., pp. 7–33). Wiley. <https://doi.org/10.1002/0470867132.ch2>

LeBlanc, D. P. M., Meier, M., Lo, F. Y., Schmidt, E., Valentine, C., Williams, A., Salk, J. J., Yauk, C. L., & Marchetti, F. (2022). Duplex sequencing identifies genomic features that determine susceptibility to benzo(a)pyrene-induced in vivo mutations. *BMC Genomics*, *23*(1), 542. <https://doi.org/10.1186/s12864-022-08752-w>

Lehr, R. E., Kumar, S., Levin, W., Wood, A. W., Chang, R. L., Conney, A. H., Yagi, H., Sayer, J. M., & Jerina, D. M. (1985). The Bay Region Theory of Polycyclic Aromatic Hydrocarbon Carcinogenesis. *American Chemical Society*, *283*, 63–84.

Long, A. S., Lemieux, C. L., Arlt, V. M., & White, P. A. (2016). Tissue-specific in vivo genetic toxicity of nine polycyclic aromatic hydrocarbons assessed using the Muta™ Mouse transgenic rodent assay. *Toxicology and Applied Pharmacology*, *290*, 31–42. <https://doi.org/10.1016/j.taap.2015.11.010>

Marchetti, F., Aardema, M., Beevers, C., Van Benthem, J., Douglas, G. R., Godschalk, R., Yauk, C. L., Young, R., & Williams, A. (2018). Simulation of mouse and rat spermatogenesis to inform genotoxicity testing using OECD test guideline 488. *Mutation Research/Genetic Toxicology and Environmental Mutagenesis*, *832–833*, 19–28. <https://doi.org/10.1016/j.mrgentox.2018.05.020>

Marchetti, F., Aardema, M. J., Beevers, C., Van Benthem, J., Godschalk, R., Williams, A., Yauk, C. L., Young, R., & Douglas, G. R. (2018). Identifying germ cell mutagens using OECD test guideline 488 (transgenic rodent somatic and germ cell gene mutation assays) and integration with somatic cell testing. *Mutation Research/Genetic Toxicology and Environmental Mutagenesis*, *832–833*, 7–18. <https://doi.org/10.1016/j.mrgentox.2018.05.021>

Marchetti, F., & Wyrobek, A. J. (2008). DNA repair decline during mouse spermiogenesis results in the accumulation of heritable DNA damage. *DNA Repair*, *7*(4), 572–581. <https://doi.org/10.1016/j.dnarep.2007.12.011>

Mass, M. J., Ross, J. A., Nesnow, S., Jeffers, A. J., Nelson, G., Galati, A. J., & Stoner, G. D. (1993). Ki-*ras* oncogene mutations in tumors and DNA adducts formed by benz[*j*]aceanthrylene and benzo[*a*]pyrene in the lungs of strain A/J mice. *Molecular Carcinogenesis*, 8(3), 186–192. <https://doi.org/10.1002/mc.2940080309>

National Center for Biotechnology Information (2025). PubChem Compound Summary for CID 9153, Benzo(B)Fluoranthene. Retrieved on January 16 from [https://pubchem.ncbi.nlm.nih.gov/compound/Benzo B Fluoranthene](https://pubchem.ncbi.nlm.nih.gov/compound/Benzo_B_Fluoranthene)

Nohmi, T., Kato, M., Suzuki, H., Matsui, M., Yamada, M., Watanabe, M., Suzuki, M., Horiya, N., Ueda, O., Shibuya, T., Ikeda, H., & Sofuni, T. (1996). Other transgenic mutation assays: A new transgenic mouse mutagenesis test system using Spi⁻ and 6-thioguanine selections. *Environmental and Molecular Mutagenesis*, 28(4), 465–470. [https://doi.org/10.1002/\(SICI\)1098-2280\(1996\)28:4<465::AID-EM24>3.0.CO;2-C](https://doi.org/10.1002/(SICI)1098-2280(1996)28:4<465::AID-EM24>3.0.CO;2-C)

Nybo Andersen, A.-M., & Urhoj, S. K. (2017). Is advanced paternal age a health risk for the offspring? *Fertility and Sterility*, 107(2), 312–318. <https://doi.org/10.1016/j.fertnstert.2016.12.019>

Oakberg, E. F. (1956). Duration of spermatogenesis in the mouse and timing of stages of the cycle of the seminiferous epithelium. *American Journal of Anatomy*, 99(3), 507–516. <https://doi.org/10.1002/aja.1000990307>

O'Brien, J. M., Beal, M. A., Gingerich, J. D., Soper, L., Douglas, G. R., Yauk, C. L., & Marchetti, F. (2014). Transgenic Rodent Assay for Quantifying Male Germ Cell Mutant Frequency. *Journal of Visualized Experiments*, 90, 51576. <https://doi.org/10.3791/51576-v>

O'Brien, J. M., Beal, M. A., Yauk, C. L., & Marchetti, F. (2016). Next generation sequencing of benzo(a)pyrene-induced lacZ mutants identifies a germ cell-specific mutation spectrum. *Scientific Reports*, 6(1), 36743. <https://doi.org/10.1038/srep36743>

OECD (2018) Test No. 408. Repeated dose 90-day oral toxicity study in rodents. *OECD guidelines for the testing of chemicals*, section 4. OECD Publishing, Paris.

OECD (2018) Test No. 453. Combined chronic toxicity/carcinogenicity studies. *OECD guidelines for the testing of chemicals*, section 4. OECD Publishing, Paris.

OECD (2022) Test No. 488. Transgenic rodent somatic and germ cell gene mutation assay. *OECD guidelines for the testing of chemicals*, section 4. OECD Publishing, Paris.

Penrose, L. (1955). PARENTAL AGE AND MUTATION. *The Lancet*, 266(6885), 312–313. [https://doi.org/10.1016/S0140-6736\(55\)92305-9](https://doi.org/10.1016/S0140-6736(55)92305-9)

Pepling, M. E. (2006). From primordial germ cell to primordial follicle: Mammalian female germ cell development. *Genesis*, 44(12), 622–632. <https://doi.org/10.1002/dvg.20258>

Sahoo, B. M., Ravi Kumar, B. V. V., Banik, B. K., & Borah, P. (2020). Polyaromatic Hydrocarbons (PAHs): Structures, Synthesis and their Biological Profile. *Current Organic Synthesis*, 17(8), 625–640. <https://doi.org/10.2174/1570179417666200713182441>

Salk, J. J., & Kennedy, S. R. (2020). Next-Generation Genotoxicology: Using Modern Sequencing Technologies to Assess Somatic Mutagenesis and Cancer Risk. *Environmental and Molecular Mutagenesis*, 61(1), 135–151. <https://doi.org/10.1002/em.22342>

Salk, J. J., Schmitt, M. W., & Loeb, L. A. (2018). Enhancing the accuracy of next-generation sequencing for detecting rare and subclonal mutations. *Nature Reviews Genetics*, 19(5), 269–285. <https://doi.org/10.1038/nrg.2017.117>

Schuster, D. M., LeBlanc, D. P. M., Zhou, G., Meier, M. J., Dodge, A. E., White, P. A., Long, A. S., Williams, A., Hobbs, C., Diesing, A., Smith-Roe, S. L., Salk, J. J., Marchetti, F., & Yauk, C. L. (2024). Dose-Related Mutagenic and Clastogenic Effects of Benzo[*b*]fluoranthene in Mouse Somatic Tissues Detected by Duplex Sequencing and the Micronucleus Assay. *Environmental Science & Technology*, 58(49), 21450–21463. <https://doi.org/10.1021/acs.est.4c07236>

Shimada, T. (2002). Arylhydrocarbon receptor-dependent induction of liver and lung cytochromes P450 1A1, 1A2, and 1B1 by polycyclic aromatic hydrocarbons and polychlorinated biphenyls in genetically engineered C57BL/6J mice. *Carcinogenesis*, 23(7), 1199–1207. <https://doi.org/10.1093/carcin/23.7.1199>

Shimada, T., & Fujii-Kuriyama, Y. (2004). Metabolic activation of polycyclic aromatic hydrocarbons to carcinogens by cytochromes P450 1A1 and 1B1. *Cancer Science*, 95(1), 1–6. <https://doi.org/10.1111/j.1349-7006.2004.tb03162.x>

Shojaeisaadi, H., Schoenrock, A., Meier, M. J., Williams, A., Norris, J. M., Palmer, N. D., Yauk, C. L., & Marchetti, F. (2024). Mutational signature analyses in multi-child families reveal sources of age-related increases in human germline mutations. *Communications Biology*, 7(1), 1451. <https://doi.org/10.1038/s42003-024-07140-2>

Shwed, P. S., Crosthwait, J., Douglas, G. R., & Seligy, V. L. (2010). Characterisation of MutaTMMouse *gt10-lacZ* transgene: Evidence for in vivo rearrangements. *Mutagenesis*, 25(6), 609–616. <https://doi.org/10.1093/mutage/geq048>

Thurston, S. W., Ryan, L., Christiani, D. C., Snow, R., Carlson, J., You, L., Cui, S., Ma, G., Wang, L., Huang, Y., & Xu, X. (2000). Petrochemical exposure and menstrual disturbances. *American Journal of Industrial Medicine*, 38(5), 555–564. [https://doi.org/10.1002/1097-0274\(200011\)38:5<555::AID-AJIM8>3.0.CO;2-E](https://doi.org/10.1002/1097-0274(200011)38:5<555::AID-AJIM8>3.0.CO;2-E)

- Tomei, G., Ciarrocca, M., Fortunato, B. R., Capozzella, A., Rosati, M. V., Cerratti, D., Tomao, E., Anzelmo, V., Monti, C., & Tomei, F. (2006). Exposure to traffic pollutants and effects on 17- β -estradiol (E2) in female workers. *International Archives of Occupational and Environmental Health*, 80(1), 70–77. <https://doi.org/10.1007/s00420-006-0105-8>
- Turner, T. N., Coe, B. P., Dickel, D. E., Hoekzema, K., Nelson, B. J., Zody, M. C., Kronenberg, Z. N., Hormozdiari, F., Raja, A., Pennacchio, L. A., Darnell, R. B., & Eichler, E. E. (2017). Genomic Patterns of De Novo Mutation in Simplex Autism. *Cell*, 171(3), 710-722.e12. <https://doi.org/10.1016/j.cell.2017.08.047>
- Rahal, Z., Scheet, P., & Kadara, H. (2024). Somatic Mutations in Normal Tissues: Calm before the Storm. *Cancer Discovery*, 14(4), 605–609. <https://doi.org/10.1158/2159-8290.CD-23-1508>
- Valentine, C. C., Young, R. R., Fielden, M. R., Kulkarni, R., Williams, L. N., Li, T., Minocherhomji, S., & Salk, J. J. (2020). Direct quantification of in vivo mutagenesis and carcinogenesis using duplex sequencing. *Proceedings of the National Academy of Sciences*, 117(52), 33414–33425. <https://doi.org/10.1073/pnas.2013724117>
- Wilson Sayres, M. A., & Makova, K. D. (2011). Genome analyses substantiate male mutation bias in many species. *BioEssays*, 33(12), 938–945. <https://doi.org/10.1002/bies.201100091>
- Wormhoudt, L. W., Commandeur, J. N. M., & Vermeulen, N. P. E. (1999). Genetic Polymorphisms of Human N -Acetyltransferase, Cytochrome P450, Glutathione-S-Transferase, and Epoxide Hydrolase Enzymes: Relevance to Xenobiotic Metabolism and Toxicity. *Critical Reviews in Toxicology*, 29(1), 59–124. <https://doi.org/10.1080/10408449991349186>
- Wynder, E. L., & Hoffmann, D. (1959). A study of tobacco carcinogenesis.VII. The role of higher polycyclic hydrocarbons. *Cancer*, 12(6), 1079–1086. [https://doi.org/10.1002/1097-0142\(195911/12\)12:6<1079::AID-CNCR2820120604>3.0.CO;2-I](https://doi.org/10.1002/1097-0142(195911/12)12:6<1079::AID-CNCR2820120604>3.0.CO;2-I)
- Wyrobek, A. J., Mulvihill, J. J., Wassom, J. S., Malling, H. V., Shelby, M. D., Lewis, S. E., Witt, K. L., Preston, R. J., Perreault, S. D., Allen, J. W., DeMarini, D. M., Woychik, R. P., Bishop, J. B., & Workshop Presenters. (2007). Assessing human germ-cell mutagenesis in the Postgenome Era: A celebration of the legacy of William Lawson (Bill) Russell. *Environmental and Molecular Mutagenesis*, 48(2), 71–95. <https://doi.org/10.1002/em.20284>
- Xavier, M. J., Mitchell, L. A., McEwan, K. E., Scott, R. J., & Aitken, R. J. (2018). Genomic integrity in the male germ line: Evidence in support of the disposable soma hypothesis. *Reproduction*, 156(3), 269–282. <https://doi.org/10.1530/REP-18-0202>
- Xue, W., & Warshawsky, D. (2005). Metabolic activation of polycyclic and heterocyclic aromatic hydrocarbons and DNA damage: A review. *Toxicology and Applied Pharmacology*, 206(1), 73–93. <https://doi.org/10.1016/j.taap.2004.11.006>

Yang, S. K. (1988). Stereoselectivity of cytochrome P-450 isozymes and epoxide hydrolase in the metabolism of polycyclic aromatic hydrocarbons. *Biochemical Pharmacology*, 37(1), 61–70. [https://doi.org/10.1016/0006-2952\(88\)90755-1](https://doi.org/10.1016/0006-2952(88)90755-1)

Zhang, Y., Liu, D., & Liu, Z. (2020). The benzo[b]fluoranthene in the atmospheric fine particulate matter induces mouse glomerular podocytes injury via inhibition of autophagy. *Ecotoxicology and Environmental Safety*, 195, 110403. <https://doi.org/10.1016/j.ecoenv.2020.110403>

CHAPTER TWO

DATA CHAPTER
MADISON T. STEWART

Long Term Exposure to Benzo[*b*]fluoranthene Does Not Induce Mutations in MutaMouse Male Germ Cells[#]

Madison T. Stewart^{1,2}, Gu Zhou¹, Danielle P.M. LeBlanc¹, Annette E. Dodge¹, Matthew J. Meier¹, Andrew Williams¹, Alexandra S. Long³, Paul A. White^{1,2}, Carole L. Yauk^{2,*}, Francesco Marchetti^{1,4,*}

¹Environmental Health Science and Research Bureau, HECSB, Health Canada, Ottawa, ON, Canada; ²Department of Biology, University of Ottawa, Ottawa, ON, Canada; ³Existing Substances Risk Assessment Bureau, HECSB, Health Canada, Ottawa, ON, Canada; ⁴Department of Biology, Carleton University, Ottawa, ON, Canada.

* Correspondence to: carole.yauk@uottawa.ca and Francesco.marchetti@hc-sc.gc.ca

[#]Manuscript in the process of being submitted to Mutagenesis

2.1 Abstract

Mutations in germ cells can be passed down to the offspring and lead to genetic disorders. Thus, it is critical to identify environmental exposures that impact the germline. Polycyclic aromatic hydrocarbons (PAHs) are widespread combustion by-products that are present in food, tobacco smoke, and urban air. Benzo[*b*]fluoranthene (BbF) is a PAH that is classified as a possible human carcinogen. Previous studies have demonstrated that BbF robustly induces mutations in somatic tissues using the *lacZ* assay in transgenic rodents and duplex sequencing (DS), an error-corrected next generation sequencing technology. However, the effects of BbF on germ cells are unknown. We investigated whether long-term exposure to BbF induces mutations in male germ cells. Adult MutaMouse males were exposed orally to BbF dissolved in olive oil at doses of 0, 3.25, 6.25, 12.5, 25, or 50 mg/kg body weight per day (BW/day) for 90 days, or to 0, 1.56, 3.125, 6.25, 12.5, or 25 mg/kg BW/day for 180 days. Mutant frequencies were determined using the *lacZ* assay ($n = 8$ per group). Control and high dose groups for each time point were then sequenced to detect mutations using DS ($n = 6$ per group). There were no significant increases in mutations following BbF exposure using either methodology. Similarly, there were no increases in C:G > A:T transversions at either time point, the main mutation subtype induced by BbF in somatic tissues. Overall, our results suggest that either BbF or its active metabolites are not reaching the seminiferous tubules in amounts sufficient to cause mutations, and/or that DNA damage response pathways are effectively repairing BbF-induced damage in germ cells.

Keywords: Germ cells, Transgenic rodent gene mutation assay, *lacZ* assay, Duplex sequencing, Mutation frequency, Mutation spectrum

2.2 Introduction

Mutations in the germline have been linked to decreased fertility and, if transmitted to offspring, increased susceptibility to cancer or other genetic diseases (1). Numerous environmental exposures cause germ cell mutations in rodents, and accumulating evidence suggests that some of these factors may also impact the human germline (2). Interest in the identification and characterization of human germ cell mutagens has been reignited in the wake of promising technological developments that allow direct detection of germline and inherited *de novo* mutations (3,4). Furthermore, the Globally Harmonized System (GHS) of classification and labelling considers germ cell mutagenicity a health risk (5), emphasizing that the assessment of both somatic tissue and germ cell mutagenicity is necessary (6).

Polycyclic aromatic hydrocarbons (PAHs) are widespread organic compounds that are abundant in the environment (7,8). PAHs are created during incomplete combustion processes and have been recognized as hazardous due to the widespread use of fuels for industrial applications, heating, and transportation (9,10). PAHs are also found in the human diet (e.g., grilled and smoked foods), tobacco products, contaminated air, water and soil, and in a variety of occupational settings (11). Humans are exposed to PAHs chronically during their lifetime, which can lead to a variety of adverse health effects including cancer in different tissues (12,13,14). In mammals and other vertebrates, several PAHs are mutagens and are classified as carcinogens by the International Agency for Research on Cancer (IARC). Currently, IARC recognizes eleven PAHs as possible human carcinogens (IARC Group 2B), three PAHs as probable human carcinogens (IARC Group 2A), and one PAH, benzo[*a*]pyrene (BaP), as a known human carcinogen (IARC Group 1) (15).

PAHs must undergo metabolic transformation to be DNA reactive and this occurs predominantly in the liver. Metabolism by cytochrome P450 (CYP450) isozymes and epoxide hydrolase produces DNA-reactive dihydrodiol-epoxides. This is the main pathway through which PAHs are converted to mutagenic compounds (16,17,18). PAH-dihydrodiol-epoxides cause bulky DNA adducts that, if improperly repaired, can lead to mutations (19,20). Benzo[*b*]fluoranthene (BbF) is an understudied PAH that is metabolized by CYP450 enzymes leading to the production of reactive epoxides (25,26,27). BbF has been linked to reproductive disorders, hormonal

alterations, carcinogenicity, genotoxicity, and kidney damage (21,22,23,24). Although there are no carcinogenicity data in humans, BbF is classified as a possible human carcinogen (Group 2B) (15) because of substantial evidence of carcinogenicity in mice (28). Previous studies have demonstrated strong, dose-dependent mutagenic effects of 28-day oral exposures to BbF in male mouse somatic tissues (20,29); however, the mutagenic effects of BbF in germ cells are unknown.

The gold standard assay for evaluating mutagenicity *in vivo* is the transgenic rodent gene (TGR) mutation assay described in the Organisation for Economic Co-operation Development (OECD) test guideline (TG) 488 (30). There are several TGR models including MutaMouse, Big Blue[®] mouse and rat, *LacZ* plasmid mouse, and the *gpt* delta mouse (31). The TGR assay is frequently used for regulatory mutagenicity assessment. This assay has previously shown that BbF is a potent mutagen in the glandular stomach, small intestine, liver, lung, and bone marrow (20). However, the utility of the TGR assay in quantifying biologically relevant mutagenic susceptibility is limited by its reliance on individual exogenous bacterial reporter genes (31,32).

Error-corrected next-generation sequencing (ecNGS) provides a more modern and highly sensitive approach to quantify and characterize mutagenicity in any cell type or tissue (33). Duplex Sequencing (DS) is an ecNGS technology that reduces the technical error rate associated with standard NGS technologies to accurately quantify mutations (34,35,36). DS uses barcoding of both strands of each double-stranded DNA sequence during library preparation, and bioinformatic approaches to create a consensus sequence for each DNA strand. Through this process, DS technology reduces sequencing-derived errors from 1 in 1000 to 1 in 10 million bases (36). Thus, DS can detect rare mutations that occur spontaneously or are caused by mutagenic exposures (32,37). Moreover, DS enables analysis of mutation spectra and the detection of mutations in any region or target gene of interest in the genome (38,39). Although several published studies have used DS to measure mutation induction in somatic tissues, application to germ cells is still limited.

In this study, I evaluated the mutagenic effects of different durations of oral exposure to BbF on mouse male germ cells using the TGR assay and DS to inform on its potential heritable genetic effects. Specifically, MutaMouse males were exposed daily by oral gavage to BbF for 90

days or 180 days using increasing doses. Chronic exposure durations were chosen based on recommendations in OECD TG 408 (40) and 453 (41). The objectives of this study are to: 1) quantify the impact of BbF exposure on mutations in MutaMouse male germ cells; 2) identify the mutation spectrum induced by BbF in male germ cells; and 3) compare spontaneous and BbF-induced mutation frequencies (MF) obtained using DS to mutant frequencies detected using the TGR assay.

2.3 Materials and Methods

2.3.1 Animal Exposures and Tissue Collection

The study was approved by the Health Canada Animal Care Committee and followed the Canadian Council on Animal Care guidelines. The mice used in this study were derived from Health Canada's MutaMouse colony. MutaMouse animals are transgenic mice that carry approximately 30 copies of the bacterial *lacZ* transgene on each copy of chromosome 3 (42,43). 10–12-week-old male mice were exposed daily via oral gavage to 0 (olive oil), 3.25, 6.25, 12.5, 25, or 50 mg/kg BW/day BbF (CAS 205-99-2; Sigma-Aldrich, Oakville, ON Canada) dissolved in olive oil for 90 days. In a separate experiment, mice were exposed to 0, 1.56, 3.25, 6.25, 12.5, or 25 mg/kg BW/day for 180 days. Eight animals were used for each dose group within each time point. These dose ranges were selected based on pilot studies to identify top doses that do not cause high levels of morbidity or toxicity (e.g., body weight loss greater than 20%) at the time points selected. Approximately 24 hours after final administration, mice were euthanized; testes were collected, weighed and processed for isolating tubule germ cells as described previously (42). After isolation, germ cells were flash frozen and stored at -80°C until use. Two animals from the 3.125 and 6.25 mg/kg BW/day dose groups at 90 days as well as two animals from the 3.125 and 25 mg/kg BW/day dose groups at 180 days died prior to euthanasia leaving 92 animals for analysis.

2.3.2 Transgenic Rodent Gene Mutation Assay (LacZ assay)

DNA extraction was performed using a phenol/chloroform-based method (44) on 7-8 mice per dose group (all surviving mice). Precipitated DNA was dissolved in 40 – 100 mL of Tris-EDTA buffer (10 mM Tris pH 7.6, 0.1 mM EDTA) and stored at 4°C. DNA purity and concentration were measured using a NanoDrop spectrophotometer at A260 (Thermo Scientific Canada, Ottawa, Canada). The λ gt10 phage vectors were recovered from genomic DNA using commercial packaging extract kits (Agilent Technology, Santa Clara, CA, USA) following the manufacturer's instructions. A phenyl β -d-galactopyranoside (P-gal) positive selection assay was used to measure mutations in the transgenic reporter gene (31, 44). A range of 200,000-500,000 plaque forming units (PFU) were counted for each animal, with an average of approximately 300,000 PFU as per OECD TG 488 (30). The ratio of mutant plaques to total PFU derived from plaques formed in bacterial lawns grown under non-selective conditions was used to calculate mutant frequency.

2.3.3 Duplex Sequencing (DS)

The highest BbF dose groups (50 mg/kg BW/day at 90 days, 25 mg/kg BW/day at 180 days) and concurrent controls were used for DS (n = 6 animals per dose group). Qiagen DNeasy blood and tissue kits were used for DNA extraction as described in the user's manual (DNeasy Blood & Tissue Handbook, Qiagen, Hilden, Germany, July 2020). Extracted DNA was measured using the Qubit 1x dsDNA Broad Range Assay Kit (Thermo Fischer, Waltham, MA, USA). DNA integrity number (DIN) was assessed using high-sensitivity DNA D1000 ScreenTapes and the Agilent TapeStation Genomic DNA ScreenTape assay (Agilent Technologies, Santa Clara, CA, USA). We confirmed a DIN > 7 prior to use in DS library preparation for all samples.

DNA was prepared for sequencing as described previously (29). Briefly, 1000 ng of isolated DNA from each sample was enzymatically fragmented to create approximately 300 bp-sized DNA fragments. Fragmented DNA was then end-polished, A-tailed, and ligated to DS Sequencing Adapters (TwinStrand Biosciences, Seattle WA, USA). 120mer biotinylated oligo probes (Integrated DNA Technologies, Coalville, IA, USA) were used to capture the Mouse

Mutagenesis panel (MMP) targets after PCR amplification (described in detail below). DS libraries were sequenced by Psomagen (Rockville, MD, USA) on an Illumina NovaSeq 6000 (San Diego, CA, USA) to produce an average of roughly 600 million raw reads per sample. We set a threshold of a minimum of 500 million informative duplex bases for subsequent DS analysis (45). One animal in the control group for the 180-day BbF exposure duration did not reach this minimum (294,277,420) and therefore was removed from the analyses (Supp. Figure 2.1).

The TwinStrand Biosciences Duplex-Seq Mutagenesis App (3.11.0) (TwinStrand Biosciences, Seattle, WA, USA) on the DNAnexus platform was used to process the FASTQ files. This application generated a variant call file (VCF) for each library, as well as sequencing summary metrics and mutagenesis metrics such as MF and base substitution spectrum. Briefly, this application extracts duplex tags, aligns raw reads, groups the reads based on strand defining elements and unique molecular identifiers, creates duplex consensus calls for error-correction of the read groups, and then performs consensus post-processing, re-alignment, and variant calling (37).

As described in more detail in Dodge et al. (46), two approaches were applied to quantify MFs. The first approach conservatively assumes that all identical mutations in a sample result from clonal expansion of a single mutational event (MF_{min}). The second approach assumes that all identical mutations in a sample occurred as independent mutational events (MF_{max}).

2.3.4 TwinStrand Mouse Mutagenesis Panel

The DS MMP consists of 20 2.4kb targets (9 genic and 11 intergenic), with one on every autosome except chromosome 1, which contains two targets (32). Distribution of intergenic and genic regions is based on gene intersection data from the Mouse GenCode gene set, version M25 (47). None of the target sites have a known role in cancer in mice or humans (i.e., the mouse orthologs in humans); the targets are assumed to be selectively neutral. The MMP loci do not contain pseudogenes or repetitive elements that can distort variant calling or alignment. The nucleotide composition of the MMP is strongly correlated to that of the entire mm10

genome. Overall, the MMP provides a balanced representation of the entire genome based on GC content, trinucleotide abundances, chromatin state, and transcription status (32).

2.3.5 Statistical Analyses

2.3.5.1 Body and Tissue Weight Analyses

Change in body weight at euthanasia relative to the start of exposure are expressed as percentages. Testes weights are presented as the sum of the left and right testes. Given that both body and tissue weights follow a normal distribution, ANOVA was performed in R using the `aov()` function to evaluate differences between control and BbF dose groups.

2.3.5.2 TGR Analyses

TGR analyses were conducted using the MutSeqR package (<https://github.com/EHSRB-BSRSE-Bioinformatics/MutSeqR>) in the R software. Mutant frequencies were expressed as phenotypically scorable mutants per *lacZ* locus for the *lacZ* assay. A generalized linear model (GLM) using the `model_mf` function based on a quasibinomial distribution was performed to estimate mutant frequency by dose. P-values for the dose versus control mutant frequency comparisons were adjusted using the Holm-Sidak correction for multiple comparisons. A Cochran-Armitage test was also performed to determine whether a statistically significant dose-dependent trend was observed at either time point across all doses. One animal within the highest dose group (25 mg/kg BW/day) at 180 days was identified as an outlier and was removed from further analyses using the approach outlined in Marchetti et al. (48). Briefly, a generalized linear mixed model (GLMM) based on a binomial error distribution was used to identify outlier replicates as each animal was sampled multiple times, once for each packaging reaction (49). Model residuals having > 3 standard deviations of the mean identified as outliers (50). Two out of 190 *lacZ* replicates were removed from the analyses. After removal of outlier replicates, data were collapsed to the animal level and analyses were reconducted. One animal (at 25 mg/kg BW/day BbF dose; 180-day time point) out of 92 animals was identified as an outlier and removed.

2.3.5.3 DS Analyses

As mentioned for the TGR assay, DS analyses were also conducted using MutSeqR. The entire MMP was used to evaluate mutation induction as MF_{\min} or MF_{\max} (expressed as mutations per bp) for DS. A GLM was used to estimate the MF_{\min} and MF_{\max} by dose in R. The "doBy" package in R was used to perform pairwise comparisons based on exposure dose (51). These estimates were subsequently back-transformed and the back-transformed standard errors (standard error of the mean; SEM) of the estimated MF were approximated using the delta method. The p-values for the BbF-induced MF and control were compared and adjusted using Holm-Sidak correction for multiple testing for both MF_{\min} and MF_{\max} .

To estimate MFs by target, a GLMM using the `model_mf` function was applied with a binomial error distribution. Pairwise comparisons were performed based on dose and location relative to genes using the "doBy" package in R as mentioned above (51).

A modified contingency table approach, as outlined in Piegorsch & Bailer (52), was employed to identify distinct mutation subtypes between the control and high dose groups. GLM analyses as described above (51) were conducted to determine whether BbF-induced mutation subtypes were significantly increased relative to controls. Only unique mutations as identified by the MF_{\min} approach were used for mutation spectra analysis.

2.3.5.4 Power Analyses

Power analyses were performed on the generated *lacZ* and DS data to determine the minimum fold change that could be detected with the number of animals used for each methodology. For these analyses, the control data for the 90- and 180-day time points were combined.

For the *lacZ* data, a GLMM was used to estimate the minimum fold changes. Given that no over-dispersion was observed within the data, an animal level variation of 0.1 was also used. The average MF for the 90-day and 180-day datasets combined and the median number of plaques for both time points were then calculated. Minimum fold-changes that were required to detect biologically significant effects were estimated to yield 80% power.

For the DS data, a GLMM was used to estimate the animal-to-animal level variation. This estimate was then used to generate random samples from an over-dispersed binomial distribution (53,54,55,56). A GLM was performed to estimate fold changes and the bisection method was used to calculate the minimum fold changes required to detect significant increases in BbF-induced MF under the conditions of our DS experiment to achieve 80% power.

2.4 Results

2.4.1 Top Dose Selection

A pilot study was used to determine the top dose that could be administered for 90 and 180 days without inducing excessive systemic toxicity. To identify these doses, we analyzed the body weight of MutaMouse animals exposed to 0, 6.25, 12.5, 25, and 50 mg/kg BW/day BbF at 60 days, 90 days, 120 days, and 180 days. For the 90-day exposure duration, we observed no statistically significant changes in body weight at 50 mg/kg BW/day BbF. However, for the 180-day time point, we detected a statistically significant 33% decrease in body weight ($p < 0.05$) at the 50 mg/kg BW/day dose group, indicating overt toxicity (Supp. Figure 2.2). Because of this, 50 mg/kg BW/day BbF was selected as the top dose at 90 days and 25 mg/kg BW/day BbF was administered as the top dose for the 180-day exposure (Supp. Table 2.1).

2.4.2 Body and Testes Weight

Body and testes weights were examined to evaluate BbF-induced toxicity. Changes in body weights at 90 days and 180 days relative to the start of exposure were analyzed for each dose group (Figure 2.1A, 2.1B). Body weight of control mice increased an average of 15.7% and 43.8% at 90 days and 180 days, respectively. BbF doses higher than 6.25 and 12.5 mg/kg/day resulted in lower increases in body weight at 90 and 180 days, respectively; these lower increases at the higher doses were statistically significant at 90 days relative to controls ($p = 0.04$ and 0.03 at 25 and 50 mg/kg BW/day, respectively). At 180 days, a borderline decline in weight gain was detected at 25 mg/kg BW/day ($p = 0.06$).

Testis weight provides an indication of toxicity to the male germline and impacts sperm count. Herein, there were no significant changes in testes weights for any of the treatment groups relative to controls after 90- or 180-day BbF exposures (Figure 2.1C, 2.1D). At 90 days, the average combined testis weights were 0.209, 0.254, 0.241, 0.198, 0.216, and 0.212 g for the 0, 3.125, 6.25, 12.5, 25, and 50 mg/kg BW/day BbF dose groups, respectively (Figure 2.1C). At 180 days, the mean testes weights were 0.252, 0.250, 0.268, 0.272, 0.214, 0.207 g for the 0, 1.5625, 3.125, 6.25, 12.5, and 25 mg/kg BW/day BbF dose groups, respectively. At this time point, a slight decrease in testes weight was observed at the highest dose (25 mg/kg BW/day BbF) relative to controls; however, this was not statistically significant (Figure 2.1D).

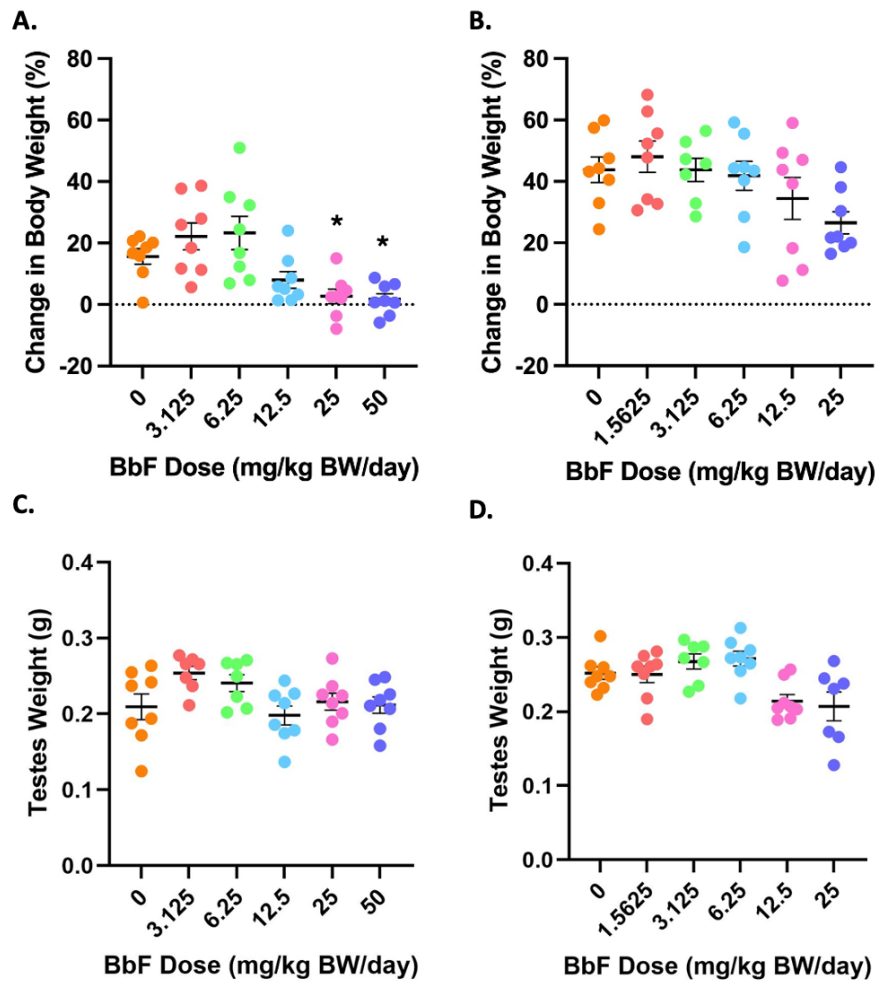


Figure 2.1. Change in body weights and sum of testes weights of MutaMouse males exposed to BbF for 90 days (A, C) and 180 days (B, D). Change in body weight data from individual animals together with the mean change in percent and SEMs per group are shown. Testes

weight data from individual mice with the mean weight in grams and SEMs per group are also indicated. Dose groups (N = 7 to 8 males per dose) in mg/kg BW/day are shown on the x-axis. Individual points indicate animal values at each dose, with the horizontal lines showing the mean, and error bars showing the SEM. *p = 0.04 and 0.03 (ANOVA) at 25 and 50 mg/kg BW/day, respectively.

2.4.3 *LacZ* Mutant Frequencies

The TGR assay was used to determine the impact of 90-day and 180-day BbF exposures on *lacZ* mutations in MutaMouse male germ cells. To calculate mutant frequency, we divided the number of mutant plaques by the total number of PFU. We analyzed an average of 300,000 PFU per mouse (Table 2.1).

BbF exposure did not cause a statistically significant increase in mutant frequency ($\times 10^{-5}$) in any of the treatment groups following the 90-day exposure. *LacZ* mutant frequencies were 2.28 ± 0.27 (\pm SEM) in controls and 2.51 ± 0.26 at the highest BbF dose (Figure 2.2A, Table 2.1). Similarly, there were no significant increases in BbF-induced *lacZ* mutant frequency in any dose groups following 180-day exposures. Mean mutant frequencies were 2.89 ± 0.38 and 3.15 ± 0.45 in the controls and highest BbF dose group, respectively (Figure 2.2B, Table 2.1). We did not observe a statistically significant trend at 90 and 180 days, and none of the mutant frequency values are outside of the historical control mutant frequency value of 2.51 ± 1.18 ($\times 10^{-5}$) (Supp. Figure 2.3, Supp. Table 2.2). Thus, the *lacZ* data adhere to the three criteria specified in TG 488 for a clearly negative result (30): 1) no statistically significant increase in mutant frequency at any dose with respect to controls; 2) no significant dose-dependent trend in mutant frequency; 3) no value outside of the historical control range.

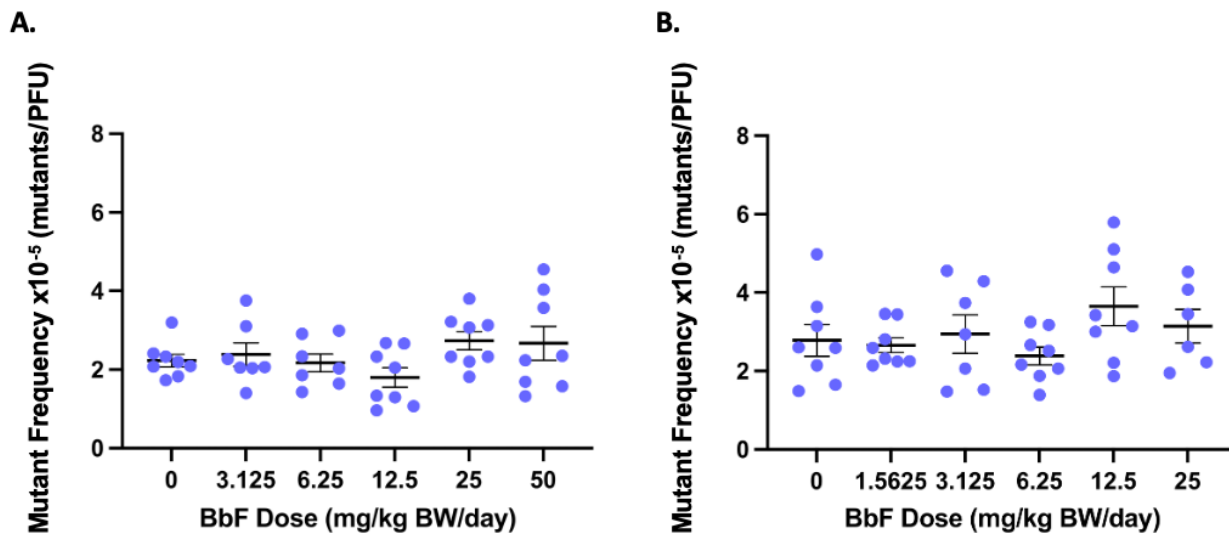


Figure 2.2. *LacZ* mutant frequencies in the germ cells of MutaMouse males exposed to BbF for 90 days (A) and 180 days (B). Mutant frequency ($\times 10^{-5}$) is represented as mutants per plaque forming units (PFU) for all animals ($N = 7$ to 8 per dose group) at each dose group. Mean mutant frequencies and SEM are shown. Actual values for each animal at each dose are represented by individual points; horizontal lines demonstrate the mean; error bars represent SEM.

Table 2.1. Average *lacZ* mutant frequencies in MutaMouse male germ cells after 90 and 180 days of exposure to BbF.

Exposure Duration	Dose (mg/kg BW/day)	# of Animals per Dose	Average PFU	Average <i>lacZ</i> MF* \pm SEM ($\times 10^{-5}$)	Fold Changes	P-values
90 days	0	8	310,314	2.28 \pm 0.27		
90 days	3.125	7	303,975	2.23 \pm 0.30	0.98	1.00
90 days	6.25	7	360,207	2.04 \pm 0.24	0.89	0.998
90 days	12.5	8	331,437	1.76 \pm 0.22	0.77	0.717
90 days	25	8	299,028	2.61 \pm 0.30	1.15	0.885
90 days	50	8	343,903	2.51 \pm 0.26	1.10	0.950
180 days	0	8	278,693	2.89 \pm 0.38		
180 days	1.5625	8	246,119	2.62 \pm 0.41	0.91	0.998
180 days	3.125	7	297,348	2.64 \pm 0.36	0.91	1.00
180 days	6.25	8	284,988	2.27 \pm 0.33	0.79	0.833
180 days	12.5	8	278,610	3.44 \pm 0.42	1.19	0.636
180 days	25	6	285,885	3.15 \pm 0.45	1.09	0.984

*Values are presented as estimates obtained using GLM

2.4.4 DS Mutation Frequencies

We next employed DS to quantify mutation frequency and spectrum across 20 endogenous loci in the mouse genome. Because of the negative *lacZ* results, DS was conducted only for the control and high dose group of each exposure duration. Given that MF is lower in germ cells than somatic cells, we used a higher DNA input (i.e., 1000 ng), and a higher average sequencing depth relative to our previous studies on somatic cell mutagenicity (53), to increase our power to detect an effect. We sequenced an average of 1.5 billion informative duplex bases per sample at the 90-day and 180-day time points, for a total of approximately 17 billion duplex bases across the cohort for each exposure duration (Table 2.2, Supp. Figure 2.1).

To estimate MF, we divided the number of mutations by the total number of duplex bases screened for each sample. Using the MF_{min} assumption, we observed a total of 381 and 379 unique mutations per mouse in both controls and BbF-exposed animals in the 90-day exposure experiment. There was no increase in MF in the BbF-treated mice relative to controls; MF was 3.70 \pm 0.40 mutations $\times 10^{-8}$ per bp (\pm SEM) in controls and 4.47 \pm 0.49 at 50 mg/kg

BW/day BbF (Figure 2.3A, Table 2.2). For the 180-day BbF exposure, we detected 363 and 453 mutations in control and BbF treated groups, respectively. There was no significant increase in MF in BbF-treated animals relative to control; MF was $4.48 \pm 0.64 \times 10^{-8}$ per bp in controls and 4.71 ± 0.60 in BbF-treated mice (Figure 2.3B, Table 2.2).

Using the MF_{max} assumption, we identified 465 and 470 mutations in total at 90 days in the control and 50 mg/kg BW/day BbF treatment groups, respectively. There were no significant increases in MF in BbF-treated animals relative to control; MF_{max} were 4.48 ± 0.54 and 5.51 ± 0.67 ($\times 10^{-8}$ per bp; \pm SEM) in controls and the 50 mg/kg BW/day BbF dose group (Figure 2.3A, Table 2.2), respectively. After 180 days of exposure, we identified a total 464 and 616 mutations in the control and 25 mg/kg BW/day BbF dose groups, respectively. There was no significant BbF-induced increase in MF in the treated dose groups relative to controls; MF_{max} was 5.80 ± 0.98 and 6.53 ± 0.95 ($\times 10^{-8}$ per bp; \pm SEM) in controls and the BbF dose (Figure 2.3B, Table 2.2), respectively.

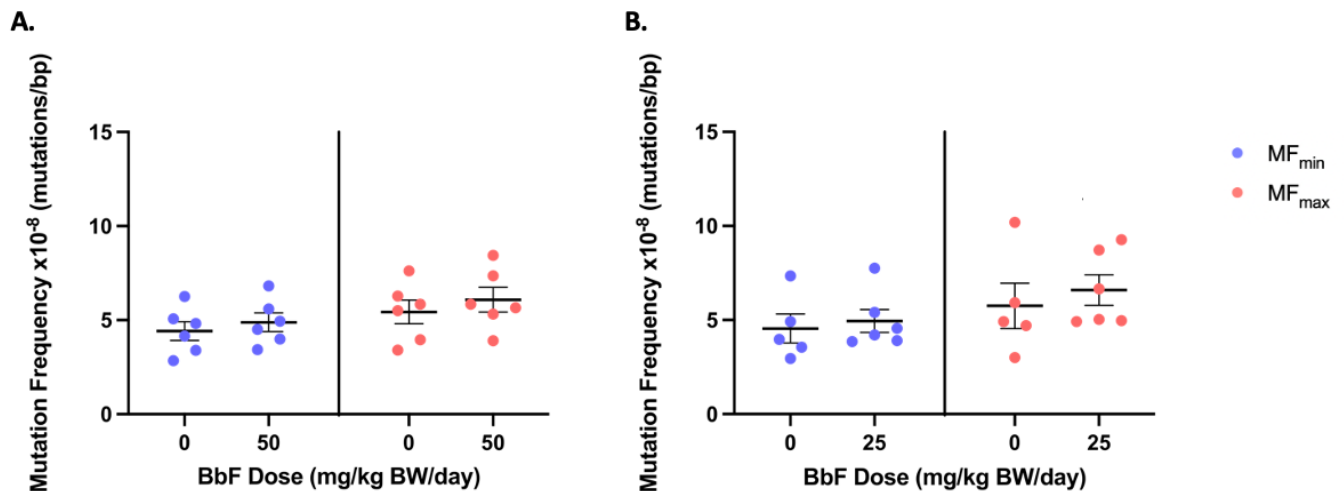


Figure 2.3. Duplex sequencing MF in germ cells of MutaMouse males in control and BbF exposed groups (N = 5 to 6 mice per dose group) at 90 days (A) and 180 days (B). MF is represented as mutations per $\times 10^{-8}$ base-pair (bp) for each animal at each dose. Mean MF and SEM are shown. Individual points report the observed values; horizontal lines indicate the calculated means.

Table 2.2. Average DS MF_{min} and MF_{max} in MutaMouse male germ cells after 90 and 180 days of exposure to BbF.

Exposure Duration	Dose* (mg/kg BW/day)	# of Animals per Dose	Average Informative Duplex Bases	Average MF _{min} ** ± SEM (x10 ⁻⁸)	Fold Changes	P-values	Average MF _{max} ** ± SEM (x10 ⁻⁸)	Fold Changes	P-values
90 days	0	6	1,569,071,844	3.70 ± 0.40			4.48 ± 0.54		
90 days	50	6	1,349,061,285	4.47 ± 0.49	1.21	0.244	5.51 ± 0.67	1.23	0.251
180 days	0	5	1,605,082,798	4.48 ± 0.64			5.80 ± 0.98		
180 days	25	6	1,570,405,624	4.71 ± 0.60	1.05	0.804	6.53 ± 0.95	1.13	0.608

*Highest BbF dose used in each experiment

**Values represent estimates from GLM

2.4.5 DS Mutation Frequency by Target

Next, we investigated whether there were locus-specific differences in response to BbF across the genic and intergenic targets of the MMP. At 90 days, the highest control MF_{min} was observed in the second target on chromosome 1 (chr1.2; 7.34 x10⁻⁸) and the lowest was on chromosome 12 (2.09 x10⁻⁸), with a 3.5-fold difference between the lowest and highest target-specific control MF. The highest MF_{min} following BbF exposure was on the second target on chromosome 1 (9.60 x10⁻⁸) and the lowest was on chromosome 6 (2.37 x10⁻⁸), corresponding to a 4.1-fold difference. There were no significant BbF-induced increases in MF_{min} in any of the 20 targets relative to control (Figure 2.4A).

At 180 days, the highest control MF_{min} on the second target of chromosome 1 (8.59 x10⁻⁸) and the lowest control MF_{min} on chromosome 5 (1.98 x10⁻⁸) differed by 4.3-fold. We detected the highest MF_{min} following BbF treatment for the second target on chromosome 1 (chr1.2; 7.58 x10⁻⁸) and the lowest MF_{min} on chromosome 3 (2.77 x10⁻⁸), with a 2.7-fold-difference between the two. We did not detect significant increases in MF_{min} for any of the 20 targets following BbF exposure (Figure 2.4B).

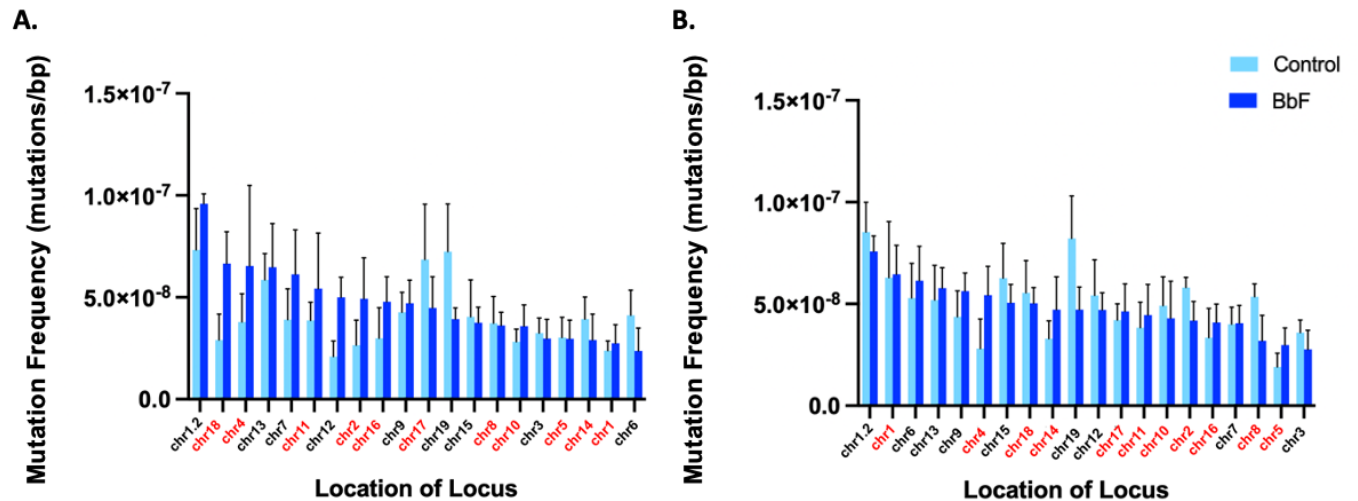


Figure 2.4. DS locus-specific MF_{min} for controls and BbF-treated mice at 90 days (A) and 180 days (B). The chromosomes on which the 20 loci are located are shown on the x-axis and they are ordered from the highest MF_{min} to lowest in the BbF treatment groups. Intergenic and genic targets on the x-axis are shown in red and black, respectively. MF_{min} and SEM for each locus are shown.

2.4.6 Mutation Spectrum

We analyzed mutation spectra to determine if specific mutation subtypes associated with BbF-induced somatic cell mutagenesis are enriched in exposed MutaMouse male germ cells. We quantified single nucleotide variants (SNVs), deletions, insertions, and multi-nucleotide variants in the control and BbF-treated mice. For both exposure durations, the mutation spectra were mainly driven by SNVs followed by insertions, deletions, and MNVs (Figure 2.5).

At 90 days, there were no significant differences between the control and BbF-induced mutation spectra. The main mutation subtypes in both groups were C:G > T:A transitions and C:G > A:T transversions, which constituted approximately 30% and 20% of total mutation subtypes, respectively. These subtypes were followed by T:A > A:T transversions (~10%) and T:A > C:G transitions (~8%; Figure 2.5A, Supp. Figure 2.4A). There were no significant increases in MF (x10⁻⁸) at C:G > A:T transversions, the main SNV expected from BbF (29), i.e., 1.48 ± 0.91 in controls and 1.61 ± 0.32 for BbF (Figure 2.5A).

At 180 days, the control mutation spectrum was mainly driven by C:G > T:A transitions and C:G > A:T transversions, constituting 33% and 16% of total mutations respectively. These subtypes were followed by T:A > A:T transversions (12%) and T:A > C:G transitions (6%) (Figure 2.5B, Supp. Figure 2.4B). However, in contrast to the 90-day exposure, we found significant differences between the overall control and BbF-induced mutation spectra ($p < 0.005$). C:G > T:A transitions and C:G > A:T transversions in the BbF-induced spectra accounted for 25% and 24% of the total mutation subtypes respectively, followed by C:G > G:C and T:A > A:T transversions, which both constituted 9% of the total mutations. Although we observed a small BbF-associated increase in C:G > A:T transversions, the 1.6-fold increase in these mutations from 1.25 ± 0.45 in the control to 1.99 ± 0.73 in the BbF treated (Figure 2.5B) was not statistically significant.

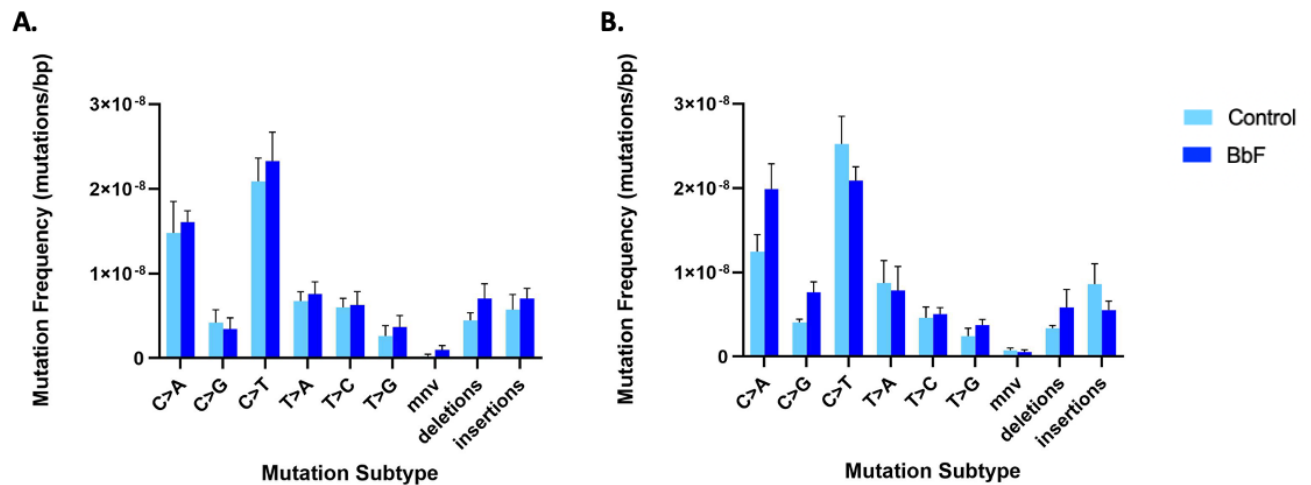


Figure 2.5. Mutation spectrum in control and BbF-treated MutaMouse male germ cells quantified using DS following 90-day (A) and 180-day (B) exposures (N = 5 to 6 per dose group). Average MF_{min} per dose group is presented for each mutation subtype. Mutations include the six single nucleotide variants, multi nucleotide variants (mnv), deletions, and insertions. Error bars are SEM. Significant differences were observed between the overall BbF-mutation spectrum relative to the spontaneous mutation spectrum at 180 days ($p < 0.005$).

2.4.7 Power Analyses

We performed power analyses on the 90- and 180-day *lacZ* and DS datasets to estimate the minimum fold change that could be detected with 80% power. For the *lacZ* data, using the median number of plaques (294,224), an animal level variation of 0.1, and the average mutant frequencies (2.83×10^{-5}) for both the 90-day and 180-day exposure durations, a 1.7-fold change is the minimum increase that could be significantly detected with 8 animals per dose group. With seven animals (i.e., one animal removed from analyses) per dose group, a 1.8-fold-increase is required (Table 2.3). For our DS data, analyses were conducted using two sample sizes (N = 5 and N = 6), given that one animal was insufficiently sequenced. Using the median informative duplex bases (1,401,511,947), the observed animal-level variation (0.2345) and the average MF (4.36×10^{-8}) for both time points, with six animals per dose group, a minimum 1.6-fold-increase could be detected with 80% power. With five animals per dose group, a minimum 1.7-fold-increase is required (Table 2.3).

Table 2.3. Power analysis of *lacZ* and DS 90-day and 180-day combined datasets.

Method	Median Informative Duplex Bases	Median PFU	Average MF	Variance	Minimum Fold Change*			
					Sample Size N = 5	Sample Size N = 6	Sample Size N = 7	Sample Size N = 8
<i>lacZ</i>	--	294,224	2.83×10^{-5}	0.10	2.03	1.87	1.79	1.72
DS	1,401,511,947	--	4.36×10^{-8}	0.23	1.70	1.60	1.54	1.48

*Minimum fold-changes shown in bold represent the fold-changes based on the corresponding number of animals used for each method.

2.5 Discussion

We investigated whether BbF is a mouse male germ cell mutagen following extended duration exposures. After 90-day BbF exposure, a significant decline in body weight relative to the control was detected at higher doses. However, we did not observe significant declines in testes weight in animals from the 90- or 180-day exposure groups relative to the controls at the top doses. There were no statistically significant increases in BbF-induced *lacZ* mutant

frequencies or significant dose-dependent trends at either time point. Consistent with these results, DS revealed no significant BbF-induced increases in MF_{min} or MF_{max} at either time point. Although C:G > A:T transversions were highly enriched in the BbF mutation spectra in somatic tissues (29), no significant increases in C:G > A:T transversions were observed in the BbF-induced mutation spectra in germ cells. Overall, our study suggests that BbF is not a mouse male germ cell mutagen under the tested conditions.

The results of this study conflict with the strong mutagenic response of BbF in somatic tissues previously observed with the *lacZ* assay (20) and DS (29). Using the *lacZ* assay Long et al. (20) observed a robust mutagenic response to BbF in liver, bone marrow, lung, small intestine, and glandular stomach following a 28-day oral exposure. Similarly, using a subset of the animals evaluated here for germ cell mutagenesis, Schuster et al. (Unpublished data) found strong dose-dependent increases in DS MF_{min} in bone marrow (4.8-fold increase at 90 days; 4.7-fold increase at 180 days) and liver (17.5-fold increase at 90 days; 16.2-fold increase at 180 days); thus, there is a clear difference in mutagenic susceptibility to BbF between germ cells and somatic tissues. Differences in biological processes may explain these findings - i.e., metabolism and distribution of BbF, DNA repair capacity, and cellular proliferation rates.

BbF must be metabolized to generate reactive species capable of forming DNA adducts. PAHs are metabolized through CYP enzymes including the CYP1A1 and CYP1B1 isoforms (57,58), and BbF's reactive metabolites can form a variety of DNA adducts (59). Both Long et al. (20) and Schuster et al. (29) reported a higher mutagenic response in the liver than in bone marrow. The liver possesses high CYP levels and is the main metabolizing tissue; however, BbF metabolites are highly unstable and therefore transportation of these metabolites to other tissues is unlikely (20). If active BbF metabolites do not reach the germ cells, we would not expect an increase in MF. Our results suggest that germ cells do not metabolize BbF or that active metabolites are not reaching the testes at levels that exceed the DNA repair capacity of germ cells.

BbF induces highly similar mutagenic effects to BaP (29, 30). BaP is the most well-studied PAH and is used as a reference for mutagenicity assessment for this class of compounds. BbF and BaP both cause bulky DNA adducts that target guanines (25,60). BaP induces mutations in mouse male germ cells that are transmitted to the offspring (61,62). Given the consistencies

between the mutagenicity of BbF and BaP in somatic tissues, and the mutagenic response of BaP in germ cells, we hypothesized that BbF exposure would similarly induce germ cell mutations. However, our results show that unlike BaP, BbF is not mutagenic in germ cells under the experimental conditions used in this study. Structural differences in BbF and BaP, and/or different metabolic activities in the testes, may lead to observed differential responses in germ cells for these two compounds.

Given their vital role as the transmitter of genetic information across generations, germ cells have highly effective DNA repair mechanisms to prevent mutations and preserve genomic integrity (63). Notably, in humans and in mice, the germline mutation rate is more than an order of magnitude lower than the mutation rate of somatic tissues (64). To achieve low germline mutation rates, DNA repair and DNA damage response mechanisms must therefore be tightly regulated. Base excision repair (BER), nucleotide excision repair (NER), homologous recombination repair, and non-homologous recombination repair are active during different phases of germ cell development and play essential roles in repairing DNA damage in germ cells (65,66). Metabolites of BbF form bulky DNA adducts that are mainly repaired by the NER pathway (67). Previous studies have shown that NER activity in male germ cells is lower than in somatic tissues, leading authors to hypothesize that male germ cells do not require high levels of NER activity because damaged cells can be removed through programmed cell death (68). Thus, germ cells may favour apoptosis over repairing extensive DNA damage, reducing the likelihood of mutations, in contrast to somatic tissues that arrest the cell cycle and execute these repair mechanisms in response to damage (63). We speculate that one possibility for the lack of mutagenicity observed following BbF exposure is the differential DNA damage response mechanisms in germ cells relative to somatic tissues.

Rates of proliferation is another factor that should be considered when comparing results between somatic tissues and germ cells. DNA replication of unrepaired damaged template is an important mechanism leading to mutations (69). Bone marrow is a rapidly proliferating tissue compared to tubule germ cells. Nonetheless, the slower proliferation rate in tubule germ cells relative to bone marrow may also partially contribute to different mutagenic responses in these tissues. In contrast, despite the very slow rate of proliferation in the liver, BbF is highly

mutagenic in this tissue (29), likely because of its primary role in the metabolism of xenobiotics. Our results suggest that differences in the distribution and metabolism of BbF between tissues, and whether active metabolites of BbF are reaching the testes, are more influential on the tissue-specific effects than proliferation rates.

One advantage of using DS over the *lacZ* assay is the ability to provide information on mutation subtypes that are induced by the exposure. Shifts in mutation spectrum may be evidence of more subtle effects not identified with the overall MF analysis. Previous studies have demonstrated that BbF metabolites favour the formation of guanine adducts (20,70,23). We observed a small, but statistically significant, difference in the overall mutation spectrum in BbF-treated mice relative to controls at 180 days, but no evidence of changes in the C:G > A:T transversions that are characteristic of BbF and BaP exposure (29,32). Overall, these findings provide further evidence for the lack of mutagenicity of BbF in mouse male germ cells with the present experimental design.

Published DS power analyses suggest that 4-5 animals per treatment group is sufficient to detect a 1.5-fold change in MF in somatic tissues (53). No such power analysis has been conducted for male germ cells. OECD TG 488 requires a minimum of 5 animals per treatment group but does not specify the power or detectable effect size (30). Herein, we investigated the minimum fold-increases we could expect with 80% power with the number of animals used for the *lacZ* and DS assays. Our power analyses show that the observed fold increases in BbF's MF are below the minimum fold increase that could have been detected with our experimental design (Table 2.3). A much larger sample size would be required to have the necessary power to detect the small changes that we observed. Identifying small fold-increases in germline mutations is important given that even minor changes can have a significant impact at the population level (71). For example, Beal et al. (72) demonstrated that a 25% increase in sperm MF due to tobacco smoking will result in the transmission of millions of smoking-induced *de novo* mutations to the offspring of smokers globally. Thus, germ cell studies may require more animals relative to somatic mutagenicity studies to detect small effects with sufficient power.

2.6 Conclusions

In summary, our study demonstrates that exposure to BbF over prolonged periods of time does not increase mutations in the male mouse germline, highlighting a clear difference with respect to somatic tissues. We propose that either insufficient distribution and metabolic activation of BbF in the testes and/or effective DNA damage response mechanisms play a role in the differential response of germ cells. It is possible that mutagenic effects are occurring below the effect size that we can detect with the present study design. It is of interest to determine whether different experimental designs (e.g., a 28-day administration followed by a 28-sampling time as recommended in TG 488) would result in a significant increase in BbF induced mutations in male germ cells.

2.7 References

1. Zorrilla, M., & Yatsenko, A. N. (2013) The Genetics of Infertility: Current Status of the Field. *Current Genetic Medicine Reports*, **1**.
2. Kessler, M. D., Loesch, D. P., Perry, J. A., Heard-Costa, N. L., Taliun, D., Cade, B. E., Wang, H., Daya, M., Ziniti, J., Datta, S., Celedón, J. C., Soto-Quiros, M. E., Avila, L., Weiss, S. T., Barnes, K., Redline, S. S., Vasan, R. S., Johnson, A. D., Mathias, R. A., ... Zoellner, S. (2020) De novo mutations across 1,465 diverse genomes reveal mutational insights and reductions in the Amish founder population. *Proceedings of the National Academy of Sciences*, **117**, 2560–2569.
3. Yauk, C. L., Aardema, M. J., Benthem, J. V., Bishop, J. B., Dearfield, K. L., DeMarini, D. M., Dubrova, Y. E., Honma, M., Lupski, J. R., Marchetti, F., Meistrich, M. L., Pacchierotti, F., Stewart, J., Waters, M. D., & Douglas, G. R. (2015) Approaches for identifying germ cell mutagens: Report of the 2013 IWGT workshop on germ cell assays☆. *Mutation Research/Genetic Toxicology and Environmental Mutagenesis*, **783**, 36–54.
4. Marchetti, F., Douglas, G. R., & Yauk, C. L. (2020) A Return to the Origin of the EMGS: Rejuvenating the Quest for Human Germ Cell Mutagens and Determining the Risk to Future Generations. *Environmental and Molecular Mutagenesis*, **61**, 42–54.
5. United Nations. (2015) *Globally Harmonized System of Classification and Labelling of Chemicals (GHS)*, sixth revised edition ed., New York and Geneva.
6. Marchetti, F., Aardema, M. J., Beevers, C., Van Benthem, J., Godschalk, R., Williams, A., Yauk, C. L., Young, R., & Douglas, G. R. (2018) Identifying germ cell mutagens using OECD test guideline 488 (transgenic rodent somatic and germ cell gene mutation assays) and integration with somatic cell testing. *Mutation Research/Genetic Toxicology and Environmental Mutagenesis*, **832–833**, 7–18.
7. Baklanov, A., Hänninen, O., Slørdal, L. H., Kukkonen, J., Bjergene, N., Fay, B., Finardi, S., Hoe, S. C., Jantunen, M., Karppinen, A., Rasmussen, A., Skouloudis, A., Sokhi, R. S., Sørensen, J. H., & Ødegaard, V. (2007) Integrated systems for forecasting urban meteorology, air pollution and population exposure. *Atmospheric Chemistry and Physics*, **7**, 855–874.
8. Latimer, J.S., & Zheng, J. The Sources, Transport, and Fate of PAHs in the Marine Environment. (2003) In Douben, P.E.T., Weeks, J.M., O’Hare, S., Rattner, B.A. (eds), *PAHs: An Ecotoxicological Perspective*. 1st ed., Wiley, pp. 7–33.
9. Boström, C.-E., Gerde, P., Hanberg, A., Jernström, B., Johansson, C., Kyrklund, T., Rannug, A., Törnqvist, M., Victorin, K., & Westerholm, R. (2002) Cancer Risk Assessment, Indicators, and Guidelines for Polycyclic Aromatic Hydrocarbons in the Ambient Air. *Environmental Health Perspectives*, **110**, 451–489.
10. Abdel-Shafy, H. I., & Mansour, M. S. M. (2016) A review on polycyclic aromatic hydrocarbons: Source, environmental impact, effect on human health and remediation. *Egyptian Journal of Petroleum*, **25**, 107–123.
11. Sahoo, B. M., Ravi Kumar, B. V. V., Banik, B. K., & Borah, P. (2020) Polyaromatic Hydrocarbons (PAHs): Structures, Synthesis and their Biological Profile. *Current Organic Synthesis*, **17**, 625–640.

12. Olsson, A. C., Fevotte, J., Fletcher, T., Cassidy, A., 'T Mannelje, A., Zaridze, D., Szeszenia-Dabrowska, N., Rudnai, P., Lissowska, J., Fabianova, E., Mates, D., Bencko, V., Foretova, L., Janout, V., Brennan, P., & Boffetta, P. (2010) Occupational exposure to polycyclic aromatic hydrocarbons and lung cancer risk: A multicenter study in Europe. *Occupational and Environmental Medicine*, **67**, 98–103.
13. Diggs, D. L., Huderson, A. C., Harris, K. L., Myers, J. N., Banks, L. D., Rekhadevi, P. V., Niaz, M. S., & Ramesh, A. (2011) Polycyclic Aromatic Hydrocarbons and Digestive Tract Cancers: A Perspective. *Journal of Environmental Science and Health, Part C*, **29**, 324–357.
14. Bach, P. B., Kelley, M. J., Tate, R. C., & McCrory, D. C. (2003) Screening for lung cancer: a review of the current literature. *Chest*, **123**, 72S-82S.
15. IARC (2010) Some non-heterocyclic polycyclic aromatic hydrocarbons and some related exposures. *IARC Monographs on the Evaluation of Carcinogenic Risks to Humans*, **92**. International Agency for Research on Cancer, Lyon.
16. Shimada, T. (2002) Arylhydrocarbon receptor-dependent induction of liver and lung cytochromes P450 1A1, 1A2, and 1B1 by polycyclic aromatic hydrocarbons and polychlorinated biphenyls in genetically engineered C57BL/6J mice. *Carcinogenesis*, **23**, 1199–1207.
17. Shimada, T., & Fujii-Kuriyama, Y. (2004) Metabolic activation of polycyclic aromatic hydrocarbons to carcinogens by cytochromes P450 1A1 and 1B1. *Cancer Science*, **95**, 1–6.
18. Xue, W., & Warshawsky, D. (2005) Metabolic activation of polycyclic and heterocyclic aromatic hydrocarbons and DNA damage: A review. *Toxicology and Applied Pharmacology*, **206**, 73–93.
19. Cairns, J. (1998) Mutation and Cancer: The Antecedents to Our Studies of Adaptive Mutation. *Genetics*, **148**, 1433–1440.
20. Long, A. S., Lemieux, C. L., Arlt, V. M., & White, P. A. (2016) Tissue-specific in vivo genetic toxicity of nine polycyclic aromatic hydrocarbons assessed using the MutaTMMouse transgenic rodent assay. *Toxicology and Applied Pharmacology*, **290**, 31–42.
21. Thurston, S. W., Ryan, L., Christiani, D. C., Snow, R., Carlson, J., You, L., Cui, S., Ma, G., Wang, L., Huang, Y., & Xu, X. (2000) Petrochemical exposure and menstrual disturbances. *American Journal of Industrial Medicine*, **38**, 555–564.
22. Tomei, G., Ciarrocca, M., Fortunato, B. R., Capozzella, A., Rosati, M. V., Cerratti, D., Tomao, E., Anzelmo, V., Monti, C., & Tomei, F. (2006) Exposure to traffic pollutants and effects on 17- β -estradiol (E2) in female workers. *International Archives of Occupational and Environmental Health*, **80**, 70–77.
23. Mass, M. J., Abu-Shakra, A., Roop, B. C., Nelson, G., Galati, A. J., Stoner, G. D., Nesnow, S., & Ross, J. A. (1996) Benzo[*b*]fluoranthene: Tumorigenicity in strain A/J mouse lungs, DNA adducts and mutations in the Ki-*ras* oncogene. *Carcinogenesis*, **17**, 1701–1704.
24. Zhang, Y., Liu, D., & Liu, Z. (2020) The benzo[*b*]fluoranthene in the atmospheric fine particulate matter induces mouse glomerular podocytes injury via inhibition of autophagy. *Ecotoxicology and Environmental Safety*, **195**, 110403.
25. Amin, S., LaVoie, E. J., & Hecht, S. S. (1982) Identification of metabolites of benzo[*b*]fluoranthene. *Carcinogenesis*, **3**, 171–174.

26. Yang, S. K. (1988) Stereoselectivity of cytochrome P-450 isozymes and epoxide hydrolase in the metabolism of polycyclic aromatic hydrocarbons. *Biochemical Pharmacology*, **37**, 61–70.
27. Lehr, R. E., Kumar, S., Levin, W., Wood, A. W., Chang, R. L., Conney, A. H., Yagi, H., Sayer, J. M., & Jerina, D. M. (1985) The Bay Region Theory of Polycyclic Aromatic Hydrocarbon Carcinogenesis. *American Chemical Society*, **283**, 63–84.
28. Wynder, E. L. & Hoffmann, D. (1959) A study of tobacco carcinogenesis. VII. The role of higher polycyclic hydrocarbons. *Cancer*, **12**, 1079–1086.
29. Schuster, D. M., LeBlanc, D. P. M., Zhou, G., Meier, M. J., Dodge, A. E., White, P. A., Long, A. S., Williams, A., Hobbs, C., Diesing, A., Smith-Roe, S. L., Salk, J. J., Marchetti, F., & Yauk, C. L. (2024) Dose-related Mutagenic and Clastogenic Effects of Benzo[b]fluoranthene in Mouse Somatic Tissues Detected by Duplex Sequencing and the Micronucleus Assay. *Environmental Science & Technology*, **58**, 21450–21463.
30. OECD (2022) Test No. 488. Transgenic rodent somatic and germ cell gene mutation assay. *OECD guidelines for the testing of chemicals*, section 4. OECD Publishing, Paris.
31. Lambert, I. B., Singer, T. M., Boucher, S. E., & Douglas, G. R. (2005) Detailed review of transgenic rodent mutation assays. *Mutation Research/Reviews in Mutation Research*, **590**, 1–280.
32. LeBlanc, D. P. M., Meier, M., Lo, F. Y., Schmidt, E., Valentine, C., Williams, A., Salk, J. J., Yauk, C. L., & Marchetti, F. (2022) Duplex sequencing identifies genomic features that determine susceptibility to benzo(a)pyrene-induced in vivo mutations. *BMC Genomics*, **23**, 542.
33. Marchetti, F., Cardoso, R., Chen, C. L., Douglas, G. R., Elloway, J., Escobar, P. A., Harper, T., Heflich, R. H., Kidd, D., Lynch, A. M., Myers, M. B., Parsons, B. L., Salk, J. J., Settivari, R. S., Smith-Roe, S. L., Witt, K. L., Yauk, C. L., Young, R., Zhang, S., & Minocherhomji, S. (2023) Error-corrected next generation sequencing – Promises and challenges for genotoxicity and cancer risk assessment. *Mutation Research/Reviews in Mutation Research*, **792**, 108466.
34. Quail, M., Smith, M. E., Coupland, P., Otto, T. D., Harris, S. R., Connor, T. R., Bertoni, A., Swerdlow, H. P., & Gu, Y. (2012) A tale of three next generation sequencing platforms: Comparison of Ion torrent, pacific biosciences and illumina MiSeq sequencers. *BMC Genomics*, **13**, 341.
35. Fox, E. J., Reid-Bayliss, K. S., Emond, M. J., & Loeb, L. A. (2014) Accuracy of Next Generation Sequencing Platforms. *Next Generation, Sequencing & Applications*, **1**, 1000106.
36. Kennedy, S. R., Schmitt, M. W., Fox, E. J., Kohn, B. F., Salk, J. J., Ahn, E. H., Prindle, M. J., Kuong, K. J., Shen, J.-C., Risques, R.-A., & Loeb, L. A. (2014) Detecting ultralow-frequency mutations by Duplex Sequencing. *Nature Protocols*, **9**, 2586–2606.
37. Valentine, C. C., Young, R. R., Fielden, M. R., Kulkarni, R., Williams, L. N., Li, T., Minocherhomji, S., & Salk, J. J. (2020) Direct quantification of in vivo mutagenesis and carcinogenesis using duplex sequencing. *Proceedings of the National Academy of Sciences*, **117**, 33414–33425.
38. Hoang, M. L., Kinde, I., Tomasetti, C., McMahon, K. W., Rosenquist, T. A., Grollman, A. P., Kinzler, K. W., Vogelstein, B., & Papadopoulos, N. (2016) Genome-wide quantification of

- rare somatic mutations in normal human tissues using massively parallel sequencing. *Proceedings of the National Academy of Sciences*, **113**, 9846–9851.
39. Abascal, F., Harvey, L. M. R., Mitchell, E., Lawson, A. R. J., Lensing, S. V., Ellis, P., Russell, A. J. C., Alcantara, R. E., Baez-Ortega, A., Wang, Y., Kwa, E. J., Lee-Six, H., Cagan, A., Coorens, T. H. H., Chapman, M. S., Olafsson, S., Leonard, S., Jones, D., Machado, H. E., ... Martincorena, I. (2021) Somatic mutation landscapes at single-molecule resolution. *Nature*, **593**, 405–410.
 40. OECD (2018) Test No. 408. Repeated dose 90-day oral toxicity study in rodents. *OECD guidelines for the testing of chemicals*, section 4. OECD Publishing, Paris.
 41. OECD (2018) Test No. 453. Combined chronic toxicity/carcinogenicity studies. *OECD guidelines for the testing of chemicals*, section 4. OECD Publishing, Paris.
 42. Shwed, P. S., Crosthwait, J., Douglas, G. R., & Seligy, V. L. (2010) Characterisation of MutaTMMouse gt10-*lacZ* transgene: Evidence for in vivo rearrangements. *Mutagenesis*, **25**, 609–616.
 43. Meier, M. J., Beal, M. A., Schoenrock, A., Yauk, C. L., & Marchetti, F. (2019) Whole Genome Sequencing of the Mutamouse Model Reveals Strain- and Colony-Level Variation, and Genomic Features of the Transgene Integration Site. *Scientific Reports*, **9**, 13775.
 44. O'Brien, J. M., Beal, M. A., Gingerich, J. D., Soper, L., Douglas, G. R., Yauk, C. L., & Marchetti, F. (2014) Transgenic Rodent Assay for Quantifying Male Germ Cell Mutant Frequency. *Journal of Visualized Experiments*, **90**, 51576.
 45. LeBlanc, D. P. M., Zhou, G., Williams, A., Meier, M. J., Valentine, C. C., Salk, J. J., Yauk, C. L., & Marchetti, F. (2025) Duplex sequencing identifies unique characteristics of ENU-induced mutations in male mouse germ cells. *Biology of Reproduction*, ioaf029.
 46. Dodge, A. E., LeBlanc, D. P. M., Zhou, G., Williams, A., Meier, M. J., Van, P., Lo, F. Y., Valentine Iii, C. C., Salk, J. J., Yauk, C. L., & Marchetti, F. (2023) Duplex sequencing provides detailed characterization of mutation frequencies and spectra in the bone marrow of MutaMouse males exposed to procarbazine hydrochloride. *Archives of Toxicology*, **97**, 2245–2259.
 47. Frankish, A., Diekhans, M., Ferreira, A.-M., Johnson, R., Jungreis, I., Loveland, J., Mudge, J. M., Sisu, C., Wright, J., Armstrong, J., Barnes, I., Berry, A., Bignell, A., Carbonell Sala, S., Chrast, J., Cunningham, F., Di Domenico, T., Donaldson, S., Fiddes, I. T., ... Flicek, P. (2019) GENCODE reference annotation for the human and mouse genomes. *Nucleic Acids Research*, **47**, D766–D773.
 48. Marchetti, F., Zhou, G., LeBlanc, D., White, P. A., Williams, A., Yauk, C. L., & Douglas, G. R. (2021) The 28 + 28 day design is an effective sampling time for analyzing mutant frequencies in rapidly proliferating tissues of MutaMouse animals. *Archives of Toxicology*, **95**, 1103–1116.
 49. Fung, K. Y., Lin, X., & Krewski, D. (1998). Use of generalized linear mixed models in analyzing mutant frequency data from the transgenic mouse assay. *Environmental and Molecular Mutagenesis*, **31**, 48–54.
 50. Gelman A., & Hill, J. (2007) Analytical Methods for Social Research. *Data analysis using regression and multilevel/hierarchical models*. Cambridge University Press, New York.

51. Højsgaard S, Halekoh U (2018) doBy: Groupwise Statistics, LSmeans, Linear Estimates, Utilities (R package 4.6.10).
52. Piegorsch, W. W., & Bailer, A. J. (1994) Statistical approaches for analyzing mutational spectra: Some recommendations for categorical data. *Genetics*, **136**, 403–416.
53. Esina, E., Dodge, A. E., Williams, A., Schuster, D. M., LeBlanc, D. P. M., Marchetti, F., & Yauk, C. L. (2024) Power analyses to inform Duplex Sequencing study designs for MutaMouse liver and bone marrow. *Environmental and Molecular Mutagenesis*, **65**, 234–242.
54. Gelman, A., & Hill, J. (2007) Sample size and power calculations. *Data analysis using regression and multilevel/hierarchical models*, 437-454. Cambridge University Press, New York.
55. Bolker, B. (2008) Ecological models and data in R. Princeton, NJ: Princeton University Press.
56. Johnson, P. C. D., Barry, S. J. E., Ferguson, H. M., & Müller, P. (2015). Power analysis for generalized linear mixed models in ecology and evolution. *Methods in Ecology and Evolution*, **6**, 133–142.
57. Sadler, N. C., Nandhikonda, P., Webb-Robertson, B.-J., Ansong, C., Anderson, L. N., Smith, J. N., Corley, R. A., & Wright, A. T. (2016) Hepatic Cytochrome P450 Activity, Abundance, and Expression Throughout Human Development. *Drug Metabolism and Disposition*, **44**, 984–991.
58. Shiizaki, K., Kawanishi, M., & Yagi, T. (2017) Modulation of benzo[a]pyrene–DNA adduct formation by CYP1 inducer and inhibitor. *Genes and Environment*, **39**, 14.
59. Patel, A. B., Shaikh, S., Jain, K. R., Desai, C., & Madamwar, D. (2020). Polycyclic Aromatic Hydrocarbons: Sources, Toxicity, and Remediation Approaches. *Frontiers in Microbiology*, **11**, 562813.
60. Verma, N., Pink, M., Rettenmeier, A. W., & Schmitz-Spanke, S. (2012) Review on proteomic analyses of benzo[a]pyrene toxicity. *PROTEOMICS*, **12**, 1731–1755.
61. Beal, M. A., Meier, M. J., Williams, A., Rowan-Carroll, A., Gagné, R., Lindsay, S. J., Fitzgerald, T., Hurles, M. E., Marchetti, F., & Yauk, C. L. (2019) Paternal exposure to benzo(a)pyrene induces genome-wide mutations in mouse offspring. *Communications Biology*, **2**, 228.
62. O’Brien, J. M., Beal, M. A., Yauk, C. L., & Marchetti, F. (2016) Next generation sequencing of benzo(a)pyrene-induced *lacZ* mutants identifies a germ cell-specific mutation spectrum. *Scientific Reports*, **6**, 36743.
63. Bloom, J. C., Loehr, A. R., Schimenti, J. C., & Weiss, R. S. (2019) Germline genome protection: Implications for gamete quality and germ cell tumorigenesis. *Andrology*, **7**, 516–526.
64. Milholland, B., Dong, X., Zhang, L., Hao, X., Suh, Y., & Vijg, J. (2017) Differences between germline and somatic mutation rates in humans and mice. *Nature Communications*, **8**, 15183.
65. Chatterjee, N., & Walker, G. C. (2017) Mechanisms of DNA damage, repair, and mutagenesis. *Environmental and Molecular Mutagenesis*, **58**, 235–263.
66. Ozturk, S., & Demir, N. (2011) DNA repair mechanisms in mammalian germ cells. *Histology and Histopathology*, **26**, 505–517.

67. Sarasin, A. (2003) An overview of the mechanisms of mutagenesis and carcinogenesis. *Mutation Research/Reviews in Mutation Research*, **544**, 99–106.
68. Xu, G., Spivak, G., Mitchell, D. L., Mori, T., McCarrey, J. R., McMahan, C. A., Walter, R. B., Hanawalt, P. C., & Walter, C. A. (2005) Nucleotide Excision Repair Activity Varies Among Murine Spermatogenic Cell Types1. *Biology of Reproduction*, **73**, 123–130.
69. Pray, L. (2008) DNA Replication and Causes of Mutation. *Nature Education*, **1**, 214
70. Schreck, I., Chudziak, D., Schneider, S., Seidel, A., Platt, K. L., Oesch, F., & Weiss, C. (2009) Influence of aryl hydrocarbon- (Ah) receptor and genotoxins on DNA repair gene expression and cell survival of mouse hepatoma cells. *Toxicology*, **259**, 91–96.
71. Varshavsky, J. R., Rayasam, S. D. G., Sass, J. B., Axelrad, D. A., Cranor, C. F., Hattis, D., Hauser, R., Koman, P. D., Marquez, E. C., Morello-Frosch, R., Oksas, C., Patton, S., Robinson, J. F., Sathyanarayana, S., Shepard, P. M., & Woodruff, T. J. (2023) Current practice and recommendations for advancing how human variability and susceptibility are considered in chemical risk assessment. *Environmental Health*, **21**, 133.
72. Beal, M. A., Yauk, C. L., & Marchetti, F. (2017) From sperm to offspring: Assessing the heritable genetic consequences of paternal smoking and potential public health impacts. *Mutation Research/Reviews in Mutation Research*, **773**, 26–50.

CHAPTER THREE

DATA CHAPTER
MADISON T. STEWART

Aging Does Not Induce Spontaneous Mutations in Unexposed MutaMouse Male Germ Cells Spanning 3 Weeks to 37 Weeks of age

Madison T. Stewart^{1,2}, Gu Zhou¹, Danielle P.M. LeBlanc¹, Annette E. Dodge¹, Matthew J. Meier¹, Andrew Williams¹, Carole L. Yauk^{2,*}, Francesco Marchetti^{1,3,*}

¹Environmental Health Science and Research Bureau, HECSB, Health Canada, Ottawa, ON, Canada; ²Department of Biology, University of Ottawa, Ottawa, ON, Canada; ³Department of Biology, Carleton University, Ottawa, ON, Canada.

* Correspondence to: carole.yauk@uottawa.ca and Francesco.marchetti@hc-sc.gc.ca

3.1 Abstract

De novo mutations occurring in male germ cells increase with age, contributing to the age-associated decline in fertility and the heightened risk of disease in progeny. Understanding the implications of aging for germ cells is important. However, studying the impact of age-related mutagenicity can be challenging given that these are incredibly rare events, occurring at frequencies of 1-2 mutations every 100,000,000 nucleotides. Herein, we investigated the effects of aging on male germ cells using the gold-standard transgenic rodent gene (TGR) mutation *lacZ* assay and an error-corrected next-generation sequencing technology known as duplex sequencing (DS). We evaluated the impact of age in mouse male germ cells to explore whether mutations would significantly increase in mice spanning 3 weeks to 37 weeks of age. MutaMouse males were analyzed at 13-15, 25-27, and 35-37 weeks using the TGR *lacZ* assay and at 3, 13-15, 25-27, and 35-37-weeks using DS. For the *lacZ* assay, eight animals per time point were analyzed and mutant frequencies were calculated. For DS, eight animals were investigated at 3 weeks and 13-15 weeks, and six animals were analyzed at 25-27 weeks and 35-37 weeks. We detected a statistically significant increase ($p = 0.004$) in *lacZ* mutant frequencies at 35-37 weeks with respect to 13-15 weeks. No significant increases in mutation frequencies (MF) were observed at 35-37 weeks relative to 3 weeks using DS; however, we identified a significant trend for increasing MF of C:G > T:A transitions ($p = 0.04$) across all time points. Thus, our findings do provide some evidence to support an increase in germ cell mutations with aging. Additional analyses on older mice should be performed to further investigate the implications of age on germline mutations.

3.2 Introduction

The process of aging is associated with molecular and cellular changes. These changes include reduced genomic stability, telomere maintenance, and mitochondrial function along with elevated inflammation, epigenetic alterations, and deregulated nutrient sensing (Lopez-Otin et al., 2023). Spontaneous mutation and epigenetic alteration rates in male germ cells increase with age and are contributing factors for the age-related decline in fertility and the elevated risk of disease in offspring (Jenkins et al., 2014). Several disorders including autism (Parner et al., 2012), schizophrenia (Pedersen et al., 2014), bipolar disorder (Hare & Moran, 1979), Huntington's disease (Goldberg et al., 1993), and childhood leukemia (Yip et al., 2006) have been linked to paternal age at conception (De Sena Brandine et al., 2023). The repercussions associated with aging in male germ cells impact future generations and therefore extensive research in this field is required.

The reproductive effects of aging are far less understood in men than women given the well-defined biological event known as menopause that marks reproductive aging in females (Broekmans et al., 2007). Spermatogenesis, the process by which sperm is produced from stem cells in the testes, is dependent on sufficient levels of testicular testosterone and an adequate number of healthy Sertoli cells; somatic cells directly involved in the development of germ cells. The number of Sertoli cells and Leydig cells, which synthesize testicular testosterone, decrease with age in humans leading to ineffective spermatogenesis (Mularoni et al. 2020). In addition, aging is associated with reduced sperm counts and sperm quality as well as elevated sperm defects, DNA damage, and epigenetic alterations (Schmid et al. 2007, Oliveira et al. 2014, Kleshchev et al. 2023). Increased genetic and epigenetic sperm abnormalities related to age can lead to greater prevalences of pregnancy loss, congenital defects, and gene mutations in humans (Yatsenko & Turek, 2018) and animals (Serre & Robaire 1998). Additionally, in mammals, female fertility ceases as they age, while male fertility and sperm quality gradually decreases over time (Wyrobek et al., 2006). Evidence suggests that aging is associated with increased DNA damage in the spermatozoa during epididymal transit, leading to lower rates of fertilization and embryo development (Endo et al., 2024). Despite this, the age-related decline

in sperm production and the effects of mutagenesis on male fertility with advanced age are not fully understood (Albani et al., 2019).

Mutations occur in every generation despite the presence of accurate DNA repair pathways in germ cells (Panier et al., 2024). DNA damage response mechanisms in germ cells are highly effective at protecting genome integrity throughout life. In contrast, DNA repair mechanisms in somatic tissues are effective early on life yet decline in the later, post-reproductive stages (Gorbunova et al., 2007). Despite this, germ cells can still acquire mutations through various mechanisms (Aitken, 2024). Studies have shown that mutation rates are positively correlated with paternal age (Kong et al., 2012) and that 75%-80% of mutations in the gene pool are contributed by males (Kong et al., 2012, Crow, 2000). For every additional year in paternal age at conception, approximately 1.2 additional *de novo* mutations (i.e., newly occurred germline mutations in one generation) occur in the offspring on average in humans (Shojaeisaadi et al., 2024, Goldmann et al., 2019). To identify genetic variations when analyzing human germ cell mutations, whole-genome sequencing of family pedigrees is often used however, this approach involves collecting data from a large number of families which can be extremely costly (Webster et al., 2018). Advanced sequencing technologies have emerged that enable direct analyses of extremely rare mutation events and can be applied to improve our understanding of the etiology of paternal age effects (Shojaeisaadi, 2024).

Error-corrected next generation sequencing technologies have now been applied to analyze the effects of aging. Notably, duplex sequencing (DS) studies have shown more mutations in germ cells associated with congenital diseases in older men relative to younger men (Salazar et al., 2022). Highly accurate, error-corrected sequencing technologies provide a powerful approach to study the implications of mutations caused by exogenous or endogenous factors on the male germline. Herein, we investigated the effects of aging on mutant frequency using a conventional laboratory methodology that characterizes mutations in a bacterial gene of transgenic rodents. In addition, we quantified mutation frequency (MF) and spectrum using the highly accurate DS technology. Specifically, germ cells from the seminiferous tubules of MutaMouse males that were 13-15, 25-27, and 35-37 weeks of age were analyzed using the transgenic rodent gene (TGR) mutation *lacZ* assay (OECD, 2022) (N = 8 per age). These germ

cells were also investigated using DS alongside an additional group of 3-week-old mice (N = 8 for 3 week and 13-15-week-old mice; N = 6 for 25-27- and 35-37-week-old mice). The objectives of our study were to: 1) measure the impact of age on spontaneous MF of MutaMouse male germ cells; and 2) identify age-related changes in the mutation spectra in male germ cells.

3.3 Materials and Methods

3.3.1 Animal and Tissue Collection

Animal handling and tissue collection followed the Health Canada Ottawa Animal Care guidelines. MutaMouse males derived from Health Canada's MutaMouse colony were used in this study. Mice were 3-, 13-15-, 25-27- and 35-37-weeks old at tissue collection. Mice of 13-15, 25-27, and 35-37 weeks of age were the controls from an exposure study to evaluate the mutagenicity of BbF, and received olive oil by gavage for 28, 90, and 180 days. Mice were then euthanized, and tubule germ cells were extracted from the seminiferous tubules as outlined in O'Brien et al. (2014). After extraction, germ cells were flash frozen and stored at -80°C.

3.3.2 Transgenic Rodent Gene Mutation Assay (LacZ assay)

A phenol/chloroform-based method was used to extract DNA as described previously (O'Brien et al., 2014) and in Chapter 2. Briefly, precipitated DNA dissolved in 40-100 µL of Tris-EDTA buffer (10 mM Tris pH 7.6, 0.1 mM EDTA) was stored at 4°C and the purity and quality of DNA was measured using a NanoDrop spectrophotometer at A260 (Thermo Scientific Canada, Ottawa, Canada). Following manufacturer's instructions, the λgt10 phage vectors were excised from genomic DNA using commercial packaging extract kits (Agilent Technology, Santa Clara, CA, USA). Mutant frequencies were determined using a phenyl β-d-galactopyranoside (P-gal) positive selection assay (Lambert et al., 2005). Eight animals at 13-15, 25-27, and 35-37 weeks were analyzed. 3-week-old mice were not evaluated using the *lacZ* assay given the insufficient amount of DNA extracted from these mice for this assay. As per OECD TG 488 (OECD, 2022), an average of 300,000 plaque forming units (PFU) were counted for each animal (ranging from 150,000 to 500,000 PFU). To calculate mutant frequencies, mutant plaques were divided by

total PFU calculated from plaques that formed in bacterial lawns grown under non-selective conditions.

3.3.3 Duplex Sequencing (DS)

Three-, 13-15-, 25-27- and 35-37-week-old mice were analyzed using DS. Eight additional animals were evaluated at 3 weeks. The same eight animals used for the *lacZ* assay were then available for sequencing at 13-15 weeks, while six animals per time point were available at 25-27 weeks and 35-37 weeks. DNA was extracted using the Qiagen DNeasy blood and tissue kits were used for DNA extraction as outlined in the user's manual (DNeasy Blood & Tissue Handbook, Qiagen, Germany, July 2020). The Qubit 1x dsDNA Broad Range Assay Kit (Thermo Fischer, Waltham, MA, USA) was used to measure extracted DNA, and the DNA integrity number (DIN) was identified using high-sensitivity DNA tapes and the Agilent TapeStation Genomic ScreenTape assay (Agilent Technologies, Santa Clara, CA, USA). A DIN > 7 was confirmed for all samples prior to use in DS library preparations.

DNA was prepared for sequencing as described in Chapter 2. Briefly, to obtain ~300 bp-sized DNA fragments, 1000 ng of extracted DNA from each sample was enzymatically fragmented. Fragmented DNA was then end-polished, A-tailed, and ligated to DS Sequencing Adapters (TwinStrand Biosciences, Seattle WA, USA). To capture the Mouse Mutagenesis panel targets after PCR amplification (described in detail in Chapter 2), 120mer biotinylated oligo probes were used (Integrated DNA Technologies, Coalville, IA, USA). DS libraries were sequenced on an Illumina NovaSeq 6000 (San Diego, CA, USA) at Psomagen (Rockville, MD, United States) to generate an average of approximately 750 million raw reads per sample. A minimum of 500 million informative duplex bases was set as a threshold for inclusion in the DS analyses.

To process the FASTQ files, the TwinStrand Biosciences Duplex-Seq Mutagenesis App (3.11.0) (TwinStrand Biosciences, Seattle, WA, USA) on the DNAnexus platform was used as described previously (Dodge et al., 2023). This software developed variant call files (VCF) for each library, as well as sequencing summary metrics and mutagenesis metrics such as MF and base substitution spectrum. Additionally, the TwinStrand Biosciences Duplex-Seq Mutagenesis

App isolates duplex tags, aligns raw reads, classifies the reads based on strand defining elements and unique molecular identifiers, generates duplex consensus calls for error-correction of the read groups, and performs consensus post-processing, re-alignment, and variant calling (Valentine et al., 2020).

Two approaches were used to quantify MF. The first approach, referred to as MF_{\min} , assumes that all identical mutations within a sample result from clonal expansion of a single mutational event. The second approach, known as MF_{\max} , assumes that all identical mutations occurred as independent mutational processes. These approaches are outlined in detail in Dodge et al. (2023).

3.3.4 Statistical Analyses

3.3.4.1 TGR Analyses

For the *lacZ* experiment, mutant frequencies were phenotypically scoreable mutants per *lacZ* locus. A generalized linear model (GLM) using the `model_mf` function based on a quasibinomial distribution was applied to estimate mutant frequency by age. P-values at each time point with respect to the 3-week-old mice were adjusted using the Holm-Sidak correction for multiple testing.

3.3.4.2 DS Analyses

DS analyses were performed using the MutSeqR package (<https://github.com/EHSRB-BSRSE-Bioinformatics/MutSeqR>). For DS, MF_{\min} and MF_{\max} expressed as mutations per 10^8 bp were used to analyze mutagenicity. To calculate MF_{\min} and MF_{\max} by age, a GLM based on a quasibinomial distribution was applied. Pairwise comparisons based on age were performed using the "doBy" package in RStudio (Højsgaard and Halekoh, 2018). These estimates were then back-transformed, and the delta method was employed to approximate the back-transformed standard errors (standard error of the mean; SEM) of the calculated MF. P-values for MF_{\min} and MF_{\max} at each age were compared to the 3-week-old mice and adjusted using Holm-Sidak correction for multiple testing.

A generalized linear mixed model (GLMM) based a binomial error distribution using the `model_mf` function was applied to estimate MFs by target. Based on time point and location relative to genes, pairwise comparisons were performed using the “doBy” package in RStudio as described above.

As outlined by Piegorsch and Bailer (1994), a modified contingency table approach was used to evaluate mutation subtypes at each time point relative to mice at 3 weeks. A GLM with a quasibinomial distribution and pairwise comparisons were employed to investigate whether mutation subtypes at each time point were significantly increased relative to the 3-week-old animals. The MF_{\min} approach was used for these mutation spectrum analyses.

3.4 Results

3.4.1 *LacZ* Mutant Frequencies

The TGR *lacZ* assay was used to investigate the effects of aging in male on mutant frequencies at 13-15, 25-27, and 35-37 weeks. An average of approximately 300,000 PFU per mouse were analyzed.

Mutant frequencies ($\times 10^{-5} \pm \text{SEM}$) were 1.55 ± 0.20 , 2.28 ± 0.29 , and 2.89 ± 0.36 at 13-15, 25-27, and 35-37 weeks respectively (Figure 3.1, Table 3.1). A significant ($p\text{-value} = 0.004$) 1.9-fold-increase in mutant frequencies was detected for the 35-37-week-old mice compared to the 13-15-week-old mice (Figure 3.1, Table 3.1). There was no difference between 13-15 weeks and 25-27 weeks.

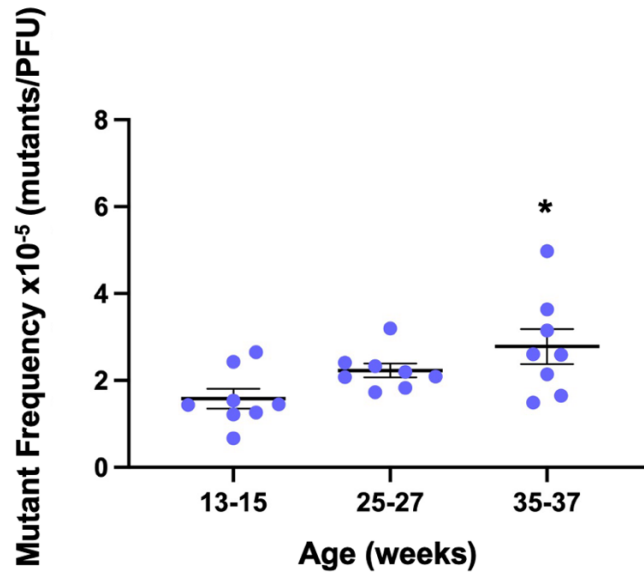


Figure 3.1. *LacZ* mutant frequencies in MutaMouse male germ cells at 13-15, 25-27, and 35-37 weeks. Mutants per plaque forming units (PFU) represent mutant frequencies for all mice at each time point. Mean mutant frequency and SEM are shown. Actual values for each animal are presented as individual points; horizontal lines indicate the mean; error bars represent SEM. The asterisk indicates statistical significance ($p = 0.004$).

Table 3.1. Average *lacZ* mutant frequencies in MutaMouse male germ cells at 13-15, 25-27, and 35-37 weeks.

Time Point	# of Animals per Time Point	Average PFU	Average <i>lacZ</i> MF* \pm SEM ($\times 10^{-5}$)	Fold Changes	P-values
13-15 weeks	8	362,872	1.55 ± 0.20	---	---
25-27 weeks	8	310,314	2.28 ± 0.28	1.47	0.118
35-37 weeks	8	278,693	2.89 ± 0.36	1.87	0.004

*Values are presented as estimates obtained using GLM

3.4.2 DS Mutation Frequencies

DS was applied to calculate MF and analyze the mutation spectra across 20 loci in the mouse genome at each time point. An input of 1000 ng DNA and an average 1-1.5 billion informative duplex bases were used relative to studies on somatic tissues given that MF is lower

in germ cells than somatic cells (Esina et al., 2024). Approximately an average of 2.0 billion informative duplex bases were obtained at 3, 13-15, 25-27, and 35-37 weeks, with a total average of around 14 billion informative duplex bases for each time point (Table 3.2, Supp. Figure 3.1).

We divided the number of mutations by the total number of duplex bases obtained for each sample to calculate MF. Using the MF_{\min} assumption, we identified 782, 947, 381, and 363 unique mutations at 3, 13-15, 25-27, and 35-37 weeks, respectively. We observed no significant increases in MF ($\times 10^{-8}$) at any of the time points relative to the 3-week-old mice. MF_{\min} was 4.18 ± 0.34 (\pm SEM) for the 3-week-old mice and 4.48 ± 0.64 for the 35-37-week-old mice. The highest MF_{\min} was at 13-15 weeks (4.81 ± 0.35), although no significant increases were detected (Figure 3.2, Table 3.2).

Using the MF_{\max} assumption, we obtained 1741, 1279, 465, and 464 mutations at 3, 13-15, 25-27, and 35-37 weeks. There were no significant age-dependent increases in MF ($\times 10^{-8}$) at any of the time points with respect to the 3-week-old mice. MF_{\max} was 9.94 ± 2.53 at 3 weeks and 5.79 ± 3.52 at 35-37 weeks. The higher average at 3 weeks was mainly driven by one mouse with a significantly higher MF_{\max} relative to the remaining animals at this time point (Figure 3.2, Table 3.2).

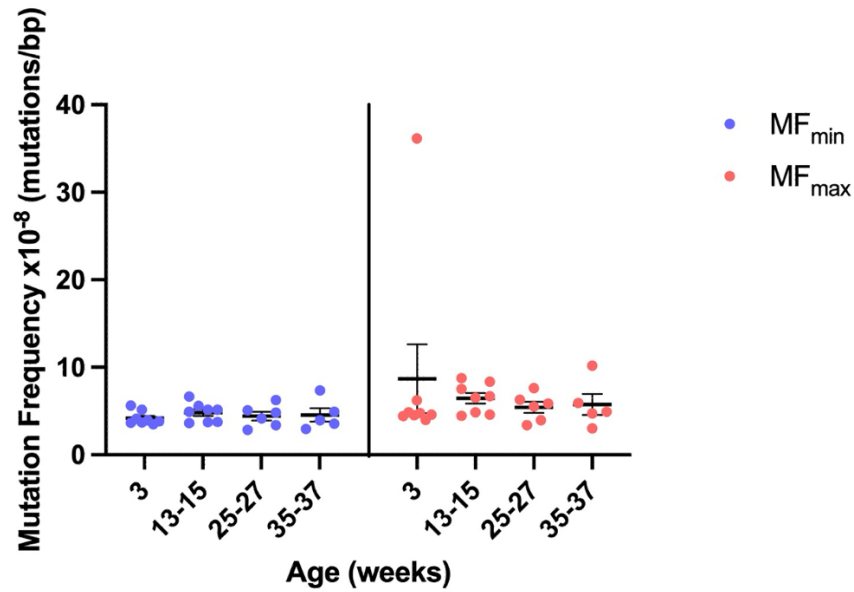


Figure 3.2. MF in MutaMouse male germ cells at 3, 13-15, 25-27, and 35-37 weeks using the MF_{min} assumption (A) and the MF_{max} assumption (B). MF_{min} and MF_{max} are represented as mutations per x10⁻⁸ basepair (bp) for each animal at each time point. Mean MF and SEM are shown. Individual points represent the observed values; horizontal lines demonstrate the calculated means.

Table 3.2. Average DS MF_{min} and MF_{max} in MutaMouse male germ cells at 3, 13-15, 25-27, and 35-37 weeks.

Time Point	# of Animals per Time Point	Average Informative Duplex Bases	Average MF _{min} ± SEM (x10 ⁻⁸)	Fold Changes	P-values	Average MF _{max} ± SEM (x10 ⁻⁸)	Fold Changes	P-values
3 weeks	8	2,340,637,008	4.18 ± 0.34	---	---	9.94 ± 2.53	---	---
13-15 weeks	8	2,460,279,000	4.81 ± 0.35	1.15	0.210	6.54 ± 1.96	0.66	0.298
25-27 weeks	6	1,569,071,844	3.70 ± 0.52	0.88	0.456	4.48 ± 2.77	0.45	0.245
35-37 weeks	5	1,605,082,798	4.48 ± 0.64	1.07	0.672	5.80 ± 3.52	0.58	0.421

*Values presented as estimates from GLM

3.4.3 DS Mutation Frequency by Target

Next, we analyzed changes in MF across the 20 genic and intergenic targets of the mouse mutagenesis panel to determine locus-specific differences with age. Given the low number of mutations identified, we combined genic vs intergenic targets for each time point rather than conducting analyses for each single target.

MF_{\min} ($\times 10^{-8}$) at genic targets were 4.51 ± 0.28 , 5.14 ± 0.33 , 5.27 ± 0.53 , and 5.18 ± 0.52 at 3, 13-15, 25-27, and 35-37 weeks, respectively. At intergenic targets, MF_{\min} were 3.89 ± 0.36 , 4.50 ± 0.33 , 3.77 ± 0.40 , and 4.05 ± 0.41 for the 3, 13-15, 25-27, and 35-37 time points, respectively. We observed higher MF_{\min} in genic regions relative to intergenic regions at each time point. The differences between regions were significant at 13-15 weeks ($p = 0.02$) and marginally significant at 25-27 and 35-37 weeks ($p = 0.058$ and 0.059 at 25-27 and 35-37 weeks, respectively) (Figure 3.3A).

Using the MF_{\max} assumption, for genic targets, MF_{\max} ($\times 10^{-8}$) at 3, 13-15, 25-27, and 35-37 weeks were 5.49 ± 0.36 , 7.35 ± 0.82 , 6.90 ± 0.79 , and 6.85 ± 0.87 , respectively. At intergenic regions, MF_{\max} for the 3-, 13-15-, 25-27- and 35-37-week time points were 11.4 ± 7.15 , 5.64 ± 0.44 , 4.31 ± 0.47 , and 4.88 ± 0.56 , respectively. At 3 weeks, we detected a higher MF_{\max} for intergenic regions with respect to genic regions (Figure 3.3B). We found significant differences between genic and intergenic regions at 13-15, 25-27, and 35-37 weeks (Figure 3.3B) ($p < 0.001$ at 13-15, 25-27 and 35-37 weeks).

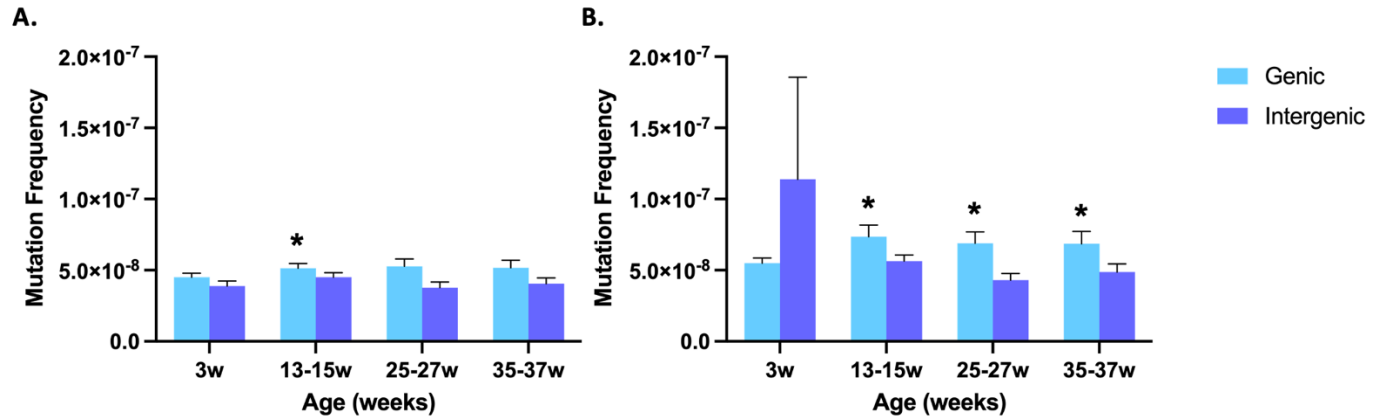


Figure 3.3. Average MF for intergenic and genic targets using MF_{min} (A) and MF_{max} (B) assumptions at 3, 13-15, 25-27, and 35-37 weeks. Mean MF and SEM for genic and intergenic targets are presented for each time point. Asterisks indicate significant differences in MF between genic and intergenic regions across time points ($p < 0.05$).

3.4.4 DS Mutation Spectrum

The spontaneous mutation spectra are comprised of small nucleotide variants (SNVs), deletions, multi-nucleotide variants, and insertions. For all time points, the mutation spectra were primarily driven by C:G > T:A transitions and C:G > A:T transversions, followed by T:A > A:T transversions (Figure 3.4).

We observed significant differences in the mutation spectra at 13-15 and 35-37 weeks relative to 3-weeks ($p < 0.001$ at 13-15 weeks; $p = 0.01$ at 35-37 weeks). Marginal significant differences were observed at 25-27 weeks ($p = 0.058$). At 3 weeks, MF for C:G > T:A transitions, C:G > A:T transversions, and T:A > A:T transversions were 1.80 ± 0.17 , 1.62 ± 0.13 , and 0.49 ± 0.08 , respectively. At 13-15 weeks, MF at these mutations were correspondingly identified as 2.31 ± 0.15 , 1.61 ± 0.16 , and 0.96 ± 0.12 . At 25-27 weeks MF were calculated as 2.09 ± 0.27 , 1.48 ± 0.3 , and 0.67 ± 0.11 for each appropriate mutation subtype. At 35-37 weeks, MF were 2.52 ± 0.33 , 1.25 ± 0.20 , and 0.87 ± 0.27 for C:G > T:A transitions, C:G > A:T transversions respectively (Figure 3.4). At all time points, we detected no statistically significant increases in MF at C:G > T:A transitions relative to 3 weeks. However, there was a significant time-dependent increasing trend in these mutations ($p < 0.04$) (Supp. Figure 3.2). In addition, there

was a significant increase in T:A > A:T transversions with respect to 3 weeks ($p = 0.01$) (Figure 3.4).

Previous human studies have shown that mutations at CpG sites increase with age (Shojaeisaadi et al., 2024). Because of this, we performed additional analyses to evaluate the trinucleotide spectra. Although not significant, this analysis revealed increases in mutations at CpG sites at 35-37 weeks with respect to 3 weeks, specifically at trinucleotides GCG (Supp. Figure 3.3).

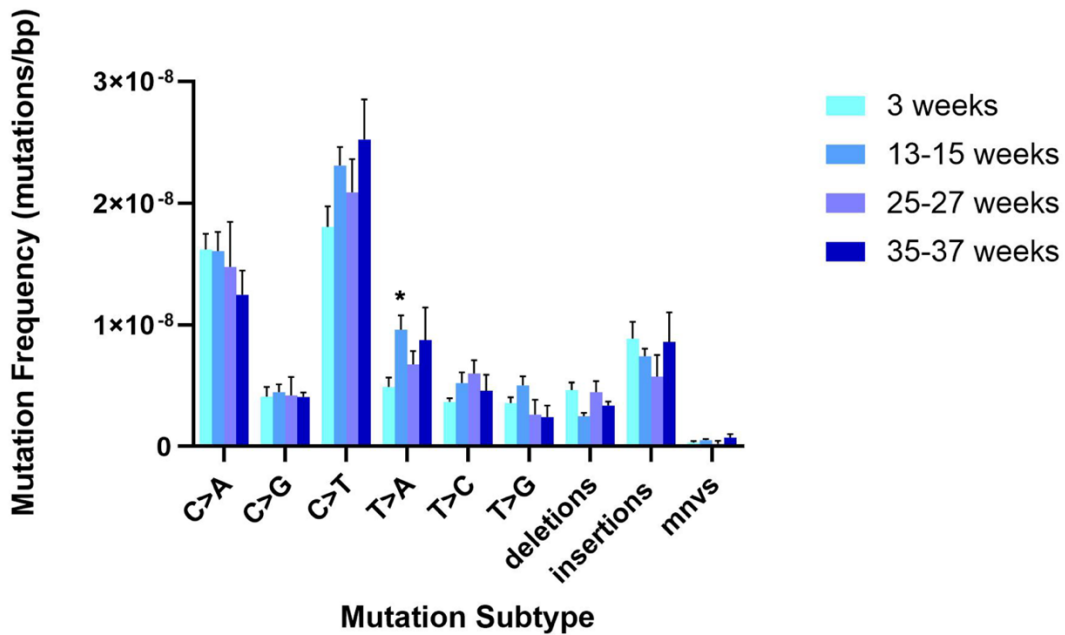


Figure 3.4. DS mutation spectrum in germ cells of MutaMouse males at 3, 13-15, 25-27, and 35-37 weeks. Average MF_{min} is presented for each mutation subtype at each time point.

Mutation subtypes shown on the x-axis include single nucleotide variants, multi nucleotide variants (mnv), deletions and insertions. Error bars are SEM. We observed significant differences in the overall mutation spectra at 13-15 weeks and 35-37 weeks with respect to 3 weeks ($p < 0.001$ at 13-15 weeks and $p = 0.01$ at 35-37 weeks). The asterisk indicates statistical significance ($p = 0.01$).

3.5 Discussion

We investigated the effects of aging on mutations in tubule germ cells of male mice using the *lacZ* assay and DS. We detected a statistically significant increase in mutant frequency at 35-37 weeks with respect to 13-15 weeks using the *lacZ* assay. However, no increases in MF were observed using DS at any time points relative to 3 weeks. Additionally, analysis of genic and intergenic regions independently did not reveal an age-associated effect. Despite no significant age-dependent increases in C:G > T:A transitions, we identified a significant increasing trend with age in MF across all time points for this SNV and a significant increase in T:A > A:T transversions at 13-15 weeks relative to 3 weeks. Overall, our study demonstrates a small impact of aging on the *lacZ* gene and marginal impacts on endogenous genic and intergenic loci over the 34-week age span studied.

We observed an age-effect for mutations with the *lacZ* assay but not with DS, even though we tested a larger age difference with the latter. This contrasting result is likely driven by the low mutant frequency observed at 13-15 weeks. An historical control database can be used as a reference for assessing mutagenic effects. Our historical control mutant frequency ($\times 10^{-5}$) is 2.51 ± 1.18 and the 95% confidence intervals of this database are 1.13 and 5.50 (Supplementary Table 2.2). Although the mutant frequency observed at 13-15 weeks (1.55×10^{-5}) is within the historical control database, it is on the low end of the distribution. Furthermore, the mutant frequency observed at 35-37 weeks is not different from the historical control frequency suggesting we must be cautious to not over-interpret the biological relevance of the observed effect.

Advancements in technology such as DS have made it possible to readily characterize mutational spectra and signatures. Previous studies have investigated age-related somatic mutations in the cancer genome and have observed age-dependent increases in the proportion of C:G > T:A transitions (Milholland et al., 2015) and increases in mutations at CpG sites in humans (Shojaeisaadi et al., 2024). Herein, we did not detect age-related significant increases in MF at C:G > T:A mutations. However, there was a significant increasing trend in MF at C:G > T:A mutations across all time points. An age-dependent increase in C:G > T:A mutations is consistent with a widespread mutational signature associated with age (Alexandrov et al.,

2013). The increase in these mutations is presumed to be initiated by spontaneous deamination of 5-methyl-cytosine and primarily occurs at CpG sites (Pfeifer, 2006). Thus, we specifically analyzed mutations at CpG sites. The analysis revealed an increase, although not significant, in mutations at CpG sites for the 35-37-week time point relative to the 3-week time point. Overall, our results provide evidence to support the potential mutagenic effects of age on male germ cells. The small impacts we observe on MF and in C:G > T:A transitions could be due to the limited age range used in this study. To our knowledge, this is the first study to ever investigate the effects of aging on spontaneous mutations in mouse male germ cells. If these mice were to live up to two years as expected, this would constitute approximately one third of their lifetime and thus the effects of aging on male germ cell mutations could be more evident in older mice. Because of this, additional analyses on older mice are required to extend these findings.

Unlike traditional mutation assays, DS can be used to differentiate between mutations that are unique and those resulting from clonal expansion. We detected more clonally expanded mutations at 3 weeks with respect to all time points. However, the greater extent of clonal expansion observed at 3 weeks was mainly driven by one mouse that could be considered an outlier. When eliminating this mouse, we observe lower clonal expansion relative to the later time points as expected. Excluding this outlier, we observe the most clonal expansion at 13-15 weeks. This finding could be explained by the higher number of informative duplex bases sequenced at this time point (2,460,279,000 bases) relative to 35-37 weeks (1,605,082,798 bases). The 13-15-week samples were sequenced more deeply and thus more mutations were identified. Overall, our results demonstrate high variability between animals when using MF_{\max} and suggest that MF_{\min} should be the primary focus of DS studies, as recommended in previous work (LeBlanc et al., In press).

Previous DS studies have observed that the occurrence of chemically induced mutations in somatic tissues are more frequent in intergenic regions than genic regions (Schuster et al., 2024, LeBlanc et al., 2022, Dodge et al., 2023). These results are consistent with transcription-coupled repair (TCR), where higher rates of DNA repair occur in transcribed regions of the genome (Luzadder et al., 2024). In our work, we observed higher MF_{\min} and MF_{\max} in genic regions compared to intergenic regions at 13-15, 25-27, and 35-37 weeks. These results could be

explained by the distinct characteristics of germ cells relative to somatic tissues. Previous studies have investigated genomic features and their influence on mutation rates in the soma and germline. Using a statistical model that predicted the mutation rate of a coding region based on GC content, expression levels, replication timing and two histonepressive marks, Chen et al. (2017) observed decreases in mutation rates with expression levels in somatic tissues; however, in the testis, increases in mutation rates with expression levels were detected. In this study, authors hypothesized that these increases may result from more DNA damage due to high transcriptional activity or due to errors that occur during TCR. In germ cells, TCR is less effective relative to somatic tissues and thus, more mutations accumulate during transcription. (Chen et al., 2017). Overall, our results suggest potential differences in damage and repair rates during transcription between somatic tissues and germ cells.

3.6 Conclusions

In summary, our study reveals marginal effects of aging at 35-37 weeks on mouse male germ cell mutagenesis. We observed statistically significant increases in mutant frequency using the TGR *lacZ* assay at 35-35 weeks relative to 13-15 weeks; however, the mutant frequency at this time point was lower than our historical control MF suggesting caution in this interpretation. Additionally there were no significant increases in MF or in C:G > T:A mutations using DS, however a significant age-related trend in these mutations was identified. We also found an age-dependent increase, although not significant, in mutations at CpG sites; regions associated with changes in DNA methylation with age. Overall, our results suggest that aging does not induce mutations at 35-37 weeks in male germ cells, however our findings could be explained by the limited age-range used to detect an effect. Thus, future work will need to focus on investigating the impact of aging in germ cells of older mice.

3.7 References

Aitken, R. J. (2024). Paternal age, *de novo* mutations, and offspring health? New directions for an ageing problem. *Human Reproduction*, deae230. <https://doi.org/10.1093/humrep/deae230>

Albani, E., Castellano, S., Gurrieri, B., Arruzzolo, L., Negri, L., Borroni, E. M., & Levi-Setti, P. E. (2019). Male age: Negative impact on sperm DNA fragmentation. *Aging*, 11(9), 2749–2761. <https://doi.org/10.18632/aging.101946>

Alexandrov, L. B., Nik-Zainal, S., Wedge, D. C., Aparicio, S. A. J. R., Behjati, S., Biankin, A. V., Bignell, G. R., Bolli, N., Borg, A., Børresen-Dale, A.-L., Boyault, S., Burkhardt, B., Butler, A. P., Caldas, C., Davies, H. R., ... Stratton, M. R. (2013). Signatures of mutational processes in human cancer. *Nature*, 500(7463), 415–421. <https://doi.org/10.1038/nature12477>

Broekmans, F. J., Knauff, E. A. H., Te Velde, E. R., Macklon, N. S., & Fauser, B. C. (2007). Female reproductive ageing: Current knowledge and future trends. *Trends in Endocrinology & Metabolism*, 18(2), 58–65. <https://doi.org/10.1016/j.tem.2007.01.004>

Chen, C., Qi, H., Shen, Y., Pickrell, J., & Przeworski, M. (2017). Contrasting Determinants of Mutation Rates in Germline and Soma. *Genetics*, 207(1), 255–267. <https://doi.org/10.1534/genetics.117.11114>

Crow, J. F. (2000). The origins, patterns and implications of human spontaneous mutation. *Nature Reviews Genetics*, 1(1), 40–47. <https://doi.org/10.1038/35049558>

De Sena Brandine, G., Aston, K. I., Jenkins, T. G., & Smith, A. D. (2023). Global effects of identity and aging on the human sperm methylome. *Clinical Epigenetics*, 15(1), 127. <https://doi.org/10.1186/s13148-023-01541-6>

DeMarini, D. M. (2012). Declaring the existence of human germ-cell mutagens. *Environmental and Molecular Mutagenesis*, 53(3), 166–172. <https://doi.org/10.1002/em.21685>

Dodge, A. E., LeBlanc, D. P. M., Zhou, G., Williams, A., Meier, M. J., Van, P., Lo, F. Y., Valentine Iii, C. C., Salk, J. J., Yauk, C. L., & Marchetti, F. (2023). Duplex sequencing provides detailed characterization of mutation frequencies and spectra in the bone marrow of MutaMouse males exposed to procarbazine hydrochloride. *Archives of Toxicology*, 97(8), 2245–2259. <https://doi.org/10.1007/s00204-023-03527-y>

Ehmcke, J., Wistuba, J., & Schlatt, S. (2006). Spermatogonial stem cells: Questions, models and perspectives. *Human Reproduction Update*, 12(3), 275–282. <https://doi.org/10.1093/humupd/dmk001>

Endo, T., Kobayashi, K., Matsumura, T., Emori, C., Ozawa, M., Kawamoto, S., Okuzaki, D., Shimada, K., Miyata, H., Shimada, K., Kodani, M., Ishikawa-Yamauchi, Y., Motooka, D., Hara, E., &

Ikawa, M. (2024). Multiple ageing effects on testicular/epididymal germ cells lead to decreased male fertility in mice. *Communications Biology*, 7(1), 16. <https://doi.org/10.1038/s42003-023-05685-2>

Fayomi, A. P., & Orwig, K. E. (2018). Spermatogonial stem cells and spermatogenesis in mice, monkeys and men. *Stem Cell Research*, 29, 207–214. <https://doi.org/10.1016/j.scr.2018.04.009>

Feuz, M. B., Nelson, D. C., Miller, L. B., Zwerdling, A. E., Meyer, R. G., & Meyer-Ficca, M. L. (2024). Reproductive Ageing: Current insights and a potential role of NAD in the reproductive health of aging fathers and their children. *Reproduction*, 167(6), e230486. <https://doi.org/10.1530/REP-23-0486>

Frankish, A., Diekhans, M., Ferreira, A.-M., Johnson, R., Jungreis, I., Loveland, J., Mudge, J. M., Sisu, C., Wright, J., Armstrong, J., Barnes, I., Berry, A., Bignell, A., Carbonell Sala, S., Chrast, J., Cunningham, F., Di Domenico, T., Donaldson, S., Fiddes, I. T., ... Flicek, P. (2019). GENCODE reference annotation for the human and mouse genomes. *Nucleic Acids Research*, 47(D1), D766–D773. <https://doi.org/10.1093/nar/gky955>

Frungieri, M. B., Calandra, R. S., Bartke, A., & Matzkin, M. E. (2021). Male and female gonadal ageing: Its impact on health span and life span. *Mechanisms of Ageing and Development*, 197, 111519. <https://doi.org/10.1016/j.mad.2021.111519>

Goldberg, Y. P., Kremer, B., Andrew, S. E., Theilmann, J., Graham, R. K., Squitieri, F., Telenius, H., Adam, S., Sajoo, A., Starr, E., Heiberg, A., Wolff, G., & Hayden, M. R. (1993). Molecular analysis of new mutations for Huntington's disease: Intermediate alleles and sex of origin effects. *Nature Genetics*, 5(2), 174–179. <https://doi.org/10.1038/ng1093-174>

Gorbunova, V., Seluanov, A., Mao, Z., & Hine, C. (2007). Changes in DNA repair during aging. *Nucleic Acids Research*, 35(22), 7466–7474. <https://doi.org/10.1093/nar/gkm756>

Hare, E. H., & Moran, P. A. P. (1979). Raised Parental Age in Psychiatric Patients: Evidence for the Constitutional Hypothesis. *British Journal of Psychiatry*, 134(2), 169–177. <https://doi.org/10.1192/bjp.134.2.169>

Højsgaard S, Halekoh U (2018) doBy: Groupwise Statistics, LSmeans, Linear Estimates, Utilities (R package 4.6.10).

Jenkins, T. G., Aston, K. I., Pflueger, C., Cairns, B. R., & Carrell, D. T. (2014). Age-Associated Sperm DNA Methylation Alterations: Possible Implications in Offspring Disease Susceptibility. *PLoS Genetics*, 10(7), e1004458. <https://doi.org/10.1371/journal.pgen.1004458>

Kaufman, J.-M., Lapauw, B., Mahmoud, A., T'Sjoen, G., & Huhtaniemi, I. T. (2019). Aging and the Male Reproductive System. *Endocrine Reviews*, 40(4), 906–972. <https://doi.org/10.1210/er.2018-00178>

Kleshchev, M., Osadchuk, L., & Osadchuk, A. (2023). Age-Related Changes in Sperm Morphology and Analysis of Multiple Sperm Defects. *Frontiers in Bioscience-Scholar*, 15(3), 12.

<https://doi.org/10.31083/j.fbs1503012>

Kong, A., Frigge, M. L., Masson, G., Besenbacher, S., Sulem, P., Magnusson, G., Gudjonsson, S. A., Sigurdsson, A., Jonasdottir, A., Jonasdottir, A., Wong, W. S. W., Sigurdsson, G., Walters, G. B., Steinberg, S., Helgason, H., Thorleifsson, G., Gudbjartsson, D. F., Helgason, A., Magnusson, O. Th., ... Stefansson, K. (2012). Rate of de novo mutations and the importance of father's age to disease risk. *Nature*, 488(7412), 471–475. <https://doi.org/10.1038/nature11396>

Lambert, I. B., Singer, T. M., Boucher, S. E., & Douglas, G. R. (2005). Detailed review of transgenic rodent mutation assays. *Mutation Research/Reviews in Mutation Research*, 590(1–3), 1–280.

<https://doi.org/10.1016/j.mrrev.2005.04.002>

LeBlanc, D. P. M., Zhou, G., Williams, A., Meier, M., Valentine, C., Salk, J. J., Yauk, C. L., & Marchetti, F. (In press). Duplex Sequencing Identifies Unique Characteristics of ENU-induced Mutations in Male Mouse Germ Cells. *Biology of Reproduction*.

López-Otín, C., Blasco, M. A., Partridge, L., Serrano, M., & Kroemer, G. (2013). The Hallmarks of Aging. *Cell*, 153(6), 1194–1217. <https://doi.org/10.1016/j.cell.2013.05.039>

Luzadder, M. M., Minko, I. G., Vartanian, V. L., Davenport, M., Fedorov, L. M., McCullough, A. K., & Lloyd, R. S. (2025). The Distinct Roles of NEIL1 and XPA in Limiting Aflatoxin B1-Induced Mutagenesis in Mice. *Molecular Cancer Research*, 23(1), 46–58. <https://doi.org/10.1158/1541-7786.MCR-24-0577>

Marchetti, F., Aardema, M., Beevers, C., Van Benthem, J., Douglas, G. R., Godschalk, R., Yauk, C. L., Young, R., & Williams, A. (2018). Simulation of mouse and rat spermatogenesis to inform genotoxicity testing using OECD test guideline 488. *Mutation Research/Genetic Toxicology and Environmental Mutagenesis*, 832–833, 19–28. <https://doi.org/10.1016/j.mrgentox.2018.05.020>

Matzkin, M. E., Calandra, R. S., Rossi, S. P., Bartke, A., & Frungieri, M. B. (2021). Hallmarks of Testicular Aging: The Challenge of Anti-Inflammatory and Antioxidant Therapies Using Natural and/or Pharmacological Compounds to Improve the Physiopathological Status of the Aged Male Gonad. *Cells*, 10(11), 3114. <https://doi.org/10.3390/cells10113114>

Meyer, R. G., & Meyer-Ficca, M. L. (2021). Metabolism in Male Reproductive Aging. *Advances in Geriatric Medicine and Research*. <https://doi.org/10.20900/agmr20210005>

Milholland, B., Auton, A., Suh, Y., & Vijg, J. (2015). Age-related somatic mutations in the cancer genome. *Oncotarget*, 6(28), 24627–24635. <https://doi.org/10.18632/oncotarget.5685>

- Mularoni, V., Esposito, V., Di Persio, S., Vicini, E., Spadetta, G., Berloco, P., Fanelli, F., Mezzullo, M., Pagotto, U., Pelusi, C., Nielsen, J. E., Rajpert-De Meyts, E., Jorgensen, N., Jorgensen, A., & Boitani, C. (2020). Age-related changes in human Leydig cell status. *Human Reproduction*, 35(12), 2663–2676. <https://doi.org/10.1093/humrep/deaa271>
- O'Brien, J. M., Beal, M. A., Gingerich, J. D., Soper, L., Douglas, G. R., Yauk, C. L., & Marchetti, F. (2014). Transgenic Rodent Assay for Quantifying Male Germ Cell Mutant Frequency. *Journal of Visualized Experiments*, 90, 51576. <https://doi.org/10.3791/51576-v>
- OECD (2022) Test No. 488. Transgenic rodent somatic and germ cell gene mutation assay. *OECD guidelines for the testing of chemicals*, section 4. OECD Publishing, Paris.
- Oliveira, J. B. A., Petersen, C. G., Mauri, A. L., Vagnini, L. D., Baruffi, R. L. R., & Franco Jr., J. G. (2014). The effects of age on sperm quality: An evaluation of 1,500 semen samples. *JBRA Assisted Reproduction*, 18(2). <https://doi.org/10.5935/1518-0557.20140002>
- Panier, S., Wang, S., & Schumacher, B. (2024). Genome Instability and DNA Repair in Somatic and Reproductive Aging. *Annual Review of Pathology: Mechanisms of Disease*, 19(1), 261–290. <https://doi.org/10.1146/annurev-pathmechdis-051122-093128>
- Parner, E. T., Baron-Cohen, S., Lauritsen, M. B., Jørgensen, M., Schieve, L. A., Yeargin-Allsopp, M., & Obel, C. (2012). Parental Age and Autism Spectrum Disorders. *Annals of Epidemiology*, 22(3), 143–150. <https://doi.org/10.1016/j.annepidem.2011.12.006>
- Pedersen, C. B., McGrath, J., Mortensen, P. B., & Petersen, L. (2014). The importance of father's age to schizophrenia risk. *Molecular Psychiatry*, 19(5), 530–530. <https://doi.org/10.1038/mp.2013.69>
- Pfeifer, G. P. (2006). Mutagenesis at Methylated CpG Sequences. In W. Doerfler & P. Böhm (Eds.), *DNA Methylation: Basic Mechanisms* (Vol. 301, pp. 259–281). Springer-Verlag. https://doi.org/10.1007/3-540-31390-7_10
- Piegorsch, W. W., & Bailer, A. J. (1994). Statistical approaches for analyzing mutational spectra: Some recommendations for categorical data. *Genetics*, 136(1), 403–416. <https://doi.org/10.1093/genetics/136.1.403>
- Salazar, R., Arbeithuber, B., Ivankovic, M., Heinzl, M., Moura, S., Hartl, I., Mair, T., Lahnsteiner, A., Ebner, T., Shebl, O., Pröll, J., & Tiemann-Boege, I. (2022). Discovery of an unusually high number of de novo mutations in sperm of older men using duplex sequencing. *Genome Research*, 32(3), 499–511. <https://doi.org/10.1101/gr.275695.121>
- Schmid, T. E., Eskenazi, B., Baumgartner, A., Marchetti, F., Young, S., Weldon, R., Anderson, D., & Wyrobek, A. J. (2007). The effects of male age on sperm DNA damage in healthy non-smokers. *Human Reproduction*, 22(1), 180–187. <https://doi.org/10.1093/humrep/del338>

- Schulte, R. T., Ohl, D. A., Sigman, M., & Smith, G. D. (2010). Sperm DNA damage in male infertility: Etiologies, assays, and outcomes. *Journal of Assisted Reproduction and Genetics*, 27(1), 3–12. <https://doi.org/10.1007/s10815-009-9359-x>
- Schuster, D. M., LeBlanc, D. P. M., Zhou, G., Meier, M. J., Dodge, A. E., White, P. A., Long, A. S., Williams, A., Hobbs, C., Diesing, A., Smith-Roe, S. L., Salk, J. J., Marchetti, F., & Yauk, C. L. (2024). *Dose-related Mutagenic and Clastogenic Effects of Benzo[b]fluoranthene in Mouse Somatic Tissues Detected by Duplex Sequencing and the Micronucleus Assay*. <https://doi.org/10.1101/2024.07.26.605228>
- Serre, V., & Robaire, B. (1998). Paternal age affects fertility and progeny outcome in the Brown Norway rat. *Fertility and Sterility*, 70(4), 625–631. [https://doi.org/10.1016/S0015-0282\(98\)00259-3](https://doi.org/10.1016/S0015-0282(98)00259-3)
- Shojaeisaadi, H., Schoenrock, A., Meier, M. J., Williams, A., Norris, J. M., Palmer, N. D., Yauk, C. L., & Marchetti, F. (2024). Mutational signature analyses in multi-child families reveal sources of age-related increases in human germline mutations. *Communications Biology*, 7(1), 1451. <https://doi.org/10.1038/s42003-024-07140-2>
- Shwed, P. S., Crosthwait, J., Douglas, G. R., & Seligy, V. L. (2010). Characterisation of MutaTMMouse *gt10-lacZ* transgene: Evidence for in vivo rearrangements. *Mutagenesis*, 25(6), 609–616. <https://doi.org/10.1093/mutage/geq048>
- Valentine, C. C., Young, R. R., Fielden, M. R., Kulkarni, R., Williams, L. N., Li, T., Minocherhomji, S., & Salk, J. J. (2020). Direct quantification of in vivo mutagenesis and carcinogenesis using duplex sequencing. *Proceedings of the National Academy of Sciences*, 117(52), 33414–33425. <https://doi.org/10.1073/pnas.2013724117>
- Verhofstad, N., Linschooten, J. O., Van Benthem, J., Dubrova, Y. E., Van Steeg, H., Van Schooten, F. J., & Godschalk, R. W. L. (2008). New methods for assessing male germ line mutations in humans and genetic risks in their offspring. *Mutagenesis*, 23(4), 241–247. <https://doi.org/10.1093/mutage/gen022>
- Webster, R. J., Williams, A., Marchetti, F., & Yauk, C. L. (2018). Discovering human germ cell mutagens with whole genome sequencing: Insights from power calculations reveal the importance of controlling for between-family variability. *Mutation Research/Genetic Toxicology and Environmental Mutagenesis*, 831, 24–32. <https://doi.org/10.1016/j.mrgentox.2018.04.004>
- Yatsenko, A. N., & Turek, P. J. (2018). Reproductive genetics and the aging male. *Journal of Assisted Reproduction and Genetics*, 35(6), 933–941. <https://doi.org/10.1007/s10815-018-1148-y>

Yauk, C. L., Aardema, M. J., Benthem, J. V., Bishop, J. B., Dearfield, K. L., DeMarini, D. M., Dubrova, Y. E., Honma, M., Lupski, J. R., Marchetti, F., Meistrich, M. L., Pacchierotti, F., Stewart, J., Waters, M. D., & Douglas, G. R. (2015). Approaches for identifying germ cell mutagens: Report of the 2013 IWGT workshop on germ cell assays☆. *Mutation Research/Genetic Toxicology and Environmental Mutagenesis*, 783, 36–54.

<https://doi.org/10.1016/j.mrgentox.2015.01.008>

Yip, B. H., Pawitan, Y., & Czene, K. (2006). Parental age and risk of childhood cancers: A population-based cohort study from Sweden. *International Journal of Epidemiology*, 35(6), 1495–1503. <https://doi.org/10.1093/ije/dyl177>

CHAPTER FOUR

DISCUSSION

MADISON T. STEWART

4.1 Summary of Study Outcomes

Previous research has shown mutations in germ cells accumulate with age and cause heritable genetic disorders; thus, it is critical to identify factors that cause germline mutations (Gao et al., 2019). Mutations can increase with age as a result of DNA replication errors that accumulate over time, a decline in effective DNA repair mechanisms within older tissues, or a combination of both (Chen, 2023). Polycyclic aromatic hydrocarbons (PAHs) are widespread pollutants that are present in food, tobacco smoke, and urban air (Dahlstrom & Bloomhuff, 2014, Abdel-Shafy & Mansour 2016). Across a lifetime, humans are continuously exposed to PAHs, which can cause an array of serious health effects (Olsson et al., 2009, Diggs et al., 2011, Bach et al., 2003). Long-term exposure to PAHs can cause lung cancer via inhalation, stomach cancer through consumption of food and skin cancer from dermal contact (US EPA, 2008). Based on available data, several PAHs are recognized as environmental mutagens and are known to be carcinogenic in animals (Abdel-Shafy & Mansour 2016, US EPA 2008). Specifically, previous studies have demonstrated that benzo[*b*]fluoranthene (BbF), a less studied PAH but a probable human carcinogen, induces mutations in mouse somatic tissues (Schuster et al., 2024, Long et al., 2016). Despite the observation of a substantial response of BbF within somatic tissues, the mutagenic effects of BbF in germ cells are not well understood. Current gold-standard methodologies for mutagenicity testing are limited in their assessment of mutations and do not fully capture the variation in mutation susceptibility across the genome. Advancements in technologies have modernized mutagenicity assessment, enabling the quantification of mutations across diverse genomic contexts and providing mechanistic insight through analysis of mutation spectral data. These new and advanced methodologies have the potential to revolutionize in vivo mutagenesis assessment and transform the field of genetic toxicology (Marchetti et al., 2023).

The overarching objectives of this thesis were to use the TGR *lacZ* and DS assays to: 1) evaluate the mutagenic effects of long-term exposure to BbF for 90 or 180 days in germ cells of male mice; and 2) measure mutations in the germ cells of unexposed males of different ages. Adult MutaMouse males were exposed orally to BbF concentrations ranging from 3.25 to 50 mg

BbF/kg body weight per day (BW/day) for 90 days and from 1.5625 to 25 mg BbF/kg BW/day for 180 days alongside controls. Mutant frequencies were determined using the TGR *lacZ* assay (n = 8 per group), while mutation frequencies (MF) for the control and high dose groups were determined using DS (n = 6 per group). For evaluating the impact of aging, unexposed mice spanning 3 to 37 weeks of age were used. I found no significant increases in BbF-induced mutant frequency or MF using the *lacZ* assay and DS despite a strong mutagenic effect in somatic tissues. Our results may be explained by differences in the metabolism of BbF and/or the effective DNA repair capacity of germ cells. Power analyses further demonstrated that germ cell studies may require larger sample sizes with respect to somatic tissues to detect small effects with sufficient power. I also found that aging did not induce mutations in germ cells at 37 weeks, which suggests the need for older mice to detect an aging effect on the male germline.

4.2 Fulfillment of Objectives

Objective 1. Quantify the impact of BbF exposure on mutant frequency and MF in MutaMouse male germ cells

I used the TGR *lacZ* assay to analyze mutant frequency in germ cells of MutaMouse males after exposure to BbF for 90 days and 180 days. There were no significant increases in mutant frequency at 90 days or 180 days relative to controls. There were no increasing trends in mutant frequency across doses for either time point using the *lacZ* assay. Analysis of BbF-induced mutagenicity in germ cells using DS also did not reveal increases in MF using the MF_{min} or MF_{max} assumptions at 90 days or 180 days relative to controls. The lack of an effect in germ cells is at variance with the strong mutagenic response of BbF in somatic tissues (Long et al., 2016, Schuster et al., 2023). Overall, our results suggest: (a) limited distribution of BbF, or limited metabolically activation of BbF, in the testes; and/or (b) that effective DNA damage response and repair mechanisms play a distinctive and highly protective role in germ cells relative to somatic tissues.

Objective 2. Measure spectral changes induced by BbF in male germ cell

I analyzed the mutation spectrum obtained using DS to further characterize BbF-induced mutations and identify distinct mutation subtypes. In somatic tissues, BbF induced mainly C:G > A:T transversions and C:G > T:A transitions (Schuster et al., 2024). In germ cells (this thesis), there were no significant differences between the BbF-induced and spontaneous overall mutation spectra at 90 days; however, at 180 days, significant differences between the overall induced and control spectra were found. Nonetheless, there were no significant dose-dependent increases in the expected C:G > A:T mutations after 90-day or 180-day BbF exposure. These transversions were of particular interest given their large response in somatic tissues. Research has also shown that guanine adducts are induced by metabolites of BbF (Long et al., 2016, Schreck et al., 2009, Mass et al., 1996). Overall, the differences in spectra between tissues further supports the contrasting responses to DNA damage between somatic tissues and germ cells and/or the inadequate metabolic activation of BbF in the testes. Additionally, because germ cell MF is an order of magnitude lower than somatic cell MF (Milholland et al., 2017) and no significant increases were found, quantifying more mutations may be required to properly characterize BbF effects (see Objective 3).

Objective 3. Perform lacZ and DS power analyses on BbF-induced male germ cell mutant frequency and MF

Previous studies have established that 4-5 animals can be used to detect a 1.5-fold increase in MF in somatic tissues using DS (Esina et al., 2024). I thus determined the effect sizes that should be detectable with 80% power with the number of animals used for the *lacZ* assay and DS. Using the *lacZ* data, I have 80% power to detect a 1.7-fold and 1.8-fold increase with eight animals and seven animals per dose group, respectively. Using DS datasets, detecting a 1.6- and 1.7-fold increase with 80% requires six animals and five animals, respectively. Comparisons with similar power analyses conducted in somatic tissues, suggest that larger number of animals are required to have the power to detect the same effect in germ cells versus somatic tissues.

Objective 4. Measure the impact of age on spontaneous mutant frequency, MF and spectrum in MutaMouse male germ cells

I evaluated the effects of age on mutations in mouse male germ cells using the *lacZ* assay and DS. Statistically significant increases in mutant frequency were observed at 35-37 weeks relative to 13-15 weeks using the *lacZ* assay; however, no significant increases in MF were identified using DS at 35-37 weeks with respect to the 13-15-week or 3-week-old mice. These contrasting results between methodologies may be explained by the low mutant frequency at 13-15 weeks based on the historical control database for the *lacZ* assay. I further observed no significant increase in C:G > T:A mutations using DS, the main mutation subtype associated with age, at 35-37 weeks relative to 3 weeks. However, a significant age-related increasing trend was observed in these mutations across all time points. Overall, our findings did not reveal clear effects of age on mutations in mouse male germ cells. The impact of aging may be more apparent in mice older than 35-37 weeks.

4.3 Contribution to Scientific Knowledge

My thesis contributes to scientific knowledge in three domains: 1) characterizing BbF mutagenicity in mouse germ cells; 2) supporting distinct responses to DNA damage in germ cells relative to somatic tissues; and 3) understanding the impact of age on germ cell mutations.

4.3.1 BbF Does Not Induce Mutations in Mouse Germ Cells after 90-day and 180-day Exposures

Germ cell mutagenicity data is important for regulatory and risk assessment. Germ cell mutagenicity is a hazard characterization criterion within the Globally Harmonized System of Classification and Labelling (GHS) (United Nations, 2015) and under REACH (Registration, Evaluation, Authorisation and Restriction of Chemicals) within the European Chemicals Agency (ECHA), germ cell data is required for substances that are mutagenic in somatic tissues (European Chemicals Agency, n.d.). Prior to our work, the effects of BbF on mutations in mouse

male germ cells were unknown. I found that BbF does not induce mutations after a 90 day or 180-day exposure period using the *lacZ* assay and DS, despite the observation of strong mutagenic responses of BbF in somatic tissues (Schuster et al., 2024, Long et al., 2016). Humans can be exposed to PAHs, such as BbF, through diet, tobacco use, pollution, and occupation (Sahoo et al., 2020). These harmful compounds are prevalent in the environment and have been linked to serious adverse health effects (Venkatraman et al., 2024). It is critical to understand the impact of chemicals on germ cells given their vital role as the carrier for hereditary information and given the risks associated with germ cell mutagenicity (Clancy, 2008, Zorrilla & Yatsenko, 2013). Overall, this work suggests that because the observed effects occurred at doses higher than typical human exposure, this large margin of exposure would suggest minimal risk. Despite these findings, continued research on chemical mutagenesis and its potential impact to germ cells is necessary to fully assess the implications of PAH exposure for human health.

4.3.2 Germ Cells Do Not Metabolically Activate BbF and/or Possess Differential Responses to DNA Damage

Chemicals are frequently examined for their capacity to cause mutations in somatic cells for regulatory purposes, and it is generally accepted that somatic studies are adequate to preserve the germline (Yauk et al., 2015). As a result, testing chemicals for their capacity to cause mutations in germ cells is less common (O'Brien et al., 2014). Our work shows contrasting results in germ cells relative to somatic tissues. Using the same subset of BbF-exposed animals, an ongoing study observed significantly increased fold changes in various somatic tissues (liver and bone marrow (Schuster et al., Unpublished data)). I have two potential explanations for the lack of effect. First, there may be differences in systemic distribution of BbF across tissues or its reduced metabolic activation within the testes with respect to tissues with higher metabolic capacity (i.e., liver). Second, germ cells could possess a distinct response to DNA damage with respect to somatic tissues, which further supports the need for research on germ cell mutagenicity. Overall, this work supports the unique and distinct features of germ cells and that regulatory decisions for BbF should be based on its strong mutagenic potential within the liver.

4.3.3 Aging Does Not Induce Mutations in 35-37-week-old Mice

The impact of aging on humans has been extensively studied given the associated risk of somatic disorders like cancer that increase with age (Berben et al., 2021, White et al., 2015). Although fewer studies have investigated age-related effects on reproduction in men with respect to women (Broekmans et al., 2007), the impact of paternal mutation on offspring inheritance of mutations as fathers age is well established (Shojaeisaadi et al., 2024, Kong et al., 2012, Goldmann et al., 2019, Crow, 2000). To study age-associated mutagenesis, previous studies have used very labour-intensive and costly approaches including whole genome sequencing of pedigrees (Webster et al., 2018).

I applied DS to study germ cell mutations in aging mice. Our approach uses only 8 mice per group yet quantifies hundreds of mutations enabling analysis of MF and spectrum. These approaches are now being applied in humans to further characterize germ cell mutagenicity (Axelsson et al., 2024, Kunisaki et al., 2024). Additionally, I investigated the effects of aging on mutations in male mouse germ cells and demonstrated that at 35-37 weeks old male mice do not have increased germ cell mutations with respect to younger mice. I did observe a significant age-related trend in C:G > T:A mutations, the mutation subtype associated with age in humans due to spontaneous deamination of cytosine (Pfeifer, 2006, Chen et al., 2020). This is an important finding given the limited age range used in this study, which points to a potential aging effect that could be more evident in older mice. Identifying age-related mutations would provide us with a better understanding of the physiological and molecular changes that occur as we age, which can significantly improve health and quality of life.

4.4 Future Directions

There are three main areas for follow-up work based on my thesis: 1) comparing the level of DNA damage in testes versus somatic tissues; 2) investigating BbF mutagenicity in germ cells using a different experimental design (e.g., 28 + 28d); and 3) quantifying the effects of aging on mutations in germ cells of older mice.

4.4.1 Level of DNA Damage in Testis Versus Somatic Tissues

Additional work is required to understand if BbF causes germ cell mutations and if not, explore the protective mechanisms that operate in the testes. A starting point to further understanding the differential response of germ cells vs somatic tissues would be evaluating DNA damage levels in the testes with respect to somatic tissues. Measuring the levels of DNA damage (i.e., DNA adducts) in the testes would inform whether the strong mutagenic response of BbF in somatic tissues but not in germ cells is due to effective DNA damage response mechanisms or due to other contributing factors such as differential distribution and metabolic activation. This can be determined through the presence or absence of DNA adducts in germ cells; if BbF is not metabolically activated in the germ cells, DNA adducts would not be detected.

4.4.2 Different Experimental Design (e.g., 28 + 28d)

Our study evaluated the mutagenic effects of BbF on male mouse germ cells after long-term exposure (i.e., 90 days and 180 days). Prior to this work, a pilot study was conducted to determine the top doses that should be administered at each time point to eliminate animal toxicity. Given that BbF doses higher than 50 mg/kg BW/day at 90 days and 25 mg/kg BW/day at 180 days induced overt toxicity, these were the doses administered for each respective exposure duration. A 28-day administration followed by a 28-sampling time as recommended in TG 488 would allow the use of BbF doses up to 100 mg/kg BW/day. This experimental design (i.e., 28 + 28d) is recommended in OECD TG 488 as it allows for prolonged exposure and sufficient time for DNA damage to be converted into mutations (OECD, 2022). Future work should investigate whether the 28+28d design, or a different experimental design, would result in a significant increase in germ cell mutations. This could verify whether higher doses of BbF are needed to overwhelm the DNA repair capacity of germ cells.

4.4.3 Effects of Aging in Older Mice

Our work investigated the impact of aging on male germ cells of mice spanning 3 weeks up to 37 weeks using the *lacZ* assay and DS. Although there were no significant age-related increases in MF using DS, I did observe a significant increase in mutations at 35-37 weeks relative to 13-15 weeks using the *lacZ* assay. However, the mutant frequency detected at 13-15 weeks was on the low end with respect to our historical control database. Nevertheless, there was a significant trend for increased C:G > T:A mutations with increasing age. The average lifespan of a mouse is approximately two years which indicates that the 35-37-week time point represents roughly one third of their lifespan, suggesting these mice are middle aged. Thus, future work should focus on investigating the effects of age in older mice. Studying the impact of age on germ cells of older mice would corroborate our findings and support the demand for further investigation given the implications associated with germline mutations.

4.5 Concluding Remarks

My thesis shows that despite significant increases in BbF-induced mutant frequency and MF in somatic tissues, long-term exposure to BbF did not induce mutations in male mouse germ cells. These results point to different biological processes including effective DNA damage response mechanisms and repair capacity in germ cells, or inadequate BbF distribution and/or metabolism within the testes. Power analyses revealed that larger sample sizes are required to detect the small changes I identified. This is the first study to ever investigate BbF mutagenicity in germ cells and this work provides valuable information to inform follow up studies. The project further revealed no effects of aging in 35–37-week-old mice; however, these results suggest effects could be more apparent in older mice. Overall, my findings strongly support differences between germ cells and somatic tissues and demonstrate that it is imperative for researchers to continue to assess germ cell mutagenicity.

4.6 References

Abascal, F., Harvey, L. M. R., Mitchell, E., Lawson, A. R. J., Lensing, S. V., Ellis, P., Russell, A. J. C., Alcantara, R. E., Baez-Ortega, A., Wang, Y., Kwa, E. J., Lee-Six, H., Cagan, A., Coorens, T. H. H., Chapman, M. S., Olafsson, S., Leonard, S., Jones, D., Machado, H. E., ... Martincorena, I. (2021). Somatic mutation landscapes at single-molecule resolution. *Nature*, *593*(7859), 405–410. <https://doi.org/10.1038/s41586-021-03477-4>

Abdel-Shafy, H. I., & Mansour, M. S. M. (2016). A review on polycyclic aromatic hydrocarbons: Source, environmental impact, effect on human health and remediation. *Egyptian Journal of Petroleum*, *25*(1), 107–123. <https://doi.org/10.1016/j.ejpe.2015.03.011>

Axelsson, J., LeBlanc, D., Shojaeisaadi, H., Meier, M. J., Fitzgerald, D. M., Nachmanson, D., Carlson, J., Golubeva, A., Higgins, J., Smith, T., Lo, F. Y., Pilsner, R., Williams, A., Salk, J., Marchetti, F., & Yauk, C. (2024). Frequency and spectrum of mutations in human sperm measured using duplex sequencing correlate with trio-based de novo mutation analyses. <https://doi.org/10.1101/2024.02.13.24302689>

Bach, P. B., Kelley, M. J., Tate, R. C., & McCrory, D. C. (2003). Screening for Lung Cancer*. *Chest*, *123*(1), 72S–82S. https://doi.org/10.1378/chest.123.1_suppl.72S

Berben, L., Floris, G., Wildiers, H., & Hatse, S. (2021). Cancer and Aging: Two Tightly Interconnected Biological Processes. *Cancers*, *13*(6), 1400. <https://doi.org/10.3390/cancers13061400>

Broekmans, F. J., Knauff, E. A. H., Te Velde, E. R., Macklon, N. S., & Fauser, B. C. (2007). Female reproductive ageing: Current knowledge and future trends. *Trends in Endocrinology & Metabolism*, *18*(2), 58–65. <https://doi.org/10.1016/j.tem.2007.01.004>

Chen, H., Chong, W., Yang, X., Zhang, Y., Sang, S., Li, X., & Lu, M. (2020). Age-related mutational signature negatively associated with immune activity and survival outcome in triple-negative breast cancer. *Oncotmunology*, *9*(1), 1788252. <https://doi.org/10.1080/2162402X.2020.1788252>

Chen, H., Krieg, T., Mautz, B., Jolly, C., Scofield, D., Maklakov, A. A., & Immler, S. (2023). Germline mutation rate is elevated in young and old parents in *Caenorhabditis remanei*. *Evolution Letters*, *7*(6), 478–489. <https://doi.org/10.1093/evlett/grad052>

Clancy, S. (2008) Genetic mutation. *Nature Education* *1*(1):187

Dahlstrom, D. L., & Bloomhuff, A. B. (2014). ACGIH® (American conference of governmental industrial hygienists).

Diggs, D. L., Huderson, A. C., Harris, K. L., Myers, J. N., Banks, L. D., Rekhadevi, P. V., Niaz, M. S., & Ramesh, A. (2011). Polycyclic Aromatic Hydrocarbons and Digestive Tract Cancers: A Perspective. *Journal of Environmental Science and Health, Part C*, 29(4), 324–357.

<https://doi.org/10.1080/10590501.2011.629974>

Esina, E., Dodge, A. E., Williams, A., Schuster, D. M., LeBlanc, D. P. M., Marchetti, F., & Yauk, C. L. (2024). Power analyses to inform Duplex Sequencing study designs for MutaMouse liver and bone marrow. *Environmental and Molecular Mutagenesis*, 65(8), 234–242.

<https://doi.org/10.1002/em.22619>

European Chemicals Agency. (n.d.). Standard information requirements recommendations. Retrieved January 18, 2025, from <https://echa.europa.eu/standard-information-requirements-recommendations>.

Gao, Z., Moorjani, P., Sasani, T. A., Pedersen, B. S., Quinlan, A. R., Jorde, L. B., Amster, G., & Przeworski, M. (2019). Overlooked roles of DNA damage and maternal age in generating human germline mutations. *Proceedings of the National Academy of Sciences*, 116(19), 9491–9500.

<https://doi.org/10.1073/pnas.1901259116>

Hoang, M. L., Kinde, I., Tomasetti, C., McMahon, K. W., Rosenquist, T. A., Grollman, A. P., Kinzler, K. W., Vogelstein, B., & Papadopoulos, N. (2016). Genome-wide quantification of rare somatic mutations in normal human tissues using massively parallel sequencing. *Proceedings of the National Academy of Sciences*, 113(35), 9846–9851.

<https://doi.org/10.1073/pnas.1607794113>

Kunisaki, J., Goldberg, M. E., Lulla, S., Sasani, T., Hiatt, L., Nicholas, T. J., Liu, L., Torres-Arce, E., Guo, Y., James, E., Horns, J. J., Ramsay, J. M., Chen, Q., Hotaling, J. M., Aston, K. I., & Quinlan, A. R. (2024). *Sperm from infertile, oligozoospermic men have elevated mutation rates*.

<https://doi.org/10.1101/2024.08.22.24312232>

Lambert, I. B., Singer, T. M., Boucher, S. E., & Douglas, G. R. (2005). Detailed review of transgenic rodent mutation assays. *Mutation Research/Reviews in Mutation Research*, 590(1–3), 1–280. <https://doi.org/10.1016/j.mrrev.2005.04.002>

LeBlanc, D. P. M., Meier, M., Lo, F. Y., Schmidt, E., Valentine, C., Williams, A., Salk, J. J., Yauk, C. L., & Marchetti, F. (2022). Duplex sequencing identifies genomic features that determine susceptibility to benzo(a)pyrene-induced in vivo mutations. *BMC Genomics*, 23(1), 542.

<https://doi.org/10.1186/s12864-022-08752-w>

Long, A. S., Lemieux, C. L., Arlt, V. M., & White, P. A. (2016). Tissue-specific in vivo genetic toxicity of nine polycyclic aromatic hydrocarbons assessed using the MutaTMMouse transgenic rodent assay. *Toxicology and Applied Pharmacology*, 290, 31–42.

<https://doi.org/10.1016/j.taap.2015.11.010>

Marchetti, F., Cardoso, R., Chen, C. L., Douglas, G. R., Elloway, J., Escobar, P. A., Harper Jr, T., Heflich, R. H., Kidd, D., Lynch, A. M., Myers, M. B., Parsons, B. L., Salk, J. J., Settivari, R. S., Smith-Roe, S. L., Witt, K. L., Yauk, C., Young, R. R., Zhang, S., & Minocherhomji, S. (2023). Error-corrected next-generation sequencing to advance nonclinical genotoxicity and carcinogenicity testing. *Nature Reviews Drug Discovery*, 22(3), 165–166.

<https://doi.org/10.1038/d41573-023-00014-y>

Mass, M. J., Abu-Shakra, A., Roop, B. C., Nelson, G., Galati, A. J., Stoner, G. D., Nesnow, S., & Ross, J. A. (1996). Benzo[*b*]fluoranthene: Tumorigenicity in strain A/J mouse lungs, DNA adducts and mutations in the Ki-*ras* oncogene. *Carcinogenesis*, 17(8), 1701–1704.

<https://doi.org/10.1093/carcin/17.8.1701>

Milholland, B., Dong, X., Zhang, L., Hao, X., Suh, Y., & Vijg, J. (2017). Differences between germline and somatic mutation rates in humans and mice. *Nature Communications*, 8(1), 15183. <https://doi.org/10.1038/ncomms15183>

O'Brien, J. M., Beal, M. A., Gingerich, J. D., Soper, L., Douglas, G. R., Yauk, C. L., & Marchetti, F. (2014). Transgenic Rodent Assay for Quantifying Male Germ Cell Mutant Frequency. *Journal of Visualized Experiments*, 90, 51576. <https://doi.org/10.3791/51576-v>

OECD (2022) Test No. 488. Transgenic rodent somatic and germ cell gene mutation assay. *OECD guidelines for the testing of chemicals*, section 4. OECD Publishing, Paris.

Olsson, A. C., Fevotte, J., Fletcher, T., Cassidy, A., 'T Mannetje, A., Zaridze, D., Szeszenia-Dabrowska, N., Rudnai, P., Lissowska, J., Fabianova, E., Mates, D., Bencko, V., Foretova, L., Janout, V., Brennan, P., & Boffetta, P. (2010). Occupational exposure to polycyclic aromatic hydrocarbons and lung cancer risk: A multicenter study in Europe. *Occupational and Environmental Medicine*, 67(2), 98–103. <https://doi.org/10.1136/oem.2009.046680>

Pfeifer, G. P. (2006). Mutagenesis at Methylated CpG Sequences. In W. Doerfler & P. Böhm (Eds.), *DNA Methylation: Basic Mechanisms* (Vol. 301, pp. 259–281). Springer-Verlag.

https://doi.org/10.1007/3-540-31390-7_10

Sahoo, B. M., Ravi Kumar, B. V. V., Banik, B. K., & Borah, P. (2020). Polyaromatic Hydrocarbons (PAHs): Structures, Synthesis and their Biological Profile. *Current Organic Synthesis*, 17(8), 625–640. <https://doi.org/10.2174/1570179417666200713182441>

Schreck, I., Chudziak, D., Schneider, S., Seidel, A., Platt, K. L., Oesch, F., & Weiss, C. (2009). Influence of aryl hydrocarbon- (Ah) receptor and genotoxins on DNA repair gene expression and cell survival of mouse hepatoma cells. *Toxicology*, 259(3), 91–96.

<https://doi.org/10.1016/j.tox.2009.02.006>

US EPA (Environmental Protection Agency) (2008) Polycyclic Aromatic Hydrocarbons (PAHs)—EPA Fact Sheet. *National Center for Environmental Assessment*, Office of Research and Development, Washington DC.

United Nations. (2015) *Globally Harmonized System of Classification and Labelling of Chemicals (GHS)*, sixth revised edition ed., New York and Geneva.

Venkatraman, G., Giribabu, N., Mohan, P. S., Muttiah, B., Govindarajan, V. K., Alagiri, M., Abdul Rahman, P. S., & Karsani, S. A. (2024). Environmental impact and human health effects of polycyclic aromatic hydrocarbons and remedial strategies: A detailed review. *Chemosphere*, 351, 141227. <https://doi.org/10.1016/j.chemosphere.2024.141227>

Webster, R. J., Williams, A., Marchetti, F., & Yauk, C. L. (2018). Discovering human germ cell mutagens with whole genome sequencing: Insights from power calculations reveal the importance of controlling for between-family variability. *Mutation Research/Genetic Toxicology and Environmental Mutagenesis*, 831, 24–32. <https://doi.org/10.1016/j.mrgentox.2018.04.004>

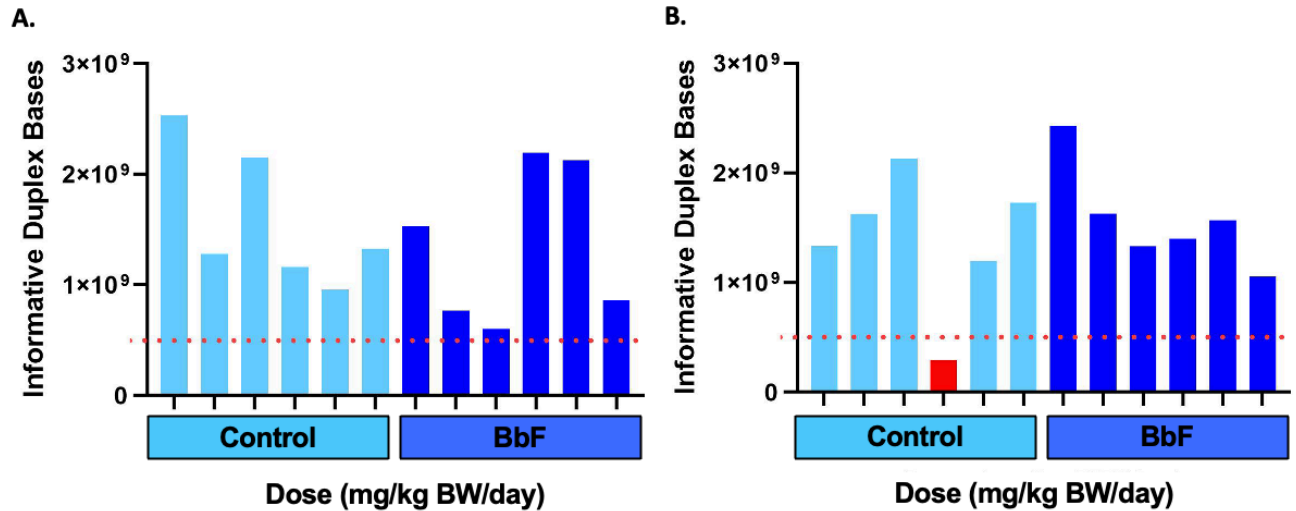
White, M. C., Holman, D. M., Boehm, J. E., Peipins, L. A., Grossman, M., & Jane Henley, S. (2014). Age and Cancer Risk. *American Journal of Preventive Medicine*, 46(3), S7–S15. <https://doi.org/10.1016/j.amepre.2013.10.029>

Yauk, C. L., Aardema, M. J., Benthem, J. V., Bishop, J. B., Dearfield, K. L., DeMarini, D. M., Dubrova, Y. E., Honma, M., Lupski, J. R., Marchetti, F., Meistrich, M. L., Pacchierotti, F., Stewart, J., Waters, M. D., & Douglas, G. R. (2015). Approaches for identifying germ cell mutagens: Report of the 2013 IWGT workshop on germ cell assays☆. *Mutation Research/Genetic Toxicology and Environmental Mutagenesis*, 783, 36–54. <https://doi.org/10.1016/j.mrgentox.2015.01.008>

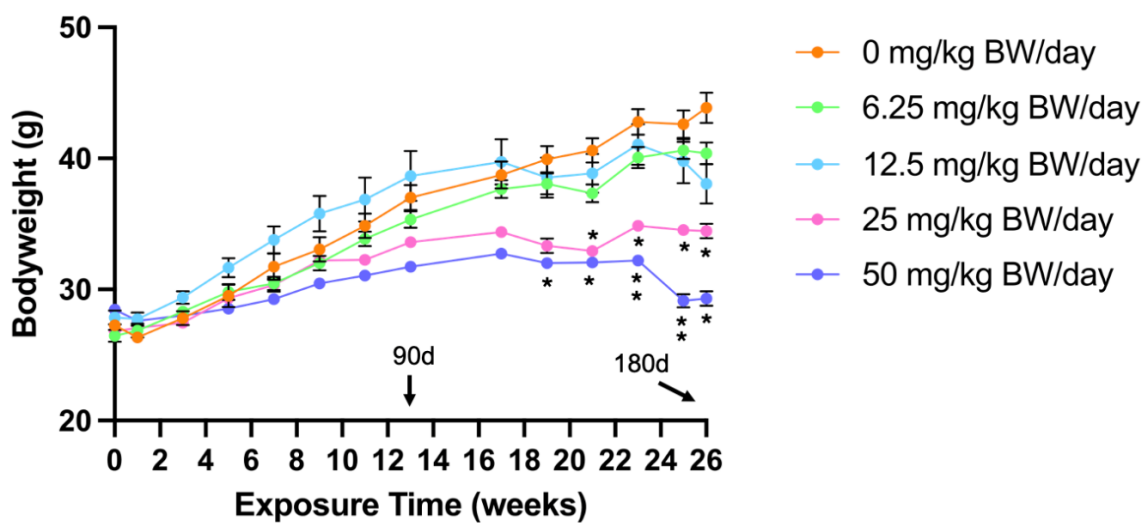
Zorrilla, M., & Yatsenko, A. N. (2013). The Genetics of Infertility: Current Status of the Field. *Current Genetic Medicine Reports*, 1(4), 247–260. <https://doi.org/10.1007/s40142-013-0027-1>

Appendix

Supplementary Material for Chapter Two



Supplementary Figure 2.1. Informative duplex bases per animal for the control and BbF treated dose groups at 90 days (A) and 180 days (B). Control and treated dose groups are indicated on the x-axis. One animal (shown in red) did not reach the minimum number of duplex bases (red dotted line) required and was therefore removed from the analyses.



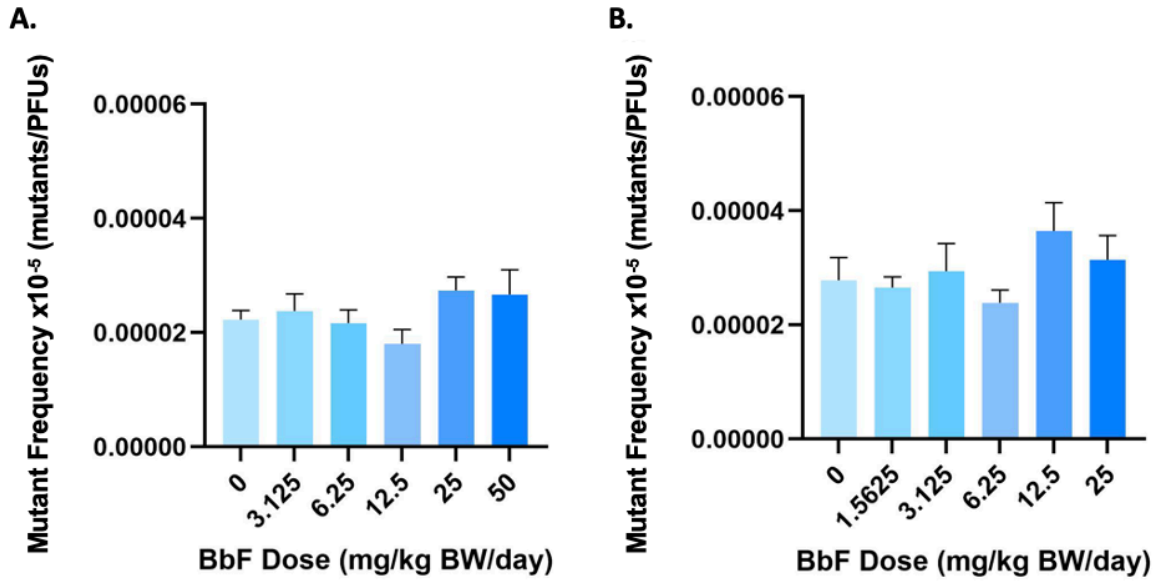
Supplementary Figure 2.2. Top dose selection for 90-day and 180-day exposure durations. Body weights of MutaMouse males were assessed over the course of each exposure period. Exposure time in weeks is represented on the x-axis with the 90-day and 180-day durations indicated by arrows. Asterisks indicate a significant decrease in body weight relative to the control ($p < 0.05$).

Supplementary Table 2.1. Body weight change in MutaMouse animals after 90 days and 180 days relative to start of exposure.

Sample ID	Exposure Duration	Dose (mg/kg BW/day)	Initial Weight (g)	Final Weight (g)	Percent change (%)
201	90 days	0	30.2	35	15.9
202	90 days	0	30.2	35.8	18.55
203	90 days	0	26.6	29.4	10.53
204	90 days	0	32.8	39.6	20.74
205	90 days	0	31.2	36.4	16.67
206	90 days	0	28.8	35.2	22.23
207	90 days	0	33.4	33.6	0.6
208	90 days	0	27.8	33.4	20.15
209	90 days	3.125	27.4	30.6	11.68
210	90 days	3.125	34.2	47.4	38.6
211	90 days	3.125	27.2	34.8	27.95
212	90 days	3.125	32	35.6	11.25
213	90 days	3.125	25	26.4	5.6
214	90 days	3.125	31.8	43.8	37.74
215	90 days	3.125	29.2	34.6	18.5
216	90 days	3.125	37.8	47.6	25.93
217	90 days	6.25	26.2	28	6.88
218	90 days	6.25	32.2	48.6	50.94
219	90 days	6.25	32.4	36.4	12.35
220	90 days	6.25	34.6	40.4	16.77
221	90 days	6.25	27.6	29.8	7.98
222	90 days	6.25	26.2	32.6	24.43
223	90 days	6.25	32.2	42.6	32.3
224	90 days	6.25	32.6	44	34.97
225	90 days	12.5	28.6	29	1.4
226	90 days	12.5	30.8	38.2	24.03
227	90 days	12.5	30.8	32.6	5.85
228	90 days	12.5	36.2	37.4	3.32
229	90 days	12.5	27.4	27.8	1.46
230	90 days	12.5	29.6	33.8	14.19
231	90 days	12.5	32.6	35.4	8.59
232	90 days	12.5	27.4	28.8	5.11
233	90 days	25	30.8	32.2	4.55
234	90 days	25	29.2	31	6.17
235	90 days	25	28	32.2	15
236	90 days	25	30.8	31.6	2.6
237	90 days	25	30.4	28	-7.9
238	90 days	25	28.4	29	2.12

239	90 days	25	32.6	31.4	-3.69
240	90 days	25	32	32.8	2.5
241	90 days	50	33	31.8	-3.64
242	90 days	50	30.8	29	-5.85
243	90 days	50	28.6	28.8	0.7
244	90 days	50	32.4	32.8	1.24
245	90 days	50	34	36	5.89
246	90 days	50	30	32.6	8.67
247	90 days	50	34	34.2	0.59
248	90 days	50	27.2	29	6.62
301	180 days	0	32.2	42.8	32.92
302	180 days	0	29.6	46.6	57.44
303	180 days	0	31.4	50.2	59.88
304	180 days	0	32	47.2	47.5
305	180 days	0	32.4	46.4	43.21
306	180 days	0	34.4	42.8	24.42
307	180 days	0	29.8	43	44.3
308	180 days	0	30.6	43	40.53
309	180 days	1.56	30.6	40.6	32.68
310	180 days	1.56	30.2	47	55.63
311	180 days	1.56	27.6	40.8	47.83
312	180 days	1.56	29.6	49.8	68.25
313	180 days	1.56	30.2	46	52.32
314	180 days	1.56	29.4	38.4	30.62
315	180 days	1.56	29	47.2	62.76
316	180 days	1.56	29.8	40	34.23
317	180 days	3.125	34.2	44	28.66
318	180 days	3.125	30	44.2	47.34
319	180 days	3.125	30.4	40.4	32.9
321	180 days	3.125	33.6	49	45.84
322	180 days	3.125	32.6	51	56.45
323	180 days	3.125	31.4	48	52.87
324	180 days	3.125	32.2	45.8	42.24
325	180 days	6.25	29.8	43	44.3
326	180 days	6.25	31.4	50	59.24
327	180 days	6.25	31.6	40.6	28.49
328	180 days	6.25	29.4	42.2	43.54
329	180 days	6.25	34.2	48	40.36
330	180 days	6.25	29.6	42.8	44.6
331	180 days	6.25	32.2	38.2	18.64
332	180 days	6.25	28.8	44.8	55.56
333	180 days	12.5	27	37.6	39.26
334	180 days	12.5	28.4	33.6	18.31

335	180 days	12.5	30	44.8	49.34
336	180 days	12.5	32.2	35.8	11.19
337	180 days	12.5	29.8	47.4	59.07
338	180 days	12.5	30.2	44.4	47.02
339	180 days	12.5	25.6	36.8	43.75
340	180 days	12.5	28.6	30.8	7.7
341	180 days	25	32.8	39	18.91
342	180 days	25	31.8	46	44.66
343	180 days	25	29.2	34	16.44
344	180 days	25	27.8	38.4	38.13
345	180 days	25	29	35.4	22.07
346	180 days	25	28.6	34.8	21.68
347	180 days	25	29.6	38.6	30.41
348	180 days	25	28	33.6	20



Supplementary Figure 2.3. Cochran-Armitage Trend Test of BbF-induced mutant frequencies at 90 days (A) and 180 days (B) using *lacZ* assay. Average *lacZ* mutant frequency values with corresponding SEMs at each dose are shown.

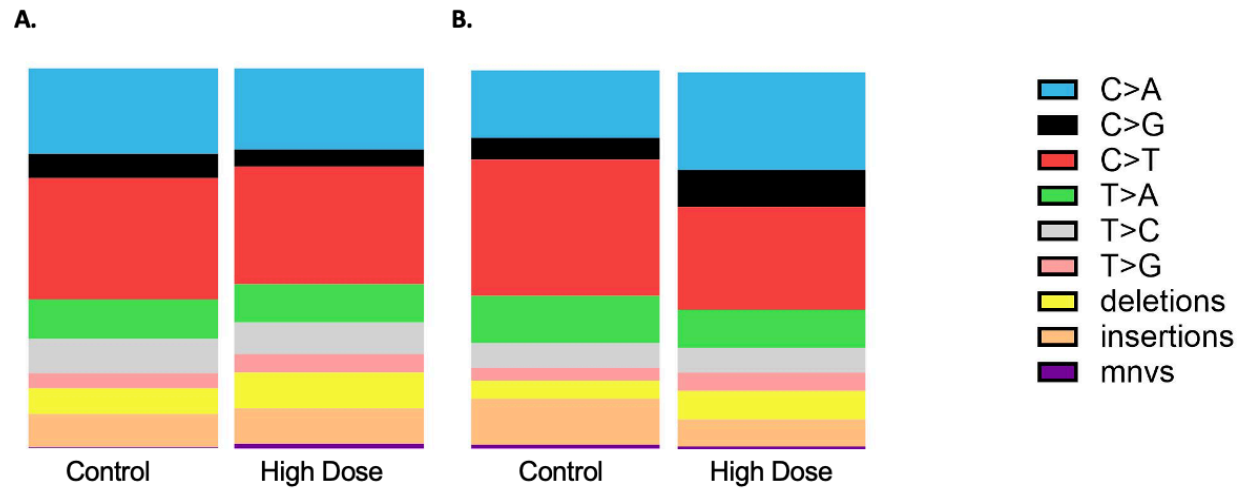
Supplementary Table 2.2. Historical control database of *lacZ* mutant frequencies in seminiferous tubules of control MutaMouse animals.

Study	Exposure Duration*	Sample ID	Mutants	PFU	Mutant Frequency (x10 ⁻⁵)	Average Mutant Frequency (x10 ⁻⁵)	Standard Deviation	Publication
BaP	28+3	1	4	243,861	1.64	2.44	1.03	O'Brien et al (2016) Tox Sci
		2	37	1,080,147	3.43			
		3	6	359,828	1.67			
		4	7	342,599	2.04			
		5	8	159,371	5.02			
		6	6	279,645	2.15			
		BM13	6	349722	1.72			
		BM14	11	357840	3.07			
		BM15	6	272025	2.21			
		BM16	5	249825	2.00			
		BM18	4	211391	1.89			
BaP in utero		11-m1A	8	261476	3.06	2.12	0.69	Meier et al (2017) Env Health Persp
		11-m2A	9	345308	2.61			
		11-m2B	12	508980	2.36			
		11-m1B	3	156682	1.91			
		11-m3B	5	330005	1.52			
		11-m3A	3	241017	1.24			
NHMA	28+3	1	5	240548	2.08	1.58	0.74	Unpublished
		2	1	141811	0.71			
		3	15	654365	2.29			
		4	5	408203	1.22			
NHMA	28+42	5	11	424107	2.59	2.98	1.85	Unpublished
		6	4	204101	1.96			
		7	5	297537	1.68			
		8	8	140485	5.69			
NHMA	28+70	11	3	118617	2.53	2.22	0.44	Unpublished
		12	3	157715	1.90			
NGS BaP	28+3	13	6	349722	1.72	2.18	0.53	PhD thesis, Marc Beal
		14	11	357840	3.07			
		15	6	272025	2.21			
		16	5	249825	2.00			
		18	4	211391	1.89			
NGS BaP	28+42	19	8	425432	1.88	3.82	2.16	PhD thesis, Marc Beal
		20	19	369768	5.14			
		21	6	241211	2.49			
		23	12	457240	2.62			
		24	10	143136	6.99			

BaP	28+28	BG101	8	418805	1.91	2.49	0.86	Zhou et al (submitted)
		BG102	13	346906	3.75			
		BG103	7	374407	1.87			
		BG104	10	288923	3.46			
		BG105	6	332659	1.80			
		BG106	5	279645	1.79			
		BG107	11	330,174	3.33			
		BG108	7	349,557	2.00			
BaP	28+42	BJ25	9	474,469	1.90	3.50	1.48	Zhou et al (submitted)
		BJ26	16	361153	4.43			
		BJ27	23	403,564	5.70			
		BJ28	20	550,676	3.63			
		BJ29	17	487,723	3.49			
		BJ30	14	748,151	1.87			
BaP	28+70	BJ49	7	345249	2.03	2.44	1.37	Zhou et al (submitted)
		BJ50	10	363804	2.75			
		BJ51	10	392961	2.54			
		BJ52	4	381033	1.05			
		BJ53	3	614955	0.49			
		BJ54	11	432721	2.54			
		BM25	10	271196	3.69			
		BM26	3	220668	1.36			
		BM27	10	289917	3.45			
		BM28	7	424107	1.65			
		BM29	11	206089	5.34			
iPMS	28+3	IG1	24	713,029	3.37	3.99	0.69	Zhou et al (submitted)
		IG2	9	261,588	3.44			
		IG3	16	362,147	4.42			
		IG4	16	338,291	4.73			
iPMS	28+28	IG5	14	477,783	2.93	2.67	0.24	Zhou et al (submitted)
		IG6	16	650,904	2.46			
		IG7	9	342,930	2.62			
iPMS	28+42	IG9	16	406,215	3.94	3.09	1.37	Zhou et al (submitted)
		IG10	5	350,385	1.43			
		IG11	23	518,205	4.44			
		IG12	10	391,636	2.55			
iPMS	28+70	IG13	5	92,773	5.39	3.62	1.38	Zhou et al (submitted)
		IG14	19	476,789	3.98			
		IG15	14	490,870	2.85			
		IG16	8	355,852	2.25			
PRC	28+3	PG113	7	318,411	2.20	2.25	0.27	Zhou et al (submitted)
		PG114	8	312,613	2.56			

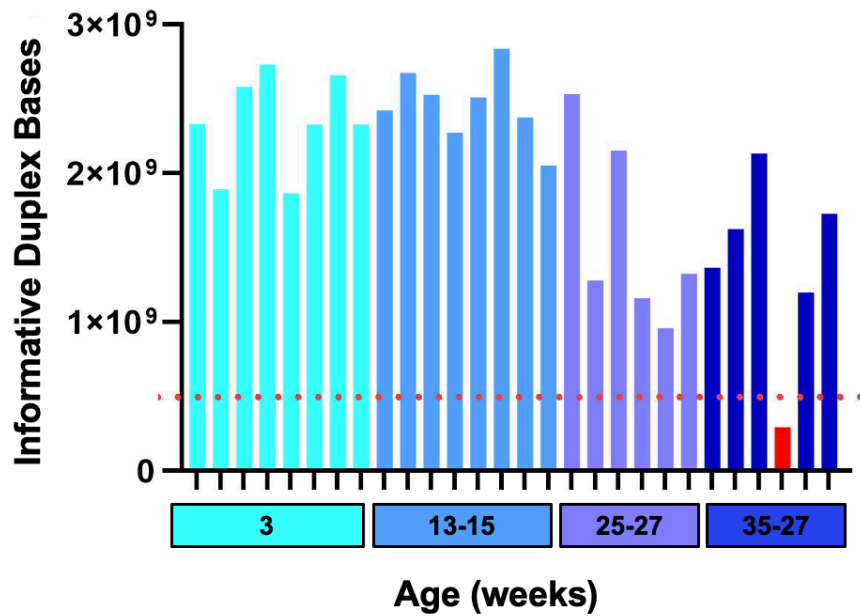
		PG115	8	344,752	2.32			
		PG116	2	104,204	1.92			
PRC	28+28	PG117	27	482,753	5.59	3.48	2.06	Zhou et al (submitted)
		PG119	17	502,467	3.38			
		PG120	8	544,381	1.47			
PRC	28+42	PG121	8	413,504	1.93	3.09	1.10	Zhou et al (submitted)
		PG123	20	624,895	3.20			
		PG124	23	557,303	4.13			
PRC	28+70	PG125	15	441,667	3.40	2.72	1.19	Zhou et al (submitted)
		PG126	5	377,720	1.32			
		PG127	19	479,771	3.96			
		PG128	11	503,627	2.18			
ENU	28+3	EJ1	8	672607	1.19	1.19	0.26	Zhou et al (submitted)
		EJ2	9	591761	1.52			
		EJ3	1	86478	1.16			
		EJ4	2	223153	0.90			
		EJ5	5	355189	1.41			
		EJ6	1	133693	0.75			
		EJ7	1	268049	0.37			
ENU	28+28	EG1	4	250819	1.59	2.47	0.93	Zhou et al (submitted)
		EG2	5	234087	2.14			
		EG3	7	244358	2.86			
		EG4	18	460553	3.91			
		EG9	5	268049	1.87			
ENU	28+42	EG5	7	251813	2.78	1.89	0.64	Zhou et al (submitted)
		EG6	3	235578	1.27			
		EG7	5	288260	1.73			
		EG8	4	227957	1.75			
ENU	28+70	EJG1	7	461216	1.52	2.15	0.85	Zhou et al (submitted)
		EJG2	4	252145	1.59			
		EJG3	10	361153	2.77			
		EJG4	12	324375	3.70			
		EJG5	3	218349	1.37			
		EJG6	12	512241	2.34			
		EJG7	6	346243	1.73			
Coal Tar	28+28	G1	10	401079	2.49	2.62	0.66	Unpublished
		G2	10	366455	2.73			
		G3	8	552333	1.45			
		G4	9	363804	2.47			
		G5	11	396937	2.77			
		G6	17	666974	2.55			
		G7	10	374738	2.67			

		G8	13	336303	3.87			
BbF	28+3	101	6	391139	1.53	1.58	0.65	Unpublished
		102	4	328186	1.22			
		103	6	417977	1.44			
		104	2	297703	0.67			
		105	4	164673	2.43			
		106	6	474469	1.26			
		107	6	414001	1.45			
		108	11	414829	2.65			
BbF	90	201	6	327357	1.83	2.23	0.45	This study
		202	10	415161	2.41			
		203	6	289254	2.07			
		204	7	300519	2.33			
		205	4	231436	1.73			
		206	6	287266	2.09			
		207	10	313110	3.19			
		208	7	318411	2.20			
BbF	180	301	7	270037	2.59	2.78	1.14	This Study
		302	9	247672	3.63			
		303	7	326860	2.14			
		304	7	221993	3.15			
		305	4	267883	1.49			
		306	18	361485	4.98			
		307	5	303336	1.65			
		308	6	230277	2.61			

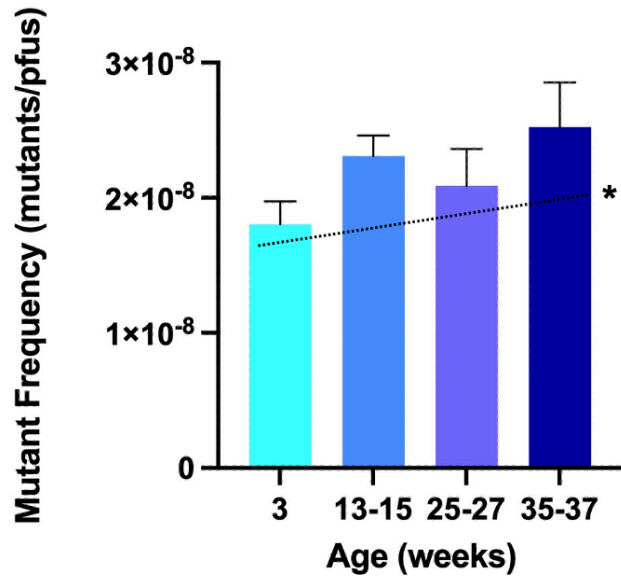


Supplementary Figure 2.4. Single nucleotide variant (SNV) proportions of total mutations in percent for the control and BbF treated mice at 90 days (A) and 180 days (B).

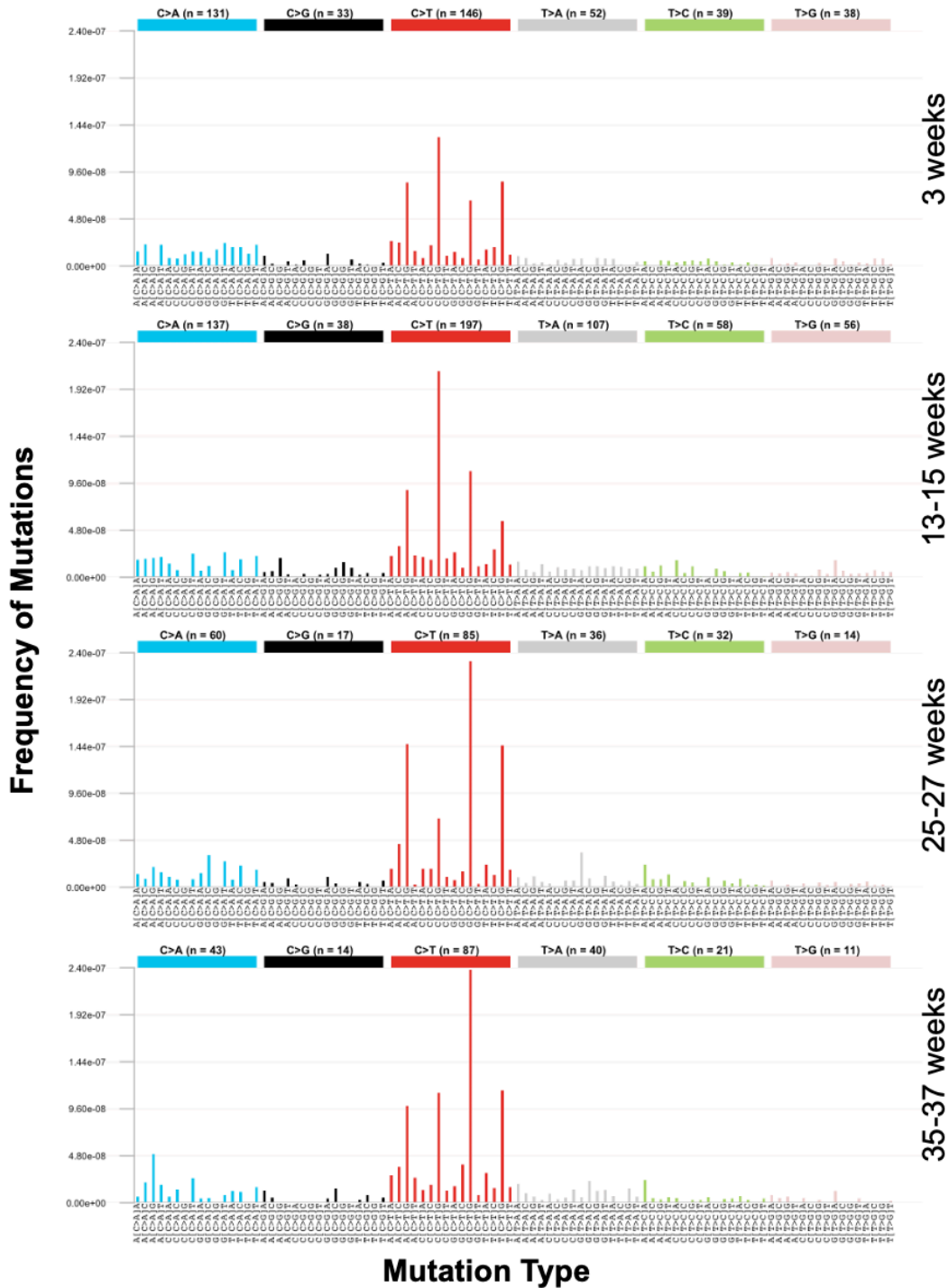
Supplementary Material for Chapter Three



Supplementary Figure 3.1. Informative duplex bases per mouse at 3, 13-15, 25-27, and 35-37 weeks. Time points are shown on the x-axis. A minimum number of duplex bases was set to ensure all animals were sufficiently sequenced (red dotted line). One animal (indicated in red) did not reach the minimum threshold and therefore was removed from the analyses.



Supplementary Figure 3.2. Cochran Armitage Trend Test of MF_{\min} for C:G > T:A transitions at the 3-, 13-15-, 25-27-, 35-37-week time points. Average MF_{\min} for C:G > T:A mutations with SEM at each time point is shown. The asterisk indicates significance ($p < 0.04$).



Supplementary Figure 3.3. Trinucleotide plots at 3, 13-15, 25-27, and 35-37 weeks. MF_{\min} shown on the y-axis and trinucleotides for each mutation type represented on the x-axis.